7-1-2012

Spectral densities and coherence of NM hydrology; NM decomposition analysis; Quantifying science education

Jennifer L. Tichy

Jennifer L. Tichy
Candidate

Biology
Department

This dissertation is approved, and it is acceptable in quality and form for publication:

Approved by the Dissertation Committee:

Robert Sinsabaugh , Chairperson

Marcy Litvak

Kathryn Watkins

Helen Wearing

Spectral Densities and Coherence of NM Hydrology; NM Decomposition Analysis; Quantifying Science Education

by

Jennifer L. Tichy

B.A., Biology, Coe College, 2004
M.S., Biology, University of New Mexico, 2008

DISSERTATION

Submitted in Partial Fulfillment of the
Requirements for the Degree of

Doctor of Philosophy
Biology

The University of New Mexico

Albuquerque, New Mexico

July, 2012

Acknowledgments

First and foremost, I would like to thank my husband, Adam Ringler, for his dedicated support and commitment through this process. He was first on the scene to provide helpful suggestions and was never-ending with encouragement and guidance. He was a key piece to this puzzle and truly bent over backwards for me. I thank him deeply. Additionally, I would like to thank my parents, Tom and Janice Tichy, for their love and encouragement through all of my years of schooling. It's been a fun, albeit long, adventure!

I would like to thank my major advisor, Bob Sinsabaugh, for his thoughtful mentorship, review of papers, and encouragement over the past few years. I am also very thankful for my committee members: the late Cliff Crawford, Marcy Litvak, Kathryn Watkins, and Helen Wearing for their support and suggestions throughout this project. I appreciate their commitment even though I went off to become a teacher!

I also am indebted to the following reviewers: Ayesha Burdett, Carolyn Donnelly, Christian Gunning, Heidi Hopkins, Kelly Isaacson, Michael Nakamaye, Etsuko Nonaka, Adam Ringler, Eric Scherff, Janice Tichy, Tom Tichy, and Cindy Walter. I greatly appreciate their suggestions and comments on my chapters along the way.

I also thank the USDA Natural Resources Conservation Service (SCAN and SNOTEL programs) for their daily measurements of snow water equivalent, soil moisture, and soil temperature, as well as the United States Geological Survey for their stream gauge data. These programs were implemented to create a nationwide soil moisture and climate information system designed to provide data to support natural resource assessments and conservation activities.

Spectral Densities and Coherence of NM Hydrology; NM Decomposition Analysis; Quantifying Science Education

by

Jennifer L. Tichy

B.A., Biology, Coe College, 2004
M.S., Biology, University of New Mexico, 2008
Ph.D., Biology, University of New Mexico, 2012

Abstract

Chapter 1: River discharge and montane snowpack play a central role in controlling processes at all levels of ecological organization, so the identification of dominant hydrological periods is an important issue in relating the physical system to the biological system. To quantitatively study the Rio Grande discharge along with the closely related snowpack, we determine the spectral densities as a function of frequency in addition to coherence estimates. This is quality-controlled through a signal to noise ratio, which also allows us to create a transfer function to model the relationship between river discharge and snowpack. By using frequency domain techniques, it becomes apparent that there are in fact three signal peaks at distinct frequencies (every 365 days, every 182 days, and every 122 days) for the riparian ecosystem of the Rio Grande in New Mexico, USA. By generalizing power spectral estimates, seasonal variation can be quantified (spring snowmelt in addition to summer monsoons) through spectrograms, yielding further amplitude estimates across a large band of frequencies of interest.

Chapter 2: To find events in both river discharge data and snow water equivalent data for the Rio Grande, New Mexico, an event detector is created through moving averages (short term average over long term average, STA/LTA). Additionally, a cross-correlation is performed on the data from the United States Geological Survey and the National Resource Conservation Service (1981-2010) to see the relationship between the river discharge data and the snow water equivalent data. Using lag times calculated from the cross correlation, the differences in peak times from discharge and snowmelt indicates a shift in snowmelt to earlier in the spring. Because of the high correlation between snow water equivalent and river discharge, plus the results of the cross-correlation, it is found that the peak in snowmelt is occurring earlier in the year and that the time lag between peak snowpack and peak river discharge is decreasing, meaning that the snowpack is generally melting faster. One implication resulting from hydrologic changes such as these is the adaptation of aquatic and terrestrial species depending on the system for survival.

Chapter 3: The temperature and moisture responses of heterotrophic soil respiration are crucial for a reliable prediction of carbon dynamics with respect to climatic change. Despite numerous studies regarding temperature and moisture effects on soil decomposition, open questions remain regarding local ecosystem response to large-scale changes in climate (i.e. If annual average soil temperature increases, will faster decay alter net ecosystem carbon exchanges?). The objective of this study was to analyze the influence of different soil and temperature response functions on decomposition rates over a time, depth, and spatial continuum, using data obtained from the USDA NRCS. According to the CENTURY soil decomposition model, decomposition was predominantly defined by temperature controls, but soil moisture provides the pulse-like activity of decomposition across the state of New Mexico. This study suggests that as the local climate changes, so will decomposition rates, which ultimately affects levels of carbon sequestration. Current measurements are on a daily time-step, but more frequent data collection could identify diel variability.

Chapter 4: In order to study the idea of teaching mainstream students how to be scientists, a literature review is performed and the data are quantitatively analyzed. The data are compared across the educational research papers and similar statistical results are then categorized and analyzed for similarities in the papers utilized. It is found that similarities in how the data are collected groups the normalized data to an extent, but the quantitative analysis finds that a more scientific approach needs to be applied to all research fields, minimizing subjective results and maximizing objective results for a given research study. A conclusion is drawn that all students need to be taught the scientific process and need to understand the importance of questioning facts and the need to critically, quantitatively, study data.

Contents

List of Figures

List of Figures

List of Tables

List of Tables

Chapter 1

Correlated Frequency Excitation of Snowpack and River Discharge

This work was published as: Tichy, J.L. Correlated discrete frequency excitation of Rio Grande Discharge and New Mexico Snowpack Data. 2011. Journal of Environmental Hydrology 19:1-14.

1.1 Introduction

Because river discharge is a function of factors such as spring snowmelt, precipitation, temperature, catchment characteristics, and anthropogenic forcings, scientists have attempted to quantify and explain regional sensitivities for particular systems (Sang et al. 2009, Hanson et al. 2004, and Daniels 2007). For example, in the western United States, approximately 50-70% of the precipitation falls as snow, and spring/early summer snowmelt runoff accounts for approximately 50-80% of the total annual runoff for snowmelt-dominated basins (Serreze et al. 1999). Despite these figures, it is predicted that there may be a reduction in mountain snowpack and

changes in snowmelt runoff timing to be earlier in the year (IPCC 2007, Daniels 2007 and Zhang et al. 2007). If the peak in snowmelt runoff is earlier in the year than it is presently, the montane storage of snowpack will be decreased, and there will be an increase in the need for alternative water management practices (Daniels 2007, Krishna 2005, and Leon et al. 2009).

Snow cover decrease has the potential to produce polar amplification of global warming caused by snow's high albedo (Stewart 2009), which could further the effects of climate change and therefore produce a positive warming feedback. Warmer winters yield less snowpack due to precipitation falling as rain rather than snow, and additionally move the peak snowmelt runoff to an earlier date, forcing severe declines in aquatic population abundance and community composition (Cayan et al. 2001, Platt and Connell 2003, and Scheffer et al. 2001). Earlier mountain snowmelt runoff results in a longer summer drought season and lessened summer and fall stream flow in adjacent dry regions. These types of changes in the annual hydrograph may cause stresses on ecosystems owing to lower flows and warmer stream temperatures (Cayan et al. 2001).

To quantify sources for environmental variation and thus how the environment may impact ecological systems, Fourier techniques are applied to create spectral densities and a transfer function to predict stream flow based on snowpack. Spectral densities allow us to see how time series data is viewed in the frequency domain (Shi et al. 2007). With this technique, the amplitude of the signal is represented as a function of frequency rather than as a function of time (Hameed 1984). The tool allows us to objectively analyze data through mathematical techniques and the strength of repetitive events in the data becomes visible (Schepers et al. 1992). For instance, it is expected that there will be a strong signal every 365 days, given our knowledge of spring river discharge. One step beyond creating the power spectrum is the spectrogram analysis, which is the process of converting the time domain

representation of a signal to a frequency domain representation that shows how different frequency components contribute to the overall signal (Sabo and Post 2008).

The idea of using power spectra to analyze hydrological data has been utilized previously around the world, but has not yet been done extensively for the semi-arid ecosystem of the Rio Grande in New Mexico, USA. Pelletier and Turcotte (1997) calculated power spectra of time series data for river discharges (636 monthly records) and precipitation (49 annual records) averaged over hundreds of stations worldwide. The average power spectrum of river discharge was found to have a power-law dependence on frequency $S(f) \sim f^{1/2}$ for time scales from 1 month to 10 years. However, they found that precipitation is spectrally white (uncorrelated, Sabo and Post 2008 and Wang et al. 2008). Because of this, the snowpack values that are directly related to the Rio Grande discharge can be analyzed in order to specify the fluctuations in this system. The analysis presented here determines if the data from the Rio Grande are spectrally white or if a signal can be teased from the data.

Others took the spectral analysis one step further by way of modeling (e.g. Dolgonosov 2008, Guo et al. 2003, Renard and Lang 2007, Mantilla et al. 2006, and Molotch and Margulis 2008). Time series data were used to model annual oscillations of river discharge through converting time series data into empirical power spectra of river discharges. The time series data were also used to construct theoretical power spectra by fitting model parameters to the data (Schaefli et al. 2007 and Labat 2005).

The aim of this paper is to use two approaches in studying data collected by the Natural Resources Conservation Service (NRCS, measuring snow water equivalent) and the United States Geological Survey (USGS, measuring river discharge) to answer our questions regarding the ecosystems surrounding the river system. With the frequency analysis, any wavelike signal can be graphically or mathematically depicted in either of two forms - the time domain and the frequency domain, as

described above. The second method is through a transfer function, which depicts the functional relationship between the Rio Grande discharge data and the NRCS data. These two approaches quantify the data and allow us to make predictions of notable frequencies in the data, such as peak spring snowmelt (fundamental mode) and the subharmonics of the data (secondary modes caused by other forcings on the system). The frequency analysis allows us to see that there are in fact three distinct peaks during different times of the year (every 365 days, every 182 days, and every 122 days).

1.2 Methods

In this analysis, NRCS SNOTEL (for SNOwpack TELemetry) data from the NRCS website (`http://www.wcc.nrcs.usda.gov/snow/`) at the Quemazon site in New Mexico is analyzed. The site number is 708, the county is Los Alamos, the latitude is 35 deg 55 min N, the longitude is 106 deg 24 min W, and the elevation is 9500 feet (Figure 1.1). The daily data, including snow water equivalent (SWE), precipitation, various air temperature quantities, and snow depth were downloaded from January 1981 through May 2010. The parameter of interest for this study is the SWE, measured in inches. To measure this parameter, a snow pillow is positioned so that it measures the water-content of the snow covering. The working principle of the sensor is based on the detection of the hydrostatic pressure caused by the layer of snow (Peterson et al. 2000). This SNOTEL site is located north of the USGS stream gauge monitoring river discharge for this project (Figure 1.1).

Additionally, United States Geological Survey stream gauge data from the USGS website (`http://water.usgs.gov/`) at the Rio Grande at Otowi Bridge site in New Mexico is analyzed. The site number is USGS 08313000, the county is Santa Fe, the latitude is 35 deg 52 min 28.2 sec, the longitude is 106 deg 8 min 32.8 sec, and the

elevation is 5488 feet (Figure 1.1). The daily data, including river discharge, were downloaded from January 1981 through May 2010. Historically, the Otowi gauge used several different types of instruments, but the technology today is the following: The stream channel cross section is divided into numerous vertical subsections and in each subsection the area is obtained by measuring the width and depth of the subsection, and the water velocity is determined using a current meter. The discharge in each subsection is computed by multiplying the subsection area by the measured velocity. The total discharge is then computed by summing the discharge of each subsection. This site is located south of the NRCS SNOTEL site used for this project (Figure 1.1).

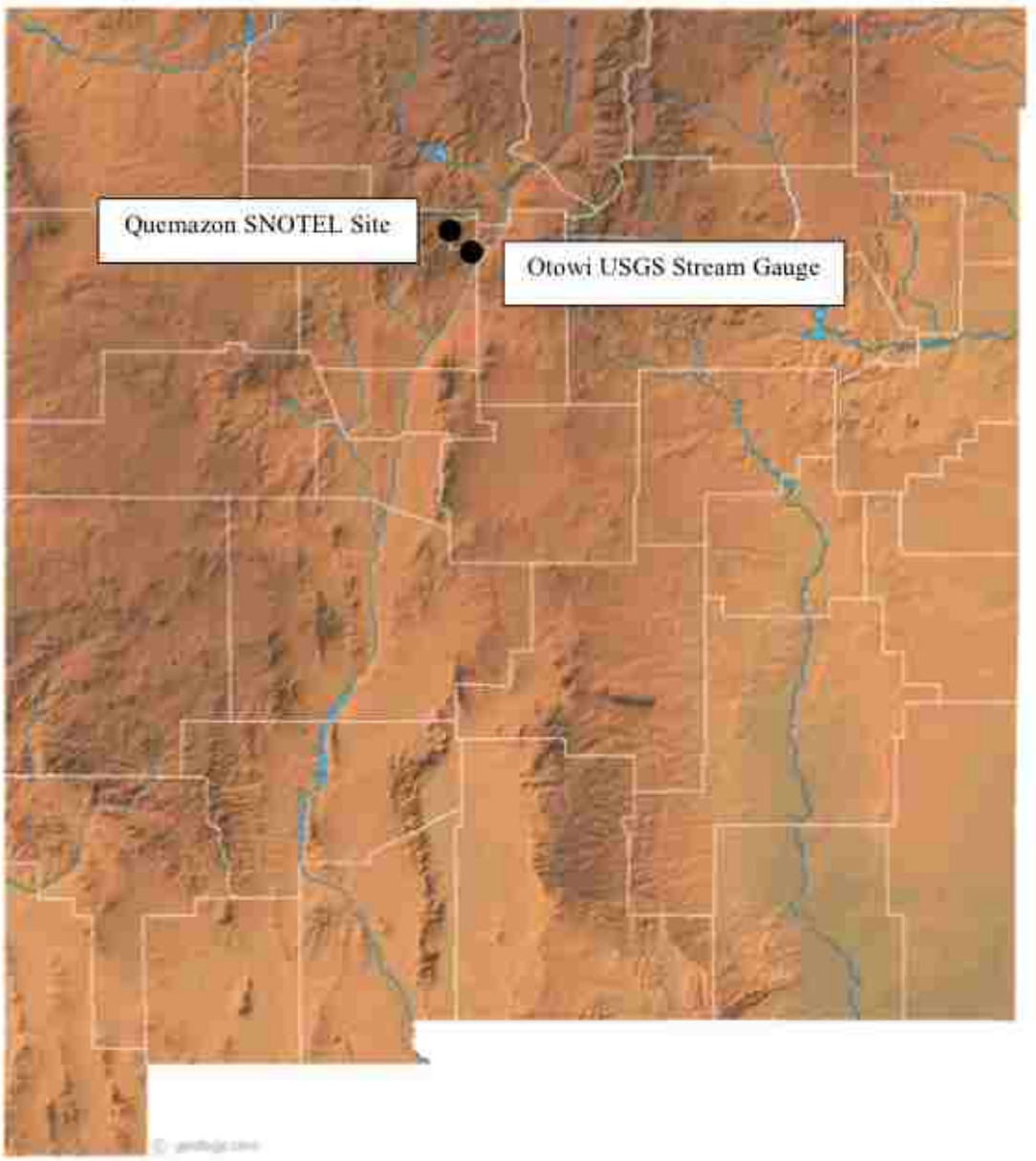

Figure 1.1: New Mexico map depicting the NRCS SNOTEL site at Quemazon and the USGS stream gauge site at the Otowi Bridge.

The fist step of the analysis is to compute power spectra of both the river discharge and the SWE data, individually. Power is the multiplication of a Fast Fourier Transform (FFT) and its conjugate, and for an FFT, a grouping of the original data set is separated and is called the window. For this analysis, an overlap of 50% is used, meaning that each window except the first and the last is analyzed twice. If there are leftover data points in the original vector, they will be discarded. Each window is then multiplied by applying a Hamming window:

$$w(n) = 0.54 - 0.46\cos\left(2\pi\frac{n}{N}\right), 0 \leq n \leq N \tag{1.1}$$

where n is the n^{th} data point and N is the number of points in the data set. This Hamming window multiplication begins the process of analyzing time-series data with cosines.

The "pwelch" function in Matlab is used with the following parameters, unless otherwise noted: window size of 256, 128 signal samples (elements of the original data vector) that are common to two adjacent segments (i.e. windows of 256 days with 50% overlap), and a sampling frequency of 1 per day. The FFT is detailed in the fully functional form:

$$FFT = X(k) = \sum_{j=1}^{N} x(j)\omega_N^{(j-1)(k-1)} \tag{1.2}$$

where j is the index of the data point in the given window, N is the number of values in the window, and k is the k^{th} term.

$$x(j) = (1/N)\sum_{k=1}^{N} X(k)\omega_N^{-(j-1)(k-1)} \tag{1.3}$$

where

$$\omega_N = e^{(-2\pi i)/N} = \cos\left(\frac{-2\pi}{N}\right) + i\sin\left(\frac{-2\pi}{N}\right) \tag{1.4}$$

Once each window is multiplied by a Hamming window, the FFT is taken of the result, and we can take an average to determine power:

$$\overline{X} = \frac{X_1 + X_2 + \cdots + X_m}{m} \tag{1.5}$$

$$\text{power} = (\overline{X})(\overline{X^*}) \tag{1.6}$$

where $\overline{X^*}$ is the conjugate of $\overline{X}$. The power can then be converted into decibels by taking the $10\log_{10}$ of the FFT times its conjugate, i.e.

$$\text{power in decibels} = 10\log_{10}((\overline{X})(\overline{X^*})) \tag{1.7}$$

A power spectra is typically plotted with either period (units of time) or frequency (units of 1/time) on the horizontal axis and power (units of [units of original data]^2*days)^2 on the vertical axis. Depending on the data, the plot may be semi-log or linear. Additionally, it is important to take note of the Nyquist frequency, which allows us to recover all Fourier components of a periodic waveform. For this to happen, the sampling rate must be at least twice the highest waveform frequency. In other words, with our sampling rate of 1/day, our Nyquist frequency is 1/2 day. If we are not cognizant of the Nyquist frequency, we are at risk of aliasing (Sabo and Post 2008).

To further analyze the power spectra, a signal to noise ratio (SNR) is calculated (Sang et al. 2009). This is performed by dividing the power spectral density by the noise in an attempt to compare noise levels to distinctive signals of biological interest. Noise in hydrological data is simply fluctuations in the flow that aren't recuring (Sabo and Post 2008). The signal to noise ratio is computed separately for both the river discharge data and the SWE data with the following equation:

$$SNR = 10\log_{10}(V_S/V_N) \tag{1.8}$$

where V_S is the spectral density power and V_N is the noise power.

After this value is calculated, it is plotted with period (in days) on the horizontal axis and power (in decibels, dB, relative to 1 ([unit]^{2}day)^2) on the vertical axis, with [unit] being either cubic feet per second (cfs) or inches (in) for this analysis. Because of how the FFTs are calculated, parts of the resulting plots are not usable (see results and discussion sections).

In order to look at the power spectral densities for each year, a spectrogram is created. This allows us to see each year's spectral density stacked with the rest of the data set. Because of the window size of 256 and an overlap of 50%, only the years 1985 through 2004 are clearly identified in this analysis.

Depending on the parameters set in the analysis, a spectrogram is able to tease further information out of the initial power spectra that would not otherwise be visible. In this analysis, the parameters are set in such a way to analyze seasonal data, closely looking at how the river and snowpack vary throughout the year as well as throughout a larger data set. Spectrograms are plotted with time on the horizontal axis, period (in days) on the vertical axis, and power (in dB relative to 1 ([unit]^{2}day)^2) shown as a color bar, with reds and oranges indicating higher power and blues indicating lower power.

The second approach used in this paper is a transfer function to represent the relationship between river discharge and SWE. The relationship between SWE and discharge is commonly studied (e.g. Hanson et al. (2004)), allowing us to relate the two parameters. To calculate the amplitude system response, the "pwelch" function is again used to calculate the power spectral densities of both the river discharge and the SWE, with a 5 point moving average to smooth the data. The mathematics behind the transfer function are as follows:

$$X_{discharge} = Y_{SWE} * T_{system} \tag{1.9}$$

where T_{system} is the overall transfer function of the system. If we then take the Fast Fourier Transform of all components, we have the following:

$$\hat{X}_{discharge} = \hat{Y}_{SWE} * \hat{T}_{system} \tag{1.10}$$

$$\frac{\hat{X}_{discharge}}{\hat{Y}_{SWE}} = \hat{T}_{system}. \tag{1.11}$$

If we then multiply all components by their respective conjugates to yield the power spectra, we can see that

$$\frac{\hat{X}_{discharge} \cdot \hat{X^*}_{discharge}}{\hat{Y}_{SWE} \cdot \hat{Y^*}_{SWE}} = \hat{T}_{system} \cdot \hat{T^*}_{system}. \tag{1.12}$$

We can then define $\hat{X}_{discharge} \cdot \hat{X^*}_{discharge}$ as P_{XX} and $\hat{Y}_{SWE} \cdot \hat{Y^*}_{SWE}$ as P_{YY} and take $10 \log_{10}$ of the values to change them into decibels (dB).

$$10 \log_{10} \frac{P_{XX}}{P_{YY}} = 10 \log_{10}(P_{XX}) - 10 \log_{10}(P_{YY}) \tag{1.13}$$

Plotting by way of a logarithmic frequency, the amplitude system response with period (in days) on the horizontal axis and the normalized amplitude (in dB) on the vertical axis, we will be able to see the constant relationship between river discharge and SWE. The figure will give us the constant that relates the two parameters, thus creating a simple model.

To then determine differences in frequencies over time, the data are divided into 5 year blocks and spectral densities are calculated with the following parameters: window size of the length of the 5 year data vector, 0 signal samples (elements of the original data vector) that are common to two adjacent segments (no overlap of windows because we were looking at the distinct 5 year periods), enough Fast Fourier Transforms (again using the above equations) to have twice the number of

data points in the 5 year vector, and a sampling frequency of 1 per day. Because of the 5-year blocks, only the years 1985 through 2005 are clearly identified in this analysis. In addition to the individual values, the means and standard deviations are also calculated. This allows us to see if the data changes over time.

1.3 Results

As described in the Methods section, the power spectra of both the Rio Grande discharge data and the Quemazon SWE data from the mountain region feeding the river are calculated with Fast Fourier Transforms. Figures 1.2 and 1.3 show the two respective power spectra. Because both plots have significant peaks under 400-day periods, both are plotted on linear plots rather than semi-log plots.

The power spectra of the discharge data (Figure 1.2) shows approximately three points of interest. There is a peak with high power at 365 days (3.81 x 10^9 Power ($(cfs^2day)^2$), a second peak with a period of 182 days (1.38 x 10^9 Power ($(cfs^2day)^2$), and a third peak with a period of 122 days (3.83 x 10^8 Power ($(cfs^2day)^2$). Additionally, the power spectra of the SWE data (Figure 1.3) also shows approximately three points of interest. There is a peak with high power at 365 days (4.14 x 10^4 Power ($(in^2day)^2$), a second peak with a period of 182 days (1.12 x 10^4 Power ($(in^2day)^2$), and a third peak with a period of 122 days (2.66 x 10^3 Power ($(in^2day)^2$).

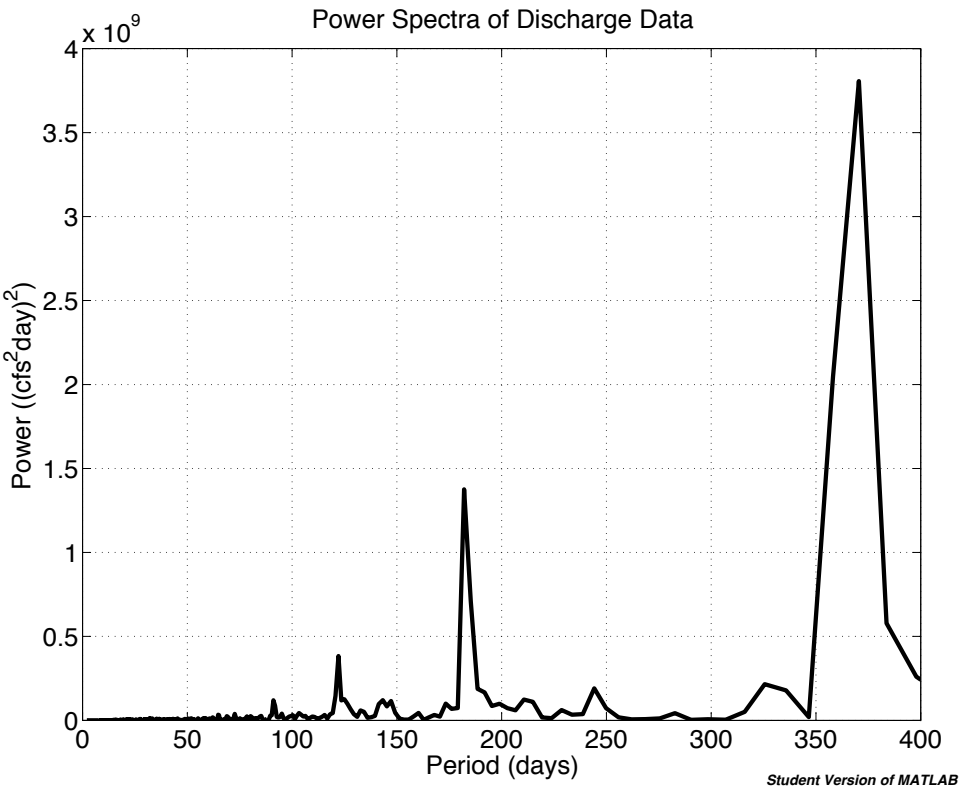

Figure 1.2: Power spectra of 1981-2010 daily Rio Grande discharge data (cfs) at the USGS Otowi gauge. The window for this analysis is the entire length of the data set with an overlap of zero.

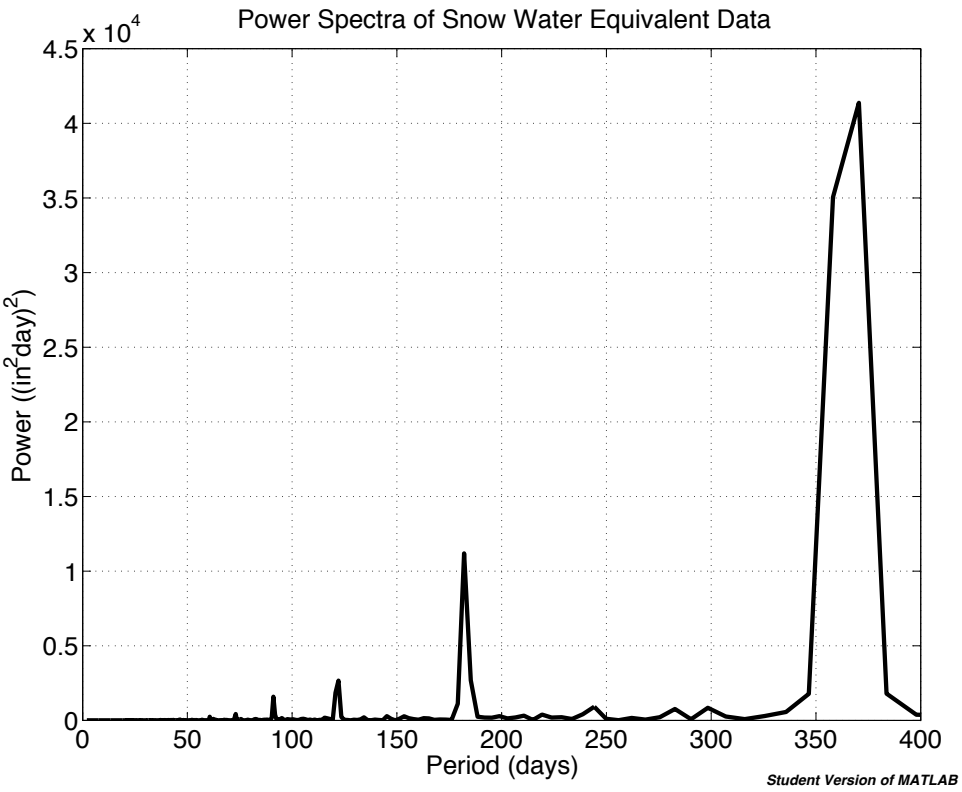

Figure 1.3: Power spectra of 1981-2010 daily snow water equivalent data (in) at the NRCS Quemazon site. The window for this analysis is the entire length of the data set with an overlap of zero.

To then separate the signal from the noise in the data, a signal to noise ratio is calculated and plotted for both the river discharge data and the SWE data (Figures 1.4 and 1.5). It is common to accept a signal to noise ratio around 20 - 40 dB (Swayze et al. 2003), meaning that there is not too much noise clouding the signal. The way that these ratios are calculated creates a band of unusable data under a period of about 50 days. The data are daily, so calculating frequencies is best done on longer periods from approximately 50 to 400 days. Additionally, powers less than zero do not make physical sense, so it is best to focus on the signal to noise ratios around our periods of interest (122 days, 182 days, and 365 days).

On the signal to noise ratio of the Rio Grande discharge data (Figure 1.4), it is apparent that the SNR around the points of interest is between 20 and 40 dB, thus showing acceptable values. Because these data have been quality-controlled, they can be used for further analyses. On the signal to noise ratio of the Quemazon SWE data (Figure 1.5), it is apparent that the SNR around the points of interest is between 0 and 40 dB, thus showing acceptable values. Given that these values are not as high quality as the Rio Grande discharge data, however, we must be cautious in further analyses.

To see the power spectra for the entire data set as individual time periods, spectrograms are created for both the river discharge data and the SWE data (Figures 1.6 and 1.7). Each vertical band in the spectrograms represents a small time period (on the order of several months) with the period length along the vertical axis. Because of the window size and overlap used for these calculations, only the years 1985-2004 are complete, thus shortening the overall data set. The power of the spectra is seen through the color bar. The spectrogram of the daily Rio Grande discharge data (Figure 1.6) shows relatively high power almost every year during the early part of the data set in the longer periods. Later in the data set, however, the signals are not as strong for this seasonal-like signal. Despite this, there are seasonal signals

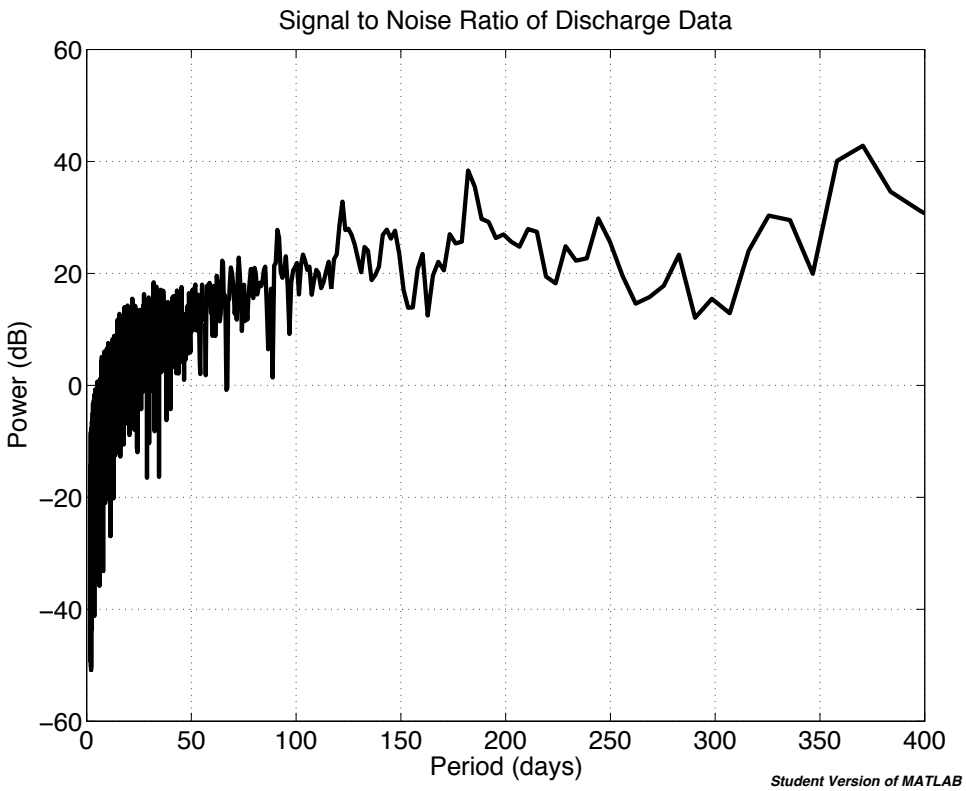

Figure 1.4: Signal to noise ratio of 1981-2010 daily Rio Grande discharge data (cfs) at the USGS Otowi gauge.

on the lower end of the power spectrum in shorter periods. The spectrogram of the daily Quemazon SWE data (Figure 1.7) shows relatively high power almost every year during the entirety of the data set as a seasonal repetition of strong power. There also are seasonal signals on the lower end of the power spectrum in the shorter periods.

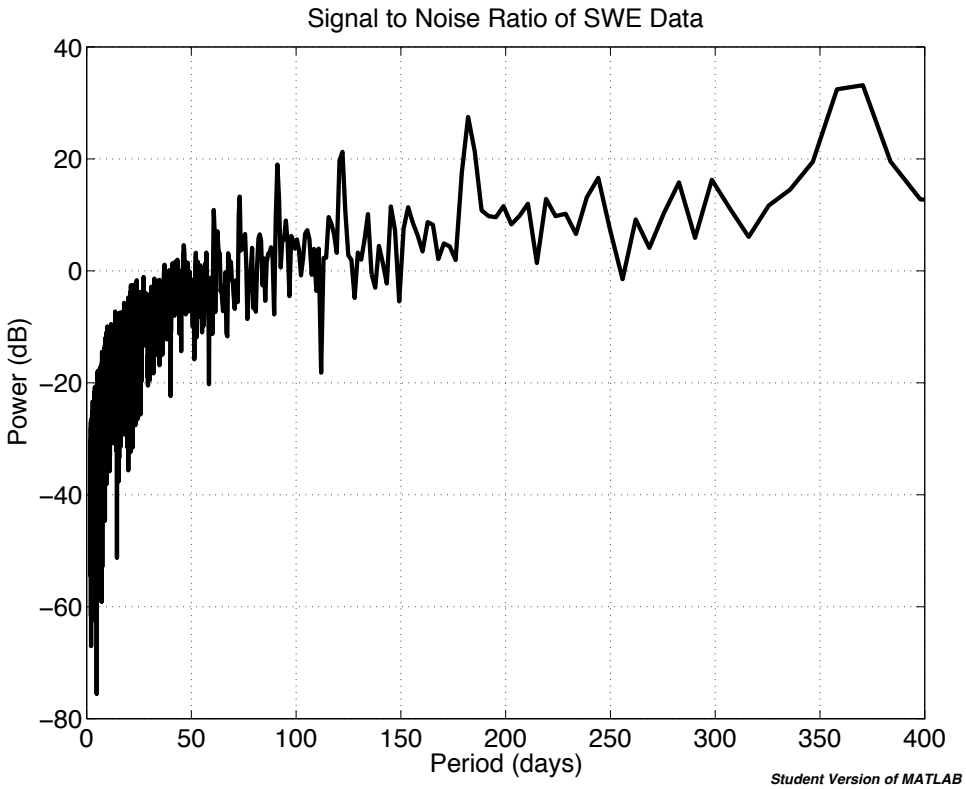

Figure 1.5: Signal to noise ratio of 1981-2010 daily snow water equivalent data (in) at the NRCS Quemazon site.

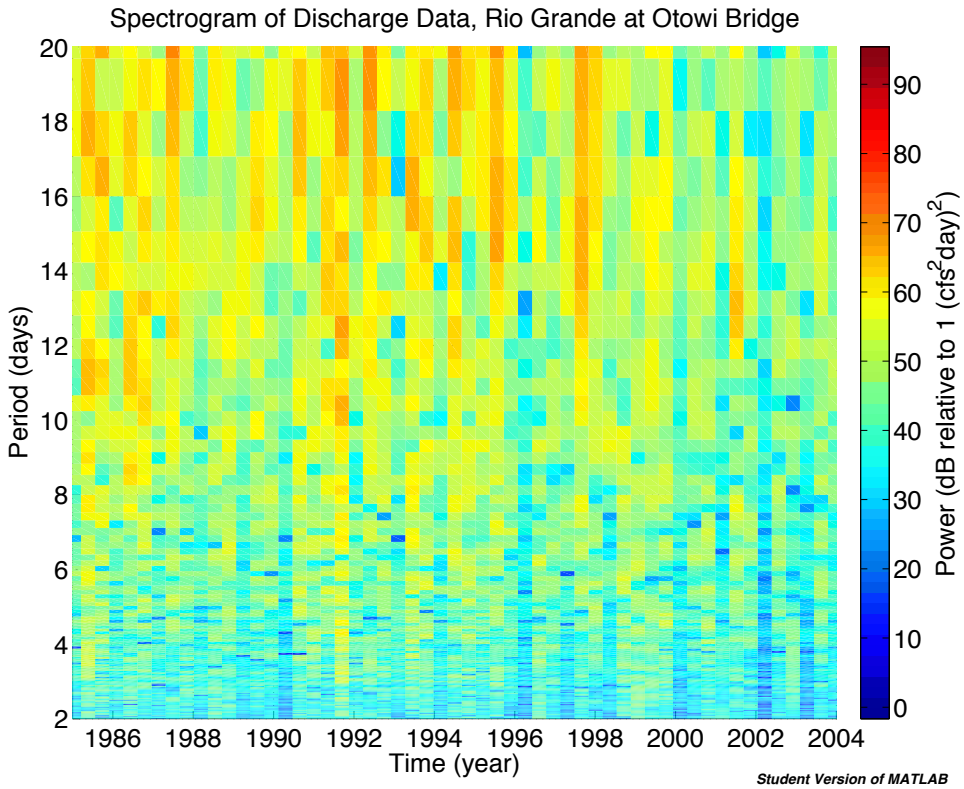

Figure 1.6: Spectrogram of 1985-2004 daily Rio Grande discharge data (cfs) at the USGS Otowi gauge. The window for this analysis is 256 with an overlap of 50%.

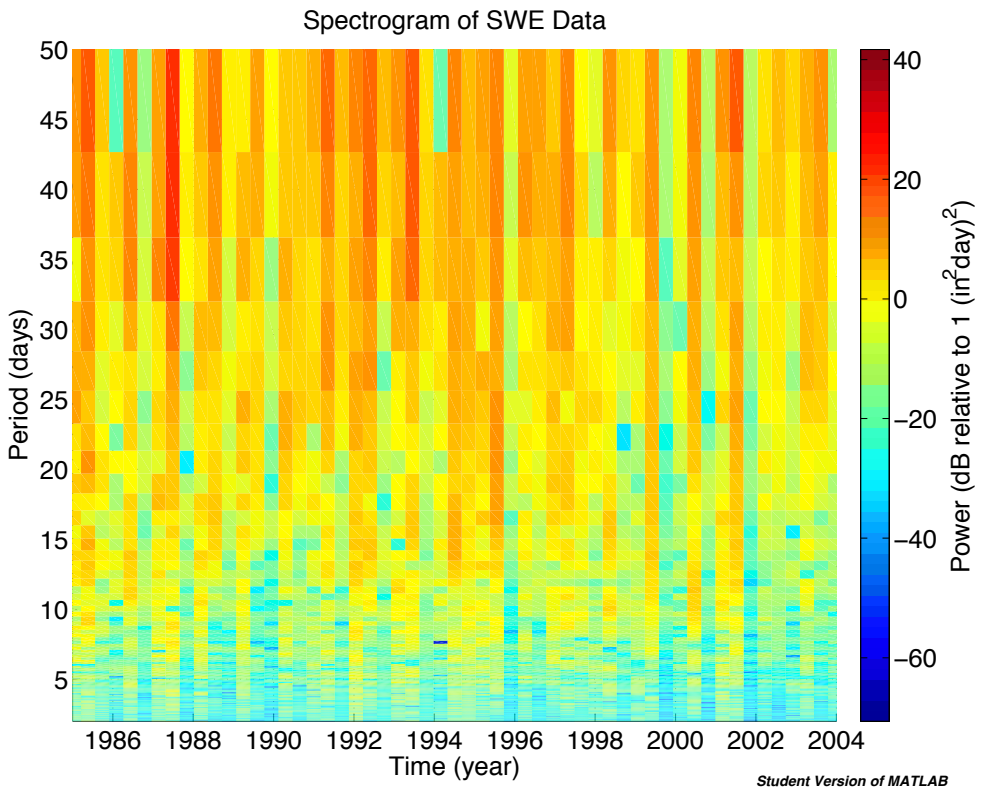

Figure 1.7: Spectrogram of 1985-2004 daily snow water equivalent data (in) at the NRCS Quemazon site. The window for this analysis is 256 with an overlap of 50%.

Using the transfer function analysis, an amplitude system response is created to see the relationship between river discharge and SWE (Figure 1.8). Because of the lack of data points, the data beyond about 100 days is unusable. Therefore, the normalized amplitude is best viewed on shorter periods.

To then look at blocks of time to see if the peak frequencies have changed over time, a power spectra analysis is performed on five year blocks of time, 1981-1985, 1986-1990, 1991-1995, 1996-2000, and 2001-2005. From each of the 5 power spectra created, the three major peaks are selected and recorded in Table 1.1. The mean of

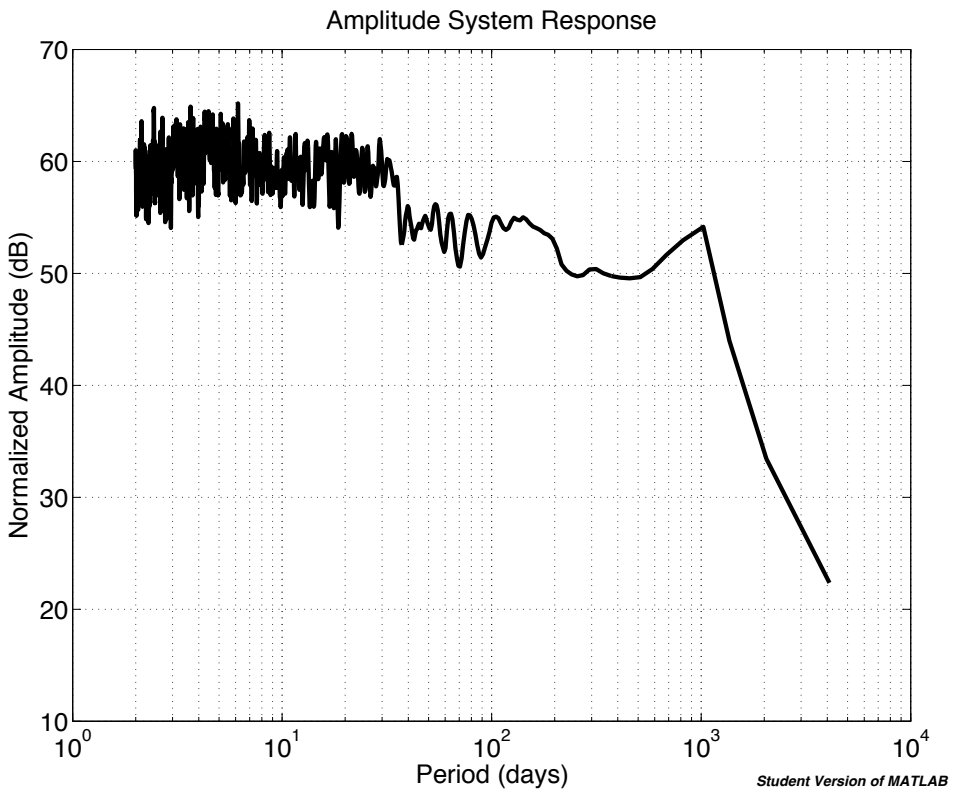

Figure 1.8: Amplitude system response of 1981-2010 Rio Grande discharge data and Quemazon snow water equivalent data.

each of the three peaks and the standard deviation are also calculated. In addition to the table, a figure is created to visually show the power spectra of the 5 year blocks of time (Figure 1.9).

Block of Years	Major Peak 365 days	2nd Peak 182 days	3rd Peak 122 days
1981-1985	2.27×10^9	1.02×10^9	2.78×10^8
1986-1990	5.98×10^8	2.50×10^8	2.53×10^7
1991-1995	1.77×10^9	7.30×10^8	2.20×10^8
1996-2000	4.46×10^8	1.79×10^8	1.32×10^8
2001-2005	2.08×10^8	4.12×10^7	1.69×10^7
mean	1.06×10^9	4.34×10^8	1.34×10^8
standard deviation	9.05×10^8	4.13×10^8	1.16×10^8

Table 1.1: Power spectra of 5 year blocks of river discharge data (cfs). The power of the three major peaks is presented, with all units in Power ($(\text{cfs}^2\text{day})^2$). See Figure 1.9 for a visual of the 3 main peak representation.

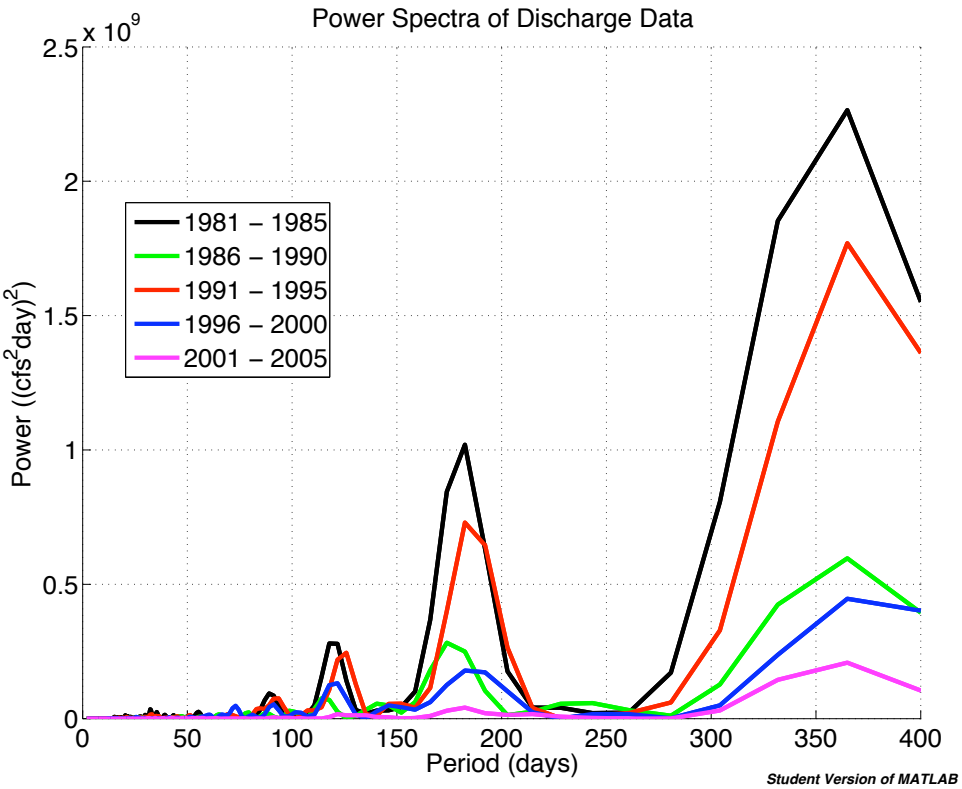

Figure 1.9: Power spectra of 5 year blocks of river discharge data (cfs). The window for this analysis is the length of a 5 year block of data with an overlap of zero.

1.4 Discussion

With predicted climate changes, there may be a reduction in mountain snowpack and changes in snowmelt runoff timing in addition to more winter precipitation falling as rain rather than snow (Sang et al. 2009, Peterson et al. 2000, and Stewart 2009). It is predicted that the peak spring runoffs will occur earlier in the year, thus reducing the montane storage of snowpack and increasing the need for alternative management practices such as reservoir storage (Peterson et al. 2000). Therefore, to ensure arid and semiarid regional water needs are met, it is important to understand the processes of snow accumulation, snowmelt, and river discharge.

To answer our questions, we can now state that there is a constant dB value that relates SWE in Quemazon to the Rio Grande discharge at the Otowi Bridge (Figure 1.8). We can use this information to effectively work backward to make predictions of summer flows. Since we know how the amplitude system response was created, we can create power spectra for SWE data and use the response of the system to predict discharge values. We can use the mathematical equations from the methods section to see the following:

$$10\log_{10}(P_{XX}) - 10\log_{10}(P_{YY}) = [\text{constant from Figure 1.8}] \tag{1.14}$$

It is then apparent to see that the SWE power spectra for any specific winter can be substituted for P_{YY} and P_{XX} can be easily solved (river discharge predictions based on power spectral densities, Figure 1.8). In order to test the transfer function, the Rio Grande discharge and Quemazon snow water equivalent data were downloaded for 2010-2011. The constant determined from the transfer function and Figure 1.8 was then used to predict the river discharge power for 2010-2011. Since the data were available, however, the actual river discharge spectral densities (power) for 2010-2011 were also calculated using the same methods listed above. The predicted and actual values were then plotted against each other to determine the accuracy of the transfer

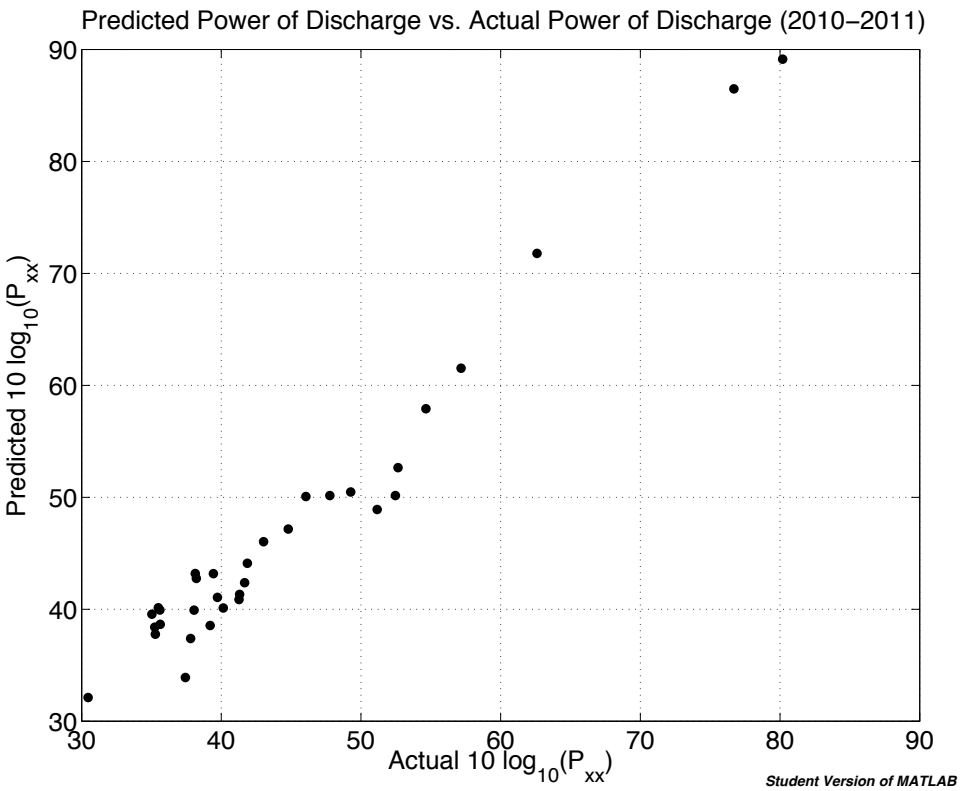

Figure 1.10: Transfer function test with the actual power (in decibels) of the 2010-2011 river discharge on the x-axis and the predicted power (in decibels) of the 2010-2011 river discharge on the y-axis.

function model. As seen in Figure 1.10, the transfer function is quite accurate, as the plot shows a clear linear trend.

The annual fluctuations of the Rio Grande are caused by several different physical parameters. The clear peak at 365 days is due to spring snowmelt runoff. High SWE and river discharge in New Mexico is generally associated with the El Niño weather phenomenon, a pattern in which warmer ocean temperatures near the equator mean more moisture for the southwestern U.S. In addition to the high yearly peak caused by springtime snowmelt, our analyses show two subharmonics, one every 182 days and one every 122 days. The analysis has revealed that these peaks are most likely due to precipitation events such as the summer monsoon and winter precipitation. The frequencies reflect regional variables such as soil saturation, catchment size, rainfall duration, and travel time from rainfall to the river. For example, in New Mexico, between 50 and 70% of the total annual precipitation falls between the months of June and September through the North American monsoon (Gosz et al. 1995), which is also reflected in our analyses. It has been found that the monsoon variability is due to surges in low-level moisture from the Gulf of California (Adams and Comrie 1997), which ultimately affects the strength of the monsoon affecting New Mexico (Hanson et al. 2004), and therefore the peaks found in our analyses.

The two spectrograms in Figures 1.6 and 1.7 show seasonal variation, indicating the presence of subharmonics due to the above parameters. The spectrogram of discharge data (Figure 1.6) shows relatively regular low power bands (blue bands), which most likely indicate winter, low flow time periods. There are also some high power bands that most likely represent spring snowmelt, but they appear to be regular during the early years of the data set but tend to fade in the later years (red/orange bands), indicating the existence of long-term trends throughout the data set analyzed. Additionally, in looking at the time series plot of the river discharge during this time, we can say that there was a period of relatively low flow from 1988 - 1991, and another from 1998 - 2004. These "dry" periods clearly affect the spectrograms. The spectrogram of SWE data (Figure 1.7) shows relatively regular low power bands (blue bands), which most likely indicate summer, no snow periods.

There are also some very distinct high power bands (red/orange bands) that most likely represent the period just before spring snowmelt, when the SWE values are the greatest. In general, the SWE spectrogram has a stronger pattern than the discharge spectrogram. This is most likely due to the more regular and less dynamic nature of snow as compared to water flow. In looking at time series plots of the data, it is apparent that there also were several spikes of high SWE, and these years are also evident on the spectrogram (1987, 1993, and 1997).

The five year block data analysis shows that if we assume a normal distribution, we can say that 68% of the major peaks occurring at 365 days are within 9.05 x 10^8 $(cfs^2day)^2$ of the mean 1.06 x 10^9 $(cfs^2day)^2$ and 95% of the major peaks occurring at 365 days are within 1.81x 10^9 $(cfs^2day)^2$ of the mean 1.06 x 10^9 $(cfs^2day)^2$. For the second peak, 68% of them occurring at 182 days are within 4.13 x 10^8 $(cfs^2day)^2$ of the mean 4.34 x 10^8 $(cfs^2day)^2$ and 95% of them occurring at 182 days are within 8.26 x 10^8 $(cfs^2day)^2$ of the mean 4.34 x 10^8 $(cfs^2day)^2$. For the third peak, 68% of them occurring at 122 days are within 1.16 x 10^8 $(cfs^2day)^2$ of the mean 1.34 x 10^8 $(cfs^2day)^2$ and 95% of the them occurring at 122 days are within 2.32 x 10^8 $(cfs^2day)^2$ of the mean 1.34 x 10^8 $(cfs^2day)^2$.

The snowpack and stream flow analysis presented here allows us to make a quantitative analysis of how the two physical parameters are related and how snowpack can be used to predict streamflow through the transfer function. Over time, there has been a general decrease in the amplitude of peaks on the spectrograms (Table 1.1 and Figure 1.9), which is evidence for a long-term trend showing a decrease in peak amplitudes at yearly frequencies.

Further questions were raised in performing this analysis, such as: What else may be causing the subharmonics found in the spectral analyses? Are there other forces on the system that could be causing the stress? It is only through further work that we will continue to understand the system and thus make the best management

decisions possible.

Chapter 2

Coherence/Event Detection of Rio Grande Flow and SWE in NM

This work was published as: Tichy, J.L. Coherence and event detection methodology of river discharge and snow water equivalent in New Mexico, USA. 2012. Journal of Environmental Hydrology 20:1-13.

2.1 Introduction

New Mexico, like many regions that rely on snowpack for water supply, is particularly vulnerable to climate change and the possibility of peak snowmelt occurring earlier in the year (Serreze et al. 1999). In the western United States, for example, approximately 50-70% of the precipitation falls as snow, and spring/early summer snowmelt runoff accounts for approximately 50-80% of the total annual runoff for snowmelt-dominated basins (Serreze et al. 1999), thus creating a need to study the interaction of spring snowmelt runoff and river discharge (Adams and Comrie 1997, Pelletier and Turcotte 1997, and Peterson et al. 2000). April 1st is typically used

as the date of maximum snow accumulation (Maurer et al. 2007 and Graf 2006) but models show that a 1 degree - 2 degree C temperature increase could yield a 10 - 15 day peak shift of discharge (IPCC 2007). Additionally, a 3 degree C temperature increase (under mid to high green house gas emission scenarios), could shift peak streamflow by 30 days (IPCC 2007). Additionally, snow has a high albedo, so there will be a positive feedback of polar amplification of global warming if there is a decrease in yearly snowpack (Mote 2003). Warmer winters yield less snowpack due to precipitation falling as rain rather than snow, and additionally move the peak snowmelt runoff to an earlier date. If the peak of spring snowmelt shifts to be earlier in the year, water managers will be faced with an annual challenge of storing winter precipitation for use later in the year (Stewart 2009).

Previous studies have found hydroclimatological changes in the last 50 years in the western United States. The changes are evident in the timing of spring runoff (Stewart 2009), in the fraction of rain versus snow (Knowles et al. 2006), in the amount of water contained in the snow (Mote 2003), in the fraction of annual streamflow throughout the year (e.g. Hidalgo et al. 2009 found that the March fraction of annual streamflow has increased while the April July fraction of annual streamflow has decreased), and in climate-sensitive biological variables (Cayan et al. 2001). It is thought that these changes are related mainly to temperature increases as they affect snowmelt-dominated basins in ways predicted in response to warming (Mote 2003), and it is suspected that the warming trends causing the changes are in part due to anthropogenic effects. Recent studies have shown that snowpack volumes and snowmelt runoff have varied with climate on many temporal and spatial levels (Zhang et al. 2007), but recent global surface temperature increases due to anthropogenic greenhouse gas emissions are now well recognized along with their potential implications on the hydrologic system.

In this study, two methods are used to quantify spring snowpack and snowmelt.

The first method is an averaging method that uses the STA/LTA algorithm, which is a short time running average divided by a long time running average. This method can be used to pick events out of time series data based on a threshold level (Wong et al. 2010). The use of this moving time-averaging method is necessary for a quantitative analysis of river discharge and SWE data because it mathematically calculates ratios without an inherent subjectivity. Additionally, with an event detector such as this, we can make proper decisions regarding water quality linked to events of interest and other management concerns (Cayan et al. 2001). The second method is a cross-correlation to analyze the similarities and differences between snowpack and spring snowmelt runoff. Lag times between peaks are also calculated in order to determine if the timing of snowmelt runoff has shifted in the last 30 years, how sensitive the Rio Grande Catchment is to mountain snowpack runoff, and if the lag time between peak snowpack and peak river discharge has also shifted in the last 30 years.

Each year, the National Weather Service and the Soil Conservation Service issue monthly forecasts of the streamflow that can be expected during the main runoff period, April through July, for much of the western United States (Redmond and Koch 1991). These forecasts are mostly based on the existing snowpack but also on expected future precipitation. They are used extensively throughout the western United States to develop reservoir operation plans for flood control and water supply plans; in turn, decisions regarding the management of many agricultural operations are also based on expected water availability (Graf 2006 and Walton and Hunter 2009). The importance of these predictions indicates the economic implications of improved estimates of snowpack and spring runoff.

Redmond and Koch (1991) suggest that the confidence interval on a water supply forecast made very early in the water year (e.g. October or November) might be increased by as much as 15% due to climate change. It is for this reason that it is

better to make predictions later in the water year. These late predictions may not give water managers sufficient time to make critical decisions regarding water use. Thus, it is important to accurately quantify the high correlation between snowpack and spring runoff (Krishna 2005).

Others have used various methods to quantify event data from hydrologic time series (e.g. Guralnik and Srivastava 1999, Smith et al. 1998, and Hamed 1998), but Norbiato et al. (2007), for instance, use the index variable method to do regional frequency analyses, allowing them to use data from nearby or similar sites to estimate quantiles of the underlying variable at their given sites. They find that attributing a single return period to a storm event is not realistic and that using a traditional rain gauge network can be too sparse to provide adequate sampling (radar data can give an advantage over actual rain gauge data (Delrieu et al. 1997 and Velasco-Forero et al. 2009)). Despite these findings, standard gauges can be used for the analysis presented here since we are studying events rather than entire volumes of precipitation for a given watershed.

Guralnik and Srivastava (1999) use a modeling approach to detect a change point by detecting the change of a model (or the parameters of the model) that describe the underlying data, and Smith et al. (1998) use wavelets to identify transient features to quantify the temporal variability of streamflow. Their study estimates precise locations of both stochastic and periodic events in time that revealed subtle structures not seen in time series data. Hamed (1998) then went on to use the Mann-Kendall test to detect trends in hydrological data. Since the test is not overly sensitive to outliers, it is accepted as a decent statistical method for hydrology.

Given the previous work, it has been recognized that further analyses and correlations will be useful information for water management techniques. The magnitude of a given peak, plus its time, are the two most important features of a hydrograph (Jain and Indurthy 2003), so those are the parameters that are analyzed here.

2.2 Methods

In this analysis, we analyze National Resource Conservation Service (NRCS) SNOTEL (for SNOwpack TELemetry) data at the Quemazon site in New Mexico from the NRCS website (`http://www.wcc.nrcs.usda.gov/snow/`). The site number is 708, the county is Los Alamos, the latitude is 35 deg 55 min N, the longitude is 106 deg 24 min W, and the elevation is 9500 feet (Figure 2.1). The daily data, including snow water equivalent (SWE), precipitation, various air temperature quantities, and snow depth were downloaded from January 1981 through May 2010. The parameter of interest for this study is the SWE, measured in inches. To measure this parameter, a snow pillow is positioned so that it measures the water-content of the snow covering. The working principle of the sensor is based on the detection of the hydrostatic pressure caused by the layer of snow (Peterson et al. 2000). This SNOTEL site is located north of the USGS stream gauge monitoring river discharge for this project (Figure 2.1).

Additionally, we also analyze United States Geological Survey (USGS) stream gauge data from the USGS website (`http://water.usgs.gov/`) at the Rio Grande at Otowi Bridge site in New Mexico. The site number is USGS 08313000, the county is Santa Fe, the latitude is 35 deg 52 min 28.2 sec, the longitude is 106 deg 8 min 32.8 sec, and the elevation is 5488 feet (Figure 2.1). The daily data, including river discharge, were downloaded from January 1981 through May 2010. Historically, the Otowi gauge used several different types of instruments, but the technology today is the following: The stream channel cross section is divided into numerous vertical subsections and in each subsection the area is obtained by measuring the width and depth of the subsection, and the water velocity is determined using a current meter. The discharge in each subsection is computed by multiplying the subsection area by the measured velocity. The total discharge is then computed by summing the discharge of each subsection. This site is located south of the NRCS SNOTEL site

used for this project (Figure 2.1).

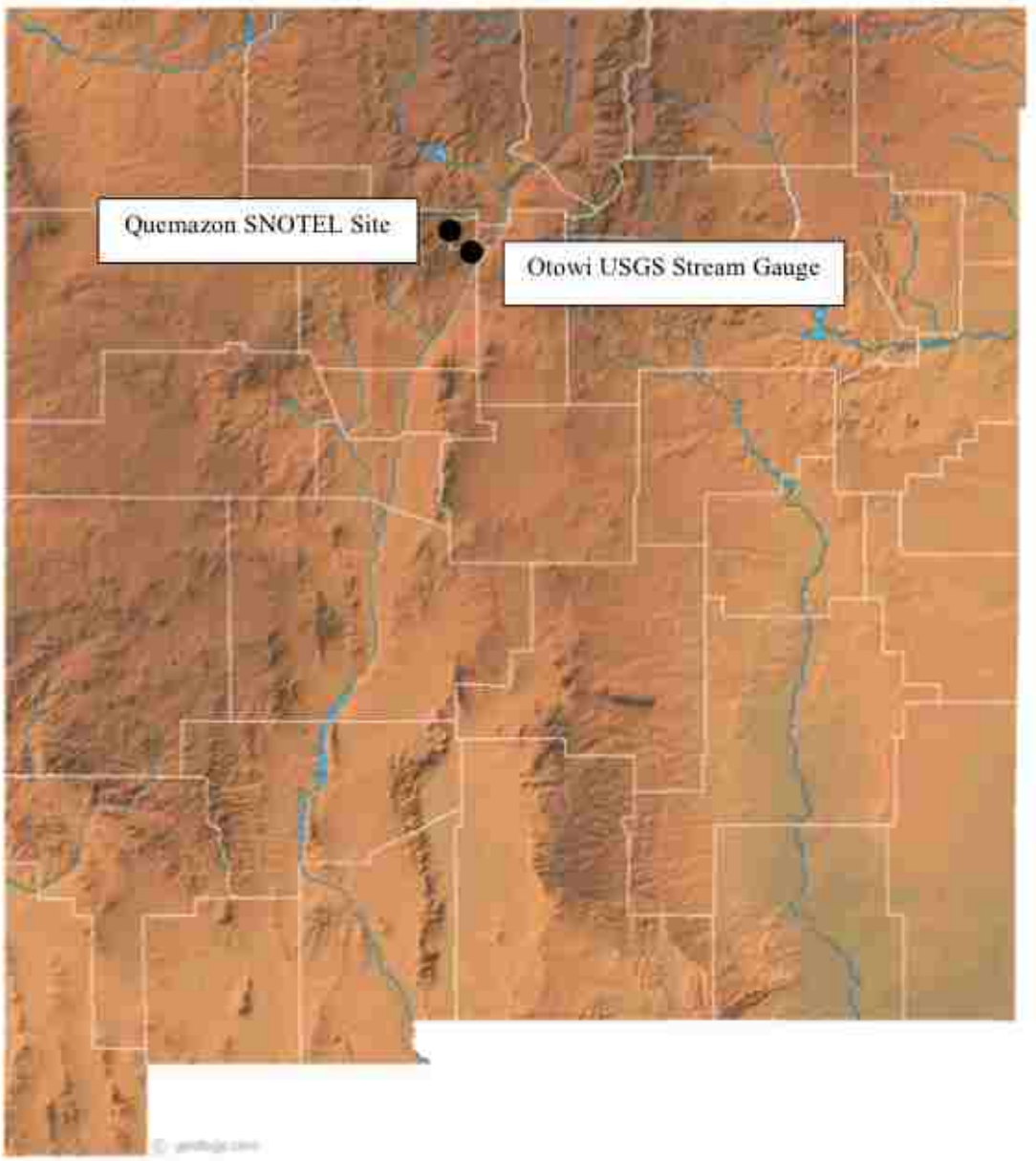

Figure 2.1: New Mexico map depicting the NRCS SNOTEL site at Quemazon and the USGS stream gauge site at the Otowi Bridge.

2.2.1 STA/LTA

The first step of the moving average analysis is to calculate short term averages (STA) and long term averages (LTA). Let x_i be the time series representing either river discharge or SWE data. Let the number of points in a short term window be ns and the number of points in a long term window be nl with $nl > ns$. Then the average values in the short term and the long term windows preceding the index i are as follows:

$$STA = \frac{1}{ns} \sum_{j=i-ns}^{i} x_j^2 \tag{2.1}$$

$$LTA = \frac{1}{nl} \sum_{j=i-nl}^{i} x_j^2 \tag{2.2}$$

If $j <= 0$, set $x_j = (x_1 + x_2)/2$ (Wong et al. 2010). We can then define the STA/LTA ratio:

$$r_i = \frac{STA}{LTA} \tag{2.3}$$

For both the river discharge and the SWE calculations, $ns = 100$ and $nl = 400$. These values are determined by optimizing the length of the data set with the length of the yearly discharge event peaks. It is not surprising that the ns and nl values for both data sets are the same, given the facts that both data sets are daily and of the same number of years. To calculate the STA/LTA, the "filter" function is utilized in Matlab. This function filters the original time series data by the ns and nl values, giving a smoothed, averaged value. The STA/LTA is then plotted for each original data point of the time series data. A threshold value is also set in order to make a quantitative cut-off point of significant events. Based on the moving average, the threshold value is set at $r_i = 1$ for discharge and $r_i = 1.5$ for SWE. This is determined

through careful exploration of average values among the years (i.e. percentages of points falling above and below the cut-off).

2.2.2 Cross Correlation

To perform the cross correlational analysis, the following procedure is employed for both the discharge data and the SWE data. To find an "average year," each annual peak is shifted to an arbitrary time scale. This allows us to normalize the data for lag time. For example, if we simply averaged each block of 365 days, there would be some years with an earlier peak and some years with a later peak. These off-years would not be included in the average and thus would not be fully represented. The goal is to see the peak of data without initially looking at the timing of the event. Once each year's maximum peak event is overlaid on the other peaks from the 30 year data set, one average year can be determined. This information is plotted as both a 2D and a 3D plot.

The Matlab function "xcorr" is used to shift each year's peak of data through the following sequence:

$$r(d) = \frac{\sum_i [x(i) - mx * (y(i-d) - my]}{\sqrt{\sum_i (x(i) - mx)^2} \sqrt{\sum_i (y(i-d) - my)^2}} \tag{2.4}$$

where $x(i)$ and $y(i)$ are the two data sets being compared, mx and my are the respective means, and d is the delay. If we assume mx and my to be zero, we have the following:

$$r(d) = \frac{\sum_i [x(i) * (y(i-d)]}{\sqrt{\sum_i (x(i))^2} \sqrt{\sum_i (y(i-d))^2}} \tag{2.5}$$

To figure the lag times associated with the correlations, a series of delays (d) are run through the above equation and the maximum value is determined. This is equal to the lag time. This function computes raw correlations without normalization, so a separate process is then employed to normalize the calculations. To do this, a cross correlation is performed between the average year and each separate year, the average year with itself, and each separate year with itself. The aforementioned 3 cross correlations are then compared. This allows us to determine the normalized correlation between each year and the average year previously determined. These calculations also allow us to determine the lag time between each year's peak and the average year's peak. The correlations are then plotted as time series to see the correlation of each year's peak to the average year's peak. Additionally, the lag times are plotted as a time series to see the time difference between each year's peak and the average year's peak (with the mean removed to normalize the data).

To then see the correlation and the lag times between each SWE peak and the consecutive river discharge peak, a cross correlation is performed between each seasonal peak (i.e. each SWE peak versus its corresponding discharge peak). This allows us to see how, exactly, each year's SWE data relates to the following spring's river discharge. We then plot a time series graph for both the correlations and the lag times. Finally, to see how the lag times and the correlations compare among both the SWE peaks and the river discharge peaks, a plot is created to compare the correlations of each SWE year to the average SWE year versus the correlations of each river discharge year to the average river discharge year. Additionally, another plot is created to compare the lag times of each SWE year from the average SWE year versus the lag times of each river discharge year from the average river discharge year.

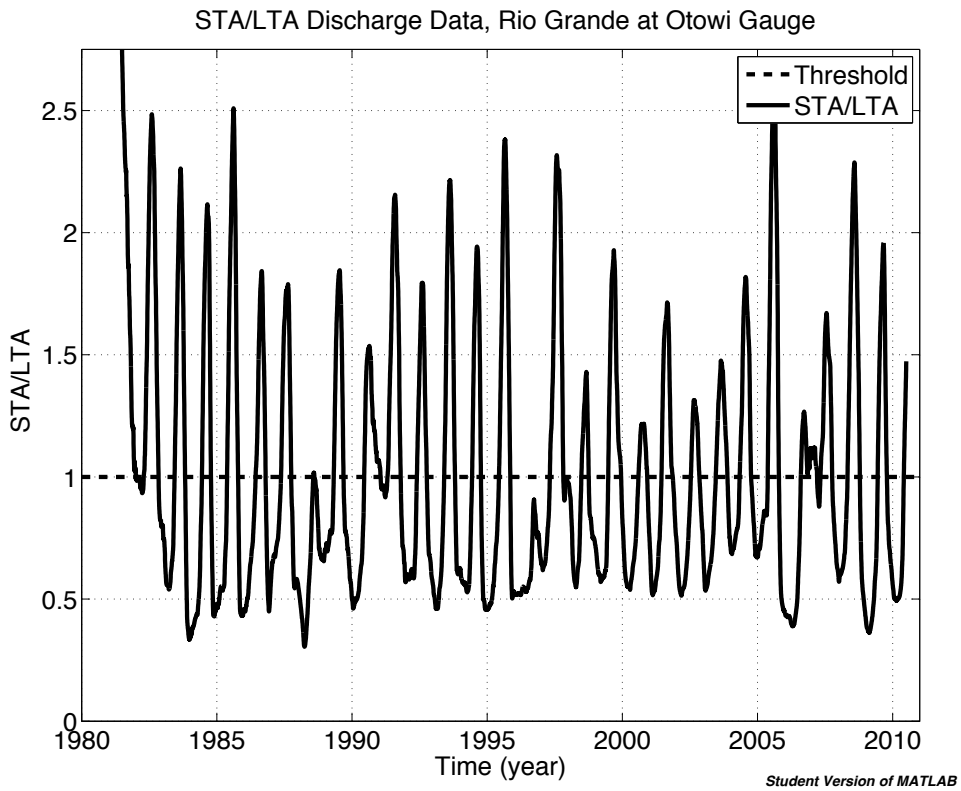

Figure 2.2: Short term average over long term average of Rio Grande discharge data at the Otowi Gauge, 1981-2010. The threshold for a significant peak on the discharge STA/LTA is 1.

2.3 Results

STA/LTA values are plotted for both the Rio Grande discharge data and the SWE data. These are presented in Figures 2.2 and 2.3, respectively. The ratio is on the vertical axis and time is on the horizontal axis. The threshold values are also plotted on each graph. The threshold for a significant peak on the discharge STA/LTA is 1 while the threshold value for the significant peak on the SWE STA/LTA is 1.5.

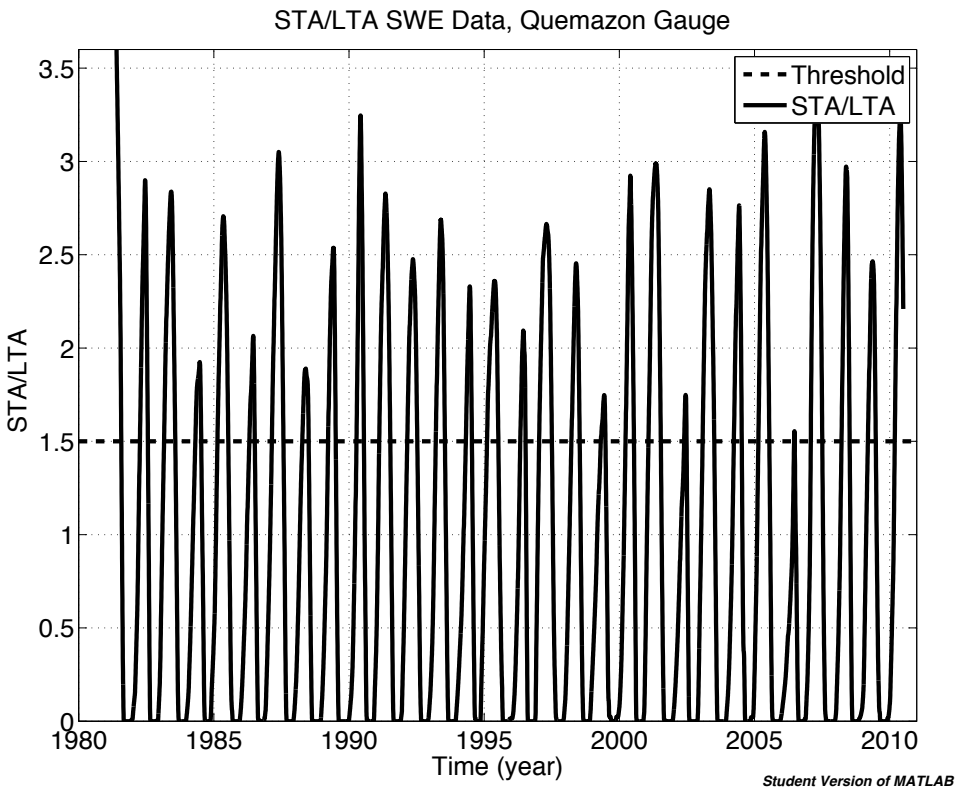

Figure 2.3: Short term average over long term average of snow water equivalent data at the Quemazon Gauge, 1981-2010. The threshold for a significant peak on the SWE STA/LTA is 1.5.

To view the average discharge year with each individual year peak, a plot is created with the shifted yearly peaks, as mentioned in the methods section. Figure 2.4 shows the average discharge peak with each of the other years' discharge peaks shifted to a generic time scale. The importance of the plot is the discharge peak value, not the time that the peak occurs. Figure 2.5 is a surface plot that shows each year's peak discharge shifted to the generic time scale. Discharge values are shown through a color bar as well as on a third axis. Trends over the 30 year time period can be seen.

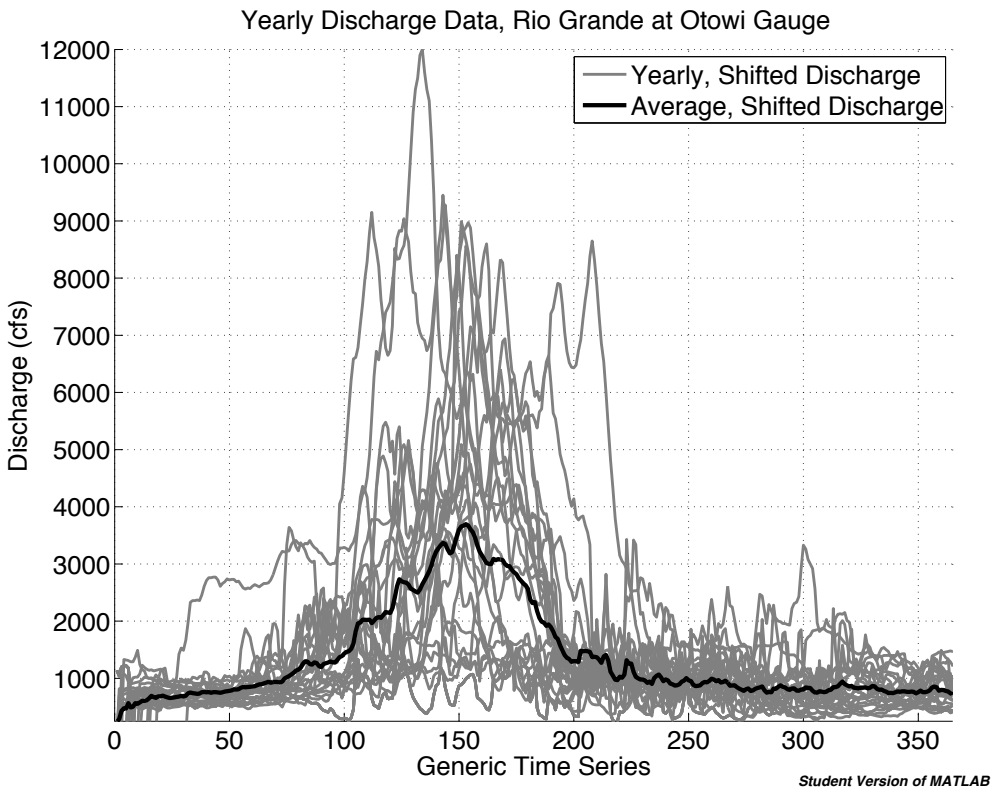

Figure 2.4: Average discharge peak and each individual discharge peak, shifted to a generic time scale for the Rio Grande discharge data at the Otowi Bridge, 1981-2010, measured in cubic feet per second.

To view the average SWE year with each individual year peak, a plot is created with the shifted yearly peaks, as mentioned in the methods section. Figure 2.6 shows the average SWE peak with each of the other years' SWE peaks shifted to a generic time scale. The importance of the plot is the SWE peak value, not the time that the peak occurs. Figure 2.7 is a surface plot that shows each year's peak SWE shifted to the generic time scale. SWE values are shown through a color bar as well as on a third axis. Trends over the 30 year time period can be seen.

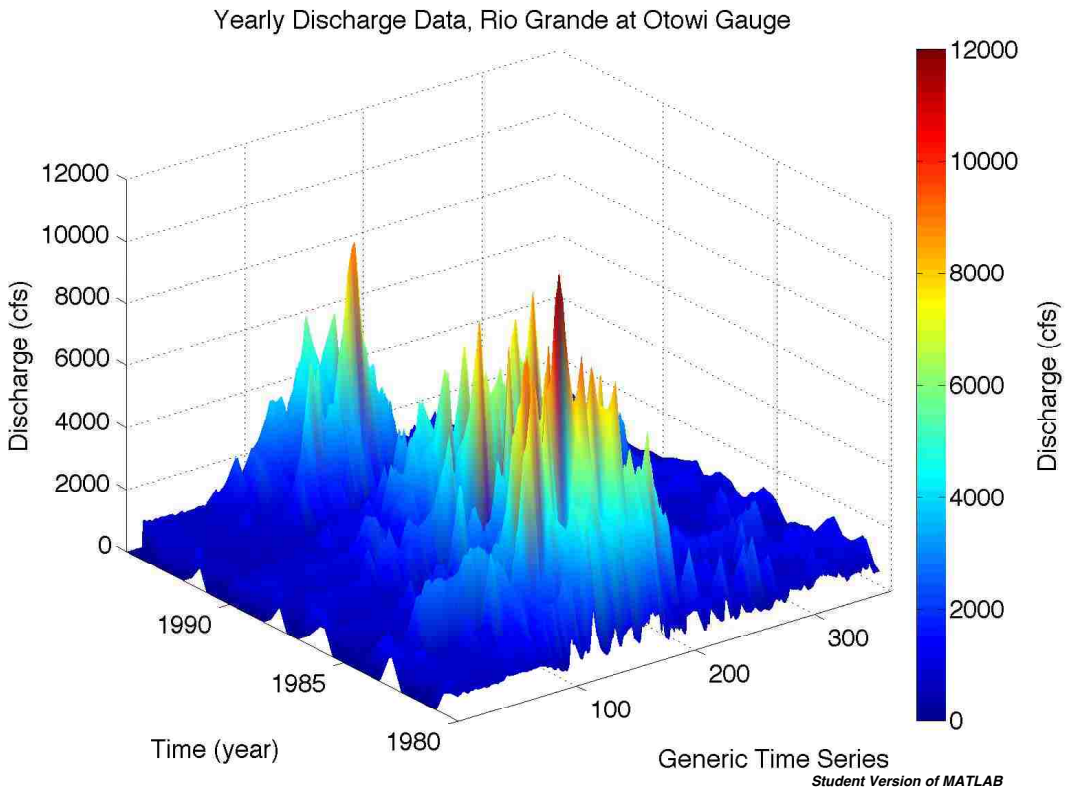

Figure 2.5: Each individual discharge peak, shifted to a generic time scale for the Rio Grande discharge data at the Otowi Bridge, 1981-2010, measured in cubic feet per second.

Several other relationships are plotted in Figures 2.8, 2.9, 2.10, and 2.11: the correlation of each year's discharge peak with the average discharge peak, the time difference of each year's discharge peak with the average discharge peak, the correlation of each year's SWE peak with the average SWE peak, and the time difference of each year's SWE peak with the average SWE peak.

The correlations are then calculated and plotted for each SWE peak and its corresponding discharge peak (Figure 2.12) where the normalized correlations are

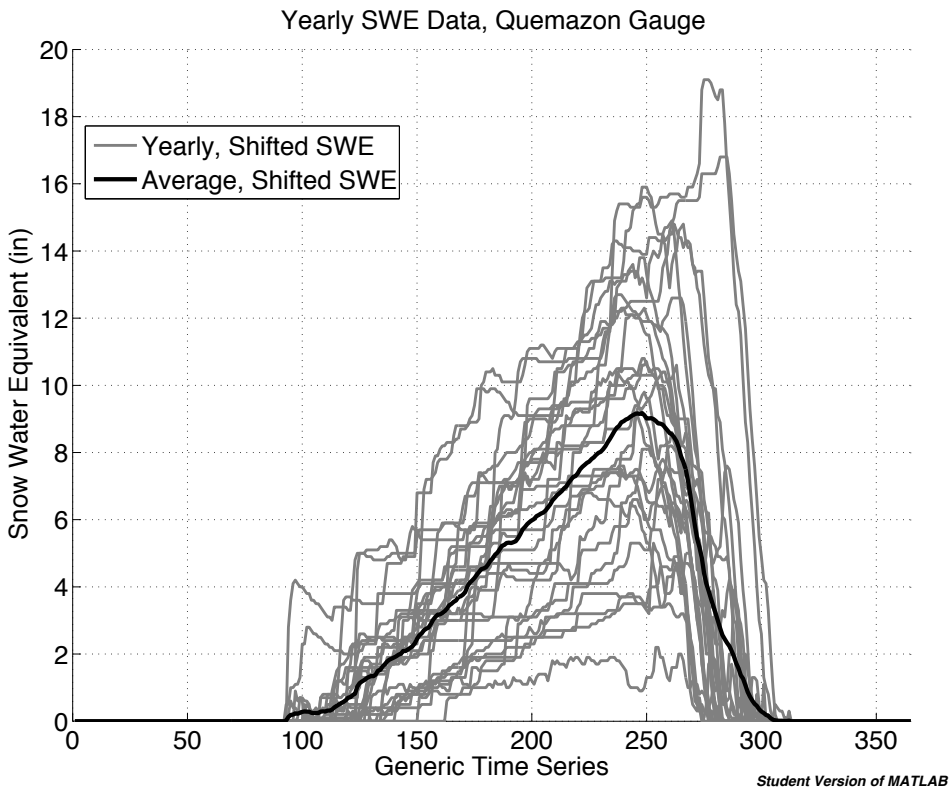

Figure 2.6: Average snow water equivalent peak and each individual snow water equivalent peak, shifted to a generic time scale for the SWE data at the Quemazon gauge, 1981-2010, measured in inches.

plotted on the vertical axis and the years are plotted on the horizontal axis. The lag times are then calculated and plotted for each SWE peak and its corresponding discharge peak (Figure 2.13) where the lag times are plotted on the vertical axis and the years are plotted on the horizontal axis.

To see the correlations between each year and the average year of both the discharge data and the SWE data, a plot is created with the normalized SWE correlations on the vertical axis and the normalized discharge correlations on the horizontal

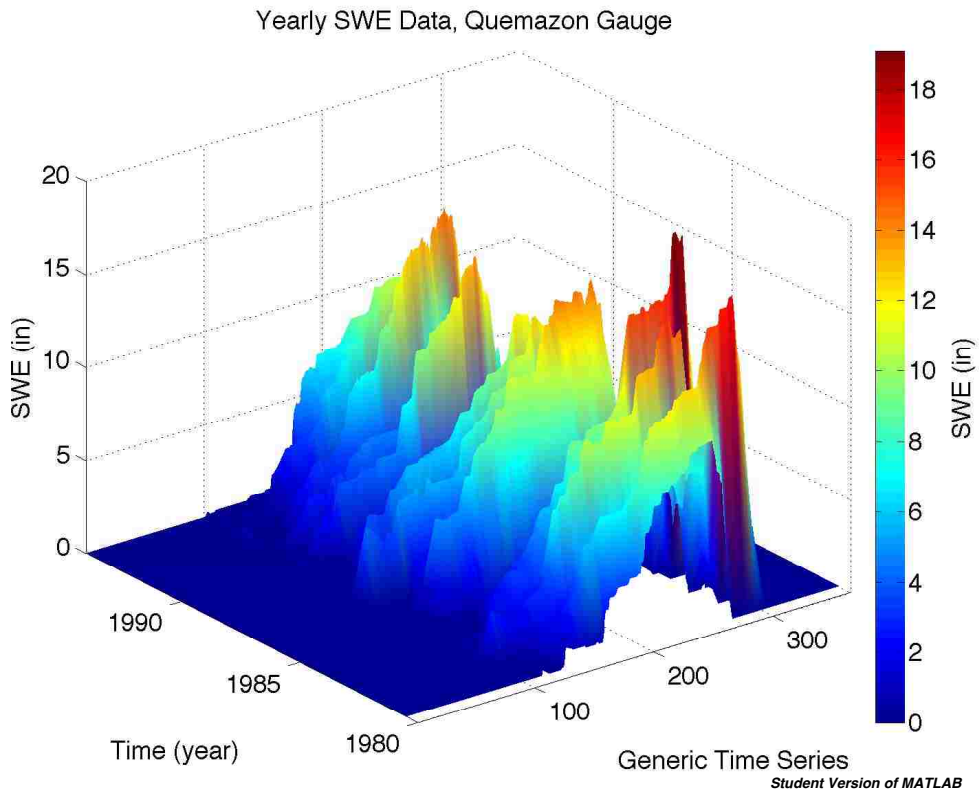

Figure 2.7: Each individual snow water equivalent peak, shifted to a generic time scale for the SWE data at the Quemazon gauge, 1981-2010, measured in inches.

axis (Figure 2.14). To see how the lag times between each year and the average year of both the discharge data and the SWE data, another plot is created with the normalized SWE lag times on the vertical axis and the normalized discharge lag times on the horizontal axis (Figure 2.15).

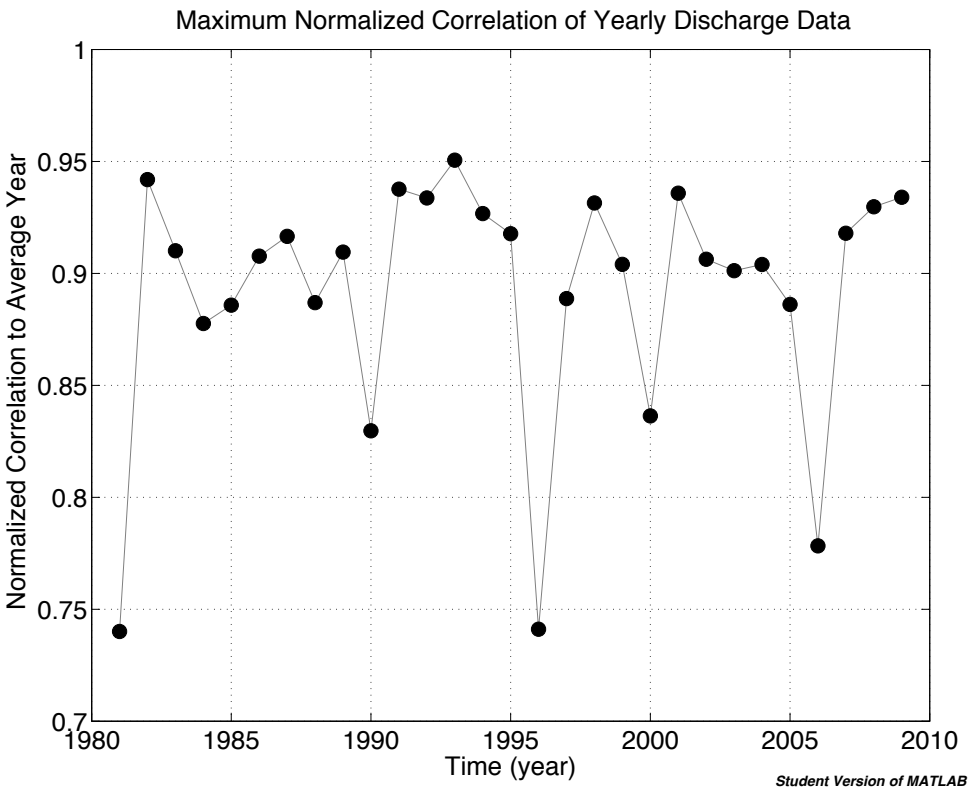

Figure 2.8: Normalized correlation between each year's discharge peak and the average discharge peak. Data are from the Rio Grande Otowi gauge.

2.4 Discussion

In this study, two methods are used to quantify spring snowpack and snowmelt. The first method is an averaging method that uses the STA/LTA algorithm. This method is used to pick events out of time series data based on a threshold level (Wong et al. 2010). Interannual variability is clearly visible in the time series data of both river discharge and SWE so the STA/LTA method allowed us to smooth the data into detecting events of significance. Figure 2.2 shows that there was a significant amount

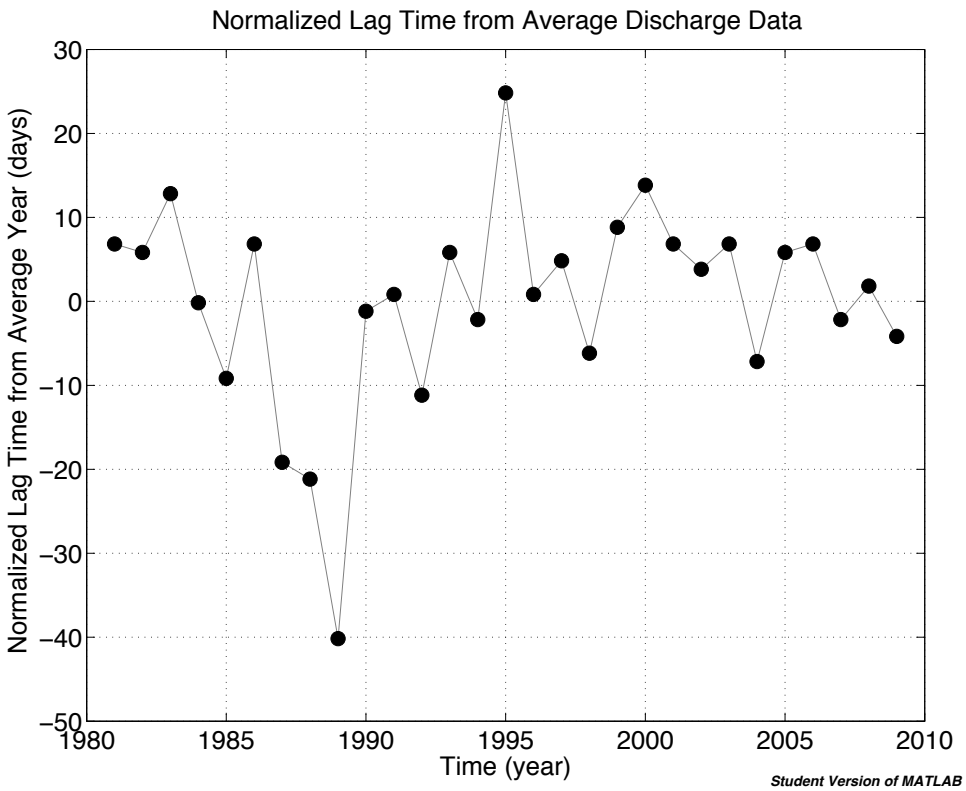

Figure 2.9: Normalized lag time between each year's discharge peak and the average discharge peak. Data are from the Rio Grande Otowi gauge.

of discharge in most years, but there were a few dry years within the 30-year data set (e.g. 1988 and 1996). The drought in 1988 was part of a drought that covered 36% of the United States and had a large effect on crop production (Riebsame et al. 2001), while the drought in 1996 covered much of Texas, New Mexico, California, Nevada, Utah, Colorado, Oklahoma, and Kansas. The depletion of ground water during both of these years affected the ecosystem for many years (Reuters 1996).

Figures 2.4, 2.5, 2.6, and 2.7 show the shifted yearly peaks with the average peaks on a generic time scale, for both river discharge and snow water equivalent,

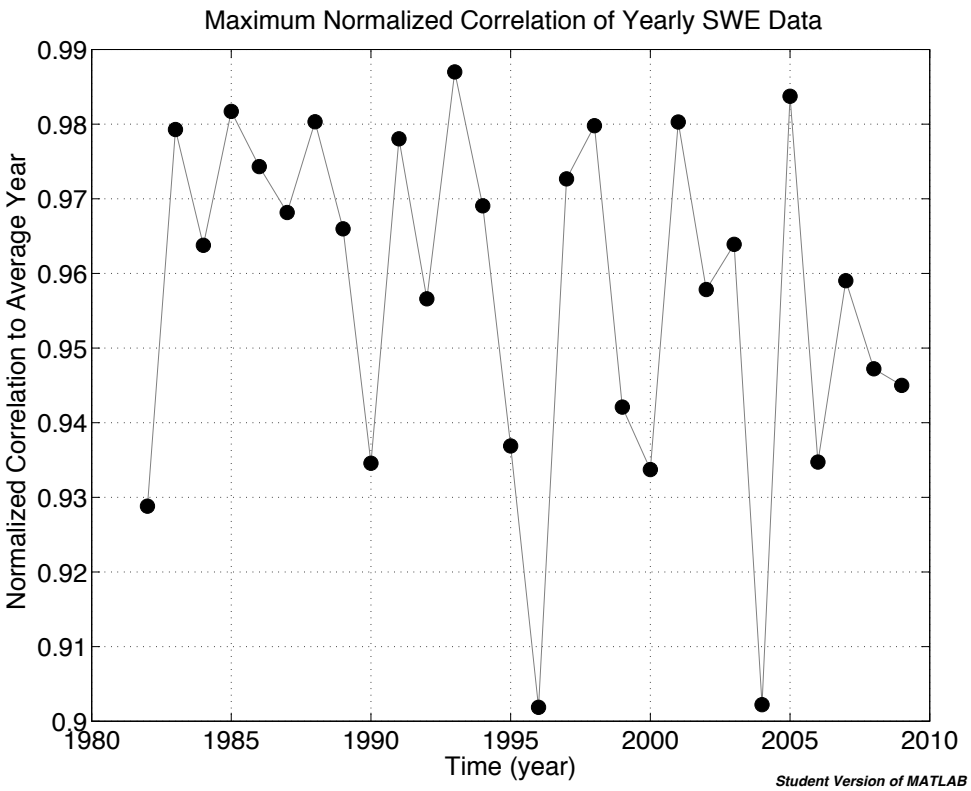

Figure 2.10: Normalized correlation between each year's SWE peak and the average SWE peak. Data are from the Quemazon gauge.

respectively. The importance of the plots is the peak values in the respective units, not the time that the peaks occurred. Due to the interannual variability of river discharge and SWE, the peaks appear diverse, which allows a further analysis of each peak's correlation and time lag in relation to the average peak as seen in the figure. Figures 2.4, 2.5, 2.6, and 2.7 also show each year's peak shifted to the generic time scale, which gives a nice visual representation of the variability over time. For instance, there are several large peaks earlier in the data sets that are not in the later part of the data sets. These results indicate a general decrease in both

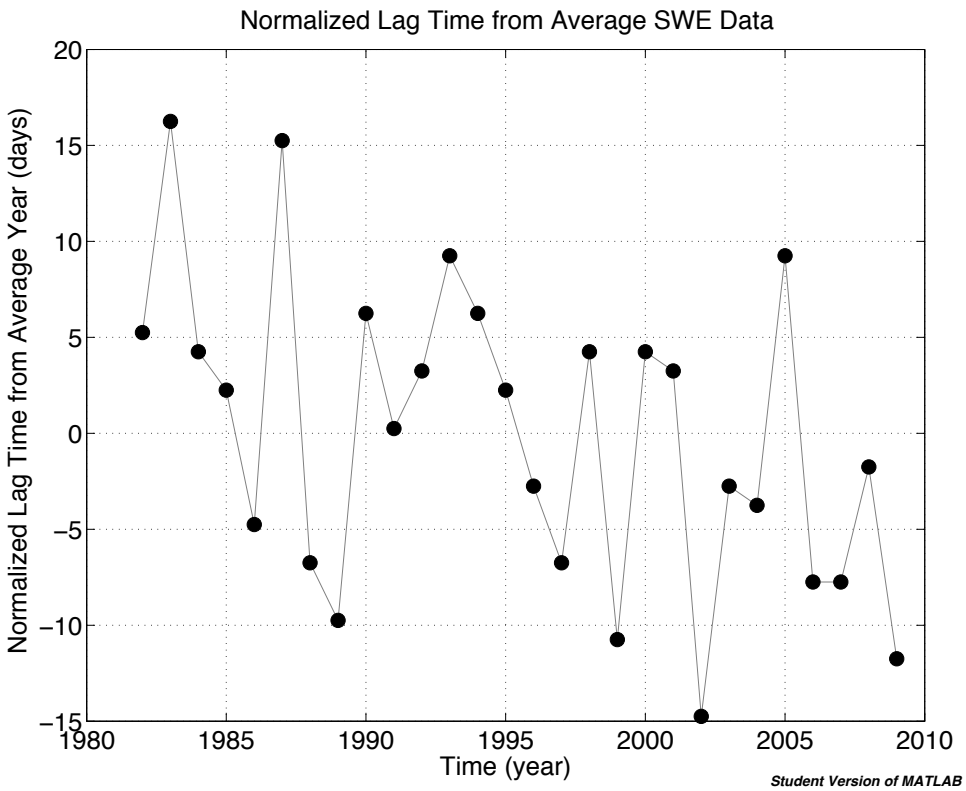

Figure 2.11: Normalized lag time between each year's SWE peak and the average SWE peak. Data are from the Quemazon gauge.

peak discharge and peak SWE over time.

In order to see the correlation of each year's discharge peak with the average discharge peak, a time series plot is created (Figure 2.8), which shows that the correlations may have a subharmonic throughout time. There is a weak oscillation among the 30 years that would have to be further studied before any conclusions can be drawn. Each year's discharge peak has a correlation of at least 0.7 with the average discharge peak, meaning that most years are similar to each other and thus the average year. Figure 2.9 shows the difference in time between each individual

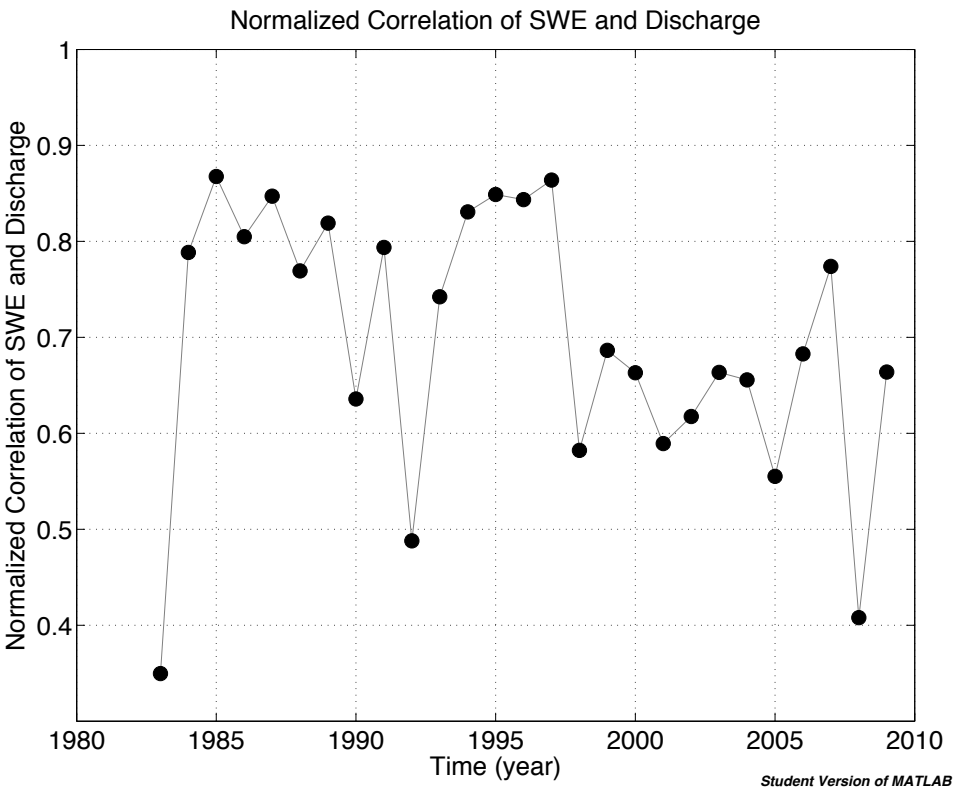

Figure 2.12: Normalized correlation between each year's SWE peak and the corresponding discharge peak. Data are from the Rio Grande at the Otowi Bridge gauge (river discharge) and the Quemazon gauge (snow water equivalent).

year of discharge data with the average discharge curve. The lag times seem to fluctuate around the zero line, with a big, distinct drop in the late 80s. In the years that have a positive lag time, the peak in discharge is actually later than average, and in the years that have a negative lag time (e.g., 1987, 1988, and 1989), the peak in discharge is actually earlier than the average. Given the drought of 1988 (Riebsame et al. 1991), the discharge that year is smaller and earlier than other years in the data set.

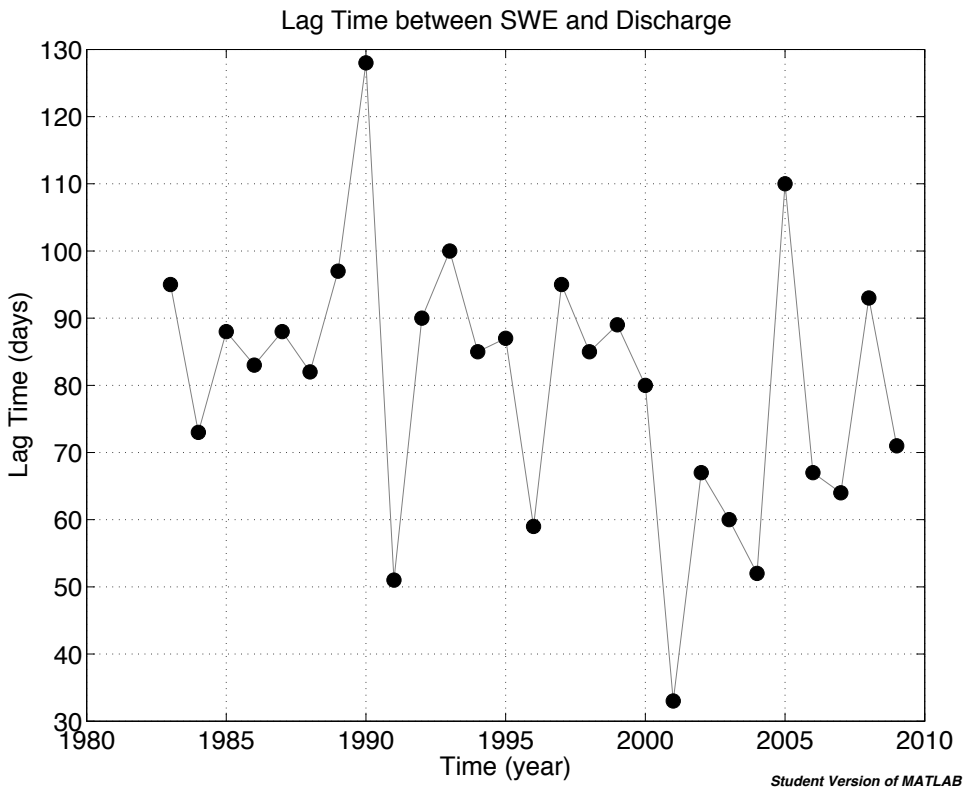

Figure 2.13: Lag times between each year's SWE peak and the corresponding discharge peak. Data are from the Rio Grande at the Otowi Bridge gauge (river discharge) and the Quemazon gauge (snow water equivalent).

Figure 2.10 presents the correlation of each year's SWE peak with the average SWE peak, and shows that the correlations may have subharmonic throughout time (perhaps every 8 years). There is a weak oscillation among the 30 years that would have to be further studied to make a conclusion. Each year's SWE peak has a correlation of at least 0.9 with the average SWE peak, meaning that the yearly SWE is quite consistent. Figure 2.11 shows that during the beginning of the data set, there are positive lag times between the yearly SWE peaks and the average SWE peak, but over time, this value switches to be primarily negative. Having a negative lag time

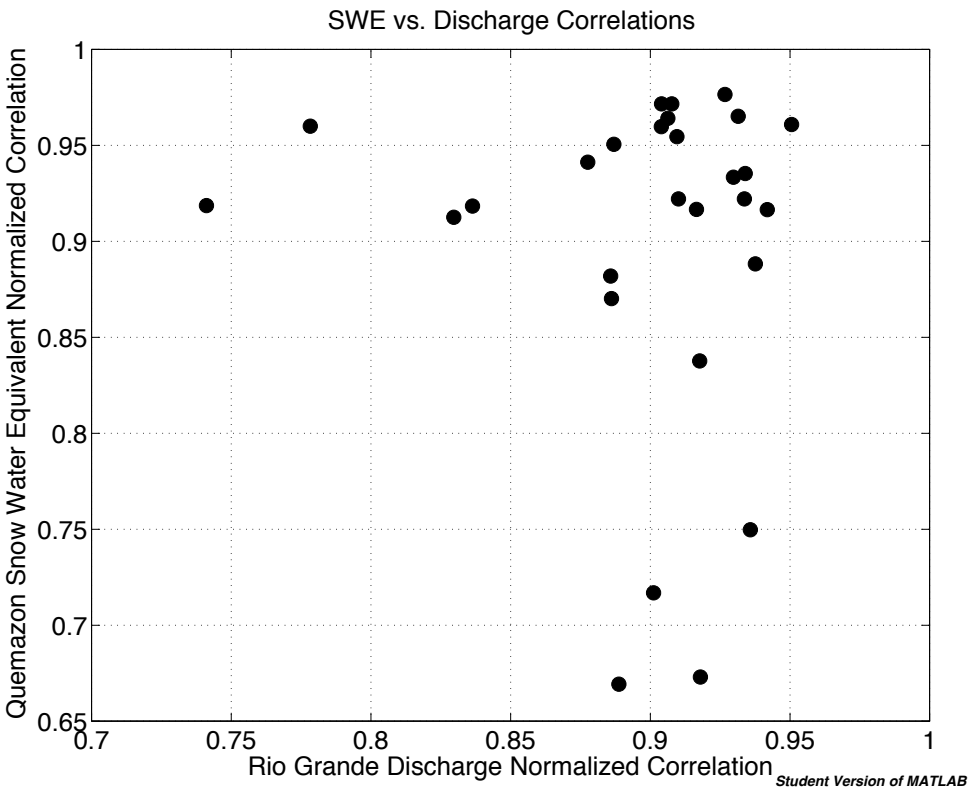

Figure 2.14: Snow water equivalent correlations between each SWE year and the average SWE year versus discharge correlations between each discharge year and the average discharge year.

means that the SWE peaks are becoming earlier in the year. SWE peaks are being seen earlier in the year, showing evidence for the hypothesis that water will have to be stored for longer periods of time given this shift. If this trend continues, the biological organisms around the Rio Grande will be forced to change their reproductive cycles to match the river system, potentially having adverse affects while the species adapt.

Figure 2.12 shows the correlation between each winter's SWE peak and each spring's discharge peak, in an attempt to see the close relationship between the two.

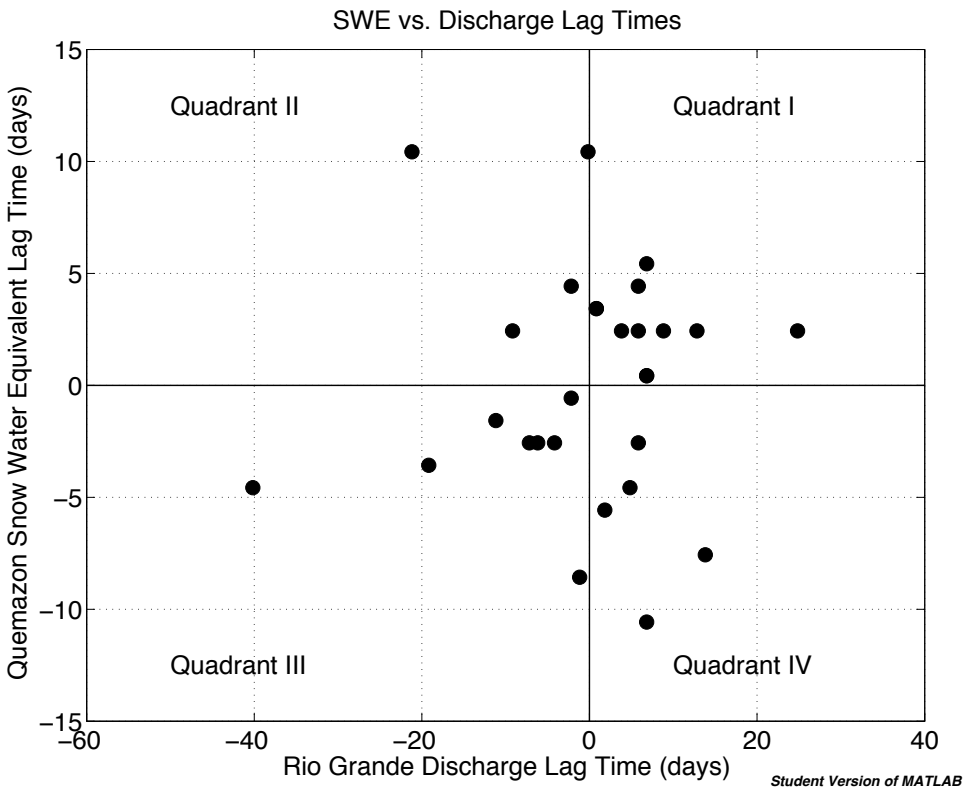

Figure 2.15: Snow water equivalent lag times between each SWE year and the average SWE year versus discharge lag times between each discharge year and the average discharge year.

The correlations range from 0.3 to 0.9, meaning that there is a high correlation in some years but not in all. This leads us to the conclusion that there are multiple other factors affecting river discharge. The STA/LTA analysis also hints at this on/off relationship, but it is apparent here. The groundwater and surface water relationship most likely has a high effect on this system (Wang et al. 2008), in addition to other anthropogenic forcings (Burkholder 1997).

In the same manner that the correlations between each winter's SWE peak and

the corresponding spring's discharge peak are not uniformly strong, neither are the lag times between each winter's SWE peak and the corresponding spring's discharge peak. The time between the 2 peaks for each year ranges from 30 to 130 days (Figure 2.13). In 1990, there is an unusually high lag time between the winter's peak in SWE and the spring's river discharge (128 days), which could indicate a colder-than-normal spring and in 2001 there is an unusually low lag time between the winter's peak in SWE and the spring's river discharge (33 days), which could indicate a warmer-than-normal spring.

Additionally, to see how the correlations compare among both the SWE peaks and the river discharge peaks, Figure 2.14 compares the correlations of each SWE year to the average SWE year versus the correlations of each river discharge year to the average river discharge year. This figure shows that, in general, when there is a high correlation between the SWE peak and the average SWE peak, there is also a high correlation between the yearly discharge peak and the average discharge peak. Although there are several years where there is a high SWE correlation with a low discharge correlation and several years where there is a high discharge correlation with a low SWE correlation, in general, most correlations are high for both SWE and discharge. The years with a high SWE correlation and a low discharge correlation (upper left hand corner of Figure 2.14) and the years with a high discharge correlation and a low SWE correlation (lower right hand corner of Figure 2.14) give us indication that other factors are at play in river discharge values. Rainfall and temperatures could have played a role with these outliers. It is interesting to see that none of the years had both a low SWE correlation and a low discharge correlation, indicating that the overarching factors of SWE and discharge are strongly related.

A comparison of the lag times of each SWE year from the average SWE year versus the lag times of each river discharge year from the average river discharge year (Figure 2.15) shows that some of the years in this 30 year data set have both a

positive SWE lag time and a positive discharge lag time, meaning that these years have peaks later than the average year for both SWE and discharge (Quadrant I). Just a few years have a positive SWE lag time and a negative discharge lag time, meaning that these years have a later-than-normal SWE peak but an earlier-than-normal discharge peak (Quadrant II). Still other years have negative lag times for both the SWE peak and the discharge peak, meaning that these years have an earlier-than-normal SWE peak and an earlier-than-normal discharge peak (Quadrant III). The final grouping of data has a positive discharge lag time and a negative SWE lag time, meaning that these years have an earlier-than-normal SWE peak and a later than normal discharge peak (Quadrant IV).

Quadrants I and III show the same-sided correlation between SWE and river discharge, meaning that the lag times are either both positive or both negative. If both lag times are positive, the peaks occur after the average peak, but if both lags are negative, the peaks occur before the average peak. With the SWE peak analysis, it is shown that the peak occurs after the average peak in the early part of the data set, but in recent years the peak occurs before the average peak. Quadrants II and IV show us that there are other factors at play in the system, such as groundwater and other anthropogenic forcings.

The analysis presented here allows us to answer several questions regarding snowpack and snowmelt but also raises others. It is found that the peak in snowmelt is occurring earlier in the year and that there is generally a high correlation between SWE and discharge. Future studies will need to analyze yearly data with an STA/LTA event detection. This will allow us to see events smaller than the annual cycle, pulling further information out of the data being collected. From this and other studies of the Rio Grande (e.g. Vivoni et al. 2009), proper management decisions can be made. Ideally, management will focus on restoring river processes, allowing the biological communities to naturally adjust to the system (Hanson et al.

2004).

Chapter 3

Effects of soil moisture and temperature on NM decomposition potential

3.1 Introduction

Understanding the impact of changing climate on local ecosystems is one of the most important and challenging tasks of the 21st century. During the 100 years from 1906 to 2005, the accumulation of greenhouse gases in the atmosphere has increased global surface temperatures between 0.56 and 0.92°C, with concurrent changes in local precipitation patterns including extreme weather events, which have likely changed in frequency and or intensity (IPCC 2007). At present, the terrestrial ecosystem is thought to be a significant sink for atmospheric carbon (C), but the future course of this sink under rising CO_2 concentrations and temperature is uncertain (Ise and Moorcroft 2006). Therefore, the heterotrophic respiration due to the decomposition of above- and below-ground plant detritus and thus pools of carbon should not be

overlooked (Jones et al. 2002). Since the amount of carbon stored in soil is estimated to be 1500 PgC (the largest pool of carbon in terrestrial ecosystems is not living organic matter but rather plant detritus and soil organic matter), approximately double as much as that in the atmosphere (Dungait et al. 2012, Gholz et al. 2000, McMurtrie et al. 2001), the potential magnitude of positive carbon feedbacks is strong. Decomposition returns nutrients to mineral forms that are needed for primary production and also transforms plant litter into humus, improving the soil quality and thus furthering the impact on carbon sequestration (Gholz et al. 2000, Moorhead and Sinsabaugh 2006, Rastetter et al. 1997).

Using a modified CENTURY model to further understand how changing climate will affect carbon cycling, specifically ecosystem respiration in the arid southwest, we analyzed a database of soil moisture and temperature assembled from 13 sites in the state of New Mexico (`http://www.wcc.nrcs.usda.gov/`, Ise and Moorhead 2006). The CENTURY model is a general model of plant-soil nutrient cycling, which has been used to simulate carbon and nutrient dynamics for different ecosystems including grasslands, agricultural lands, forests, and savannas in relation to climate, environmental factors, and land use (Parton et al. 1993, Parton 1996).

The CENTURY model is composed of a soil organic matter/decomposition submodel, a water budget model, a forest production submodel, and management and events scheduling functions (Chilcott et al. 2007). It computes the flow of carbon, nitrogen, phosphorus, and sulfur through the models compartments, and takes into account the monthly average, maximum and minimum air temperature, monthly precipitation, soil texture, plant nitrogen, phosphorus, and sulfur content, lignin content of plant material, atmospheric and soil nitrogen inputs, and initial soil carbon, nitrogen, phosphorus, and sulfur contents (Bolker et al. 1998).

The soil organic matter submodel includes three soil organic model pools (active, slow, and passive, with the decomposition term of interest being directly proportional

to the slow/passive pool of carbon: $C_{slow}\alpha \int A(t)$, where C_{slow} is the slow/passive pool of carbon, A is the decomposition term, and t is time). The slow/passive pool contains chemically recalcitrant materials derived from the transformed structural soil pool. A is the intrinsic decomposition rate for the slow/passive soil organic carbon (SOC) pool but as in the original CENTURY model, we assume that the environmental dependencies of the decomposition rates of all three pools are identical. The slow and passive pools are the largest reservoirs of carbon and have the most influence on long-term carbon sequestration in soil, since these pools function on very long time scales (Bolker et al. 1998). The submodel also includes different potential decomposition rates for each pool (focusing on the slow/passive pool in this study), above and below ground litter pools, and a surface microbial pool, which is associated with decomposing surface litter. The simplified water budget model calculates monthly evaporation, transpiration, the water content of the soil layers, snow water content, and saturated flow of water between soil layers, assuming that maximum plant production rates are controlled by temperature and moisture, but limited by nutrients if necessary (Finzi et al. 2007, Ise and Moorcraft 2006). As in many terrestrial ecosystem models (Ise and Moorcroft 2006), the effects of soil texture on SOC decomposition are not represented.

Temperature has a strong influence on all biological and physiochemical processes in the soil, so effects of this variable are most studied in the framework of soil organic matter (SOM) decomposition (Jones et al. 2002, Thongjoo et al. 2005). However, controversial discussions within the scientific community show that the treatment of temperature effects is still an unresolved problem (Davidson and Janssens 2006, Neff et al. 2002). For example, Knorr et al. (2005) found higher temperature sensitivity for more stable carbon fractions, indicating that increased soil decomposition occurs at higher temperatures, thus resulting in increased carbon dioxide emissions from soils (Eliasson et al. 2005). However, Fang et al. (2005) found no significant differences between the temperature sensitivity of labile and more stable carbon,

suggesting that soil decomposition is not dependent on temperature but rather the heterogeneity of soil carbon. If the decomposition of soil labile carbon is sensitive to temperature variation but the resistant components are not sensitive to temperature variation, then this resistant carbon or organic matter in mineral soil is unresponsive to climate warming (Fang et al. 2005). The activation energy for mineralization of recalcitrant soil organic matter is greater than that of more labile material, such as litter, fine roots, and exudates, so the passive pool in theory should have the greatest relative temperature sensitivity, but other factors such as physical protection and nutrient availability also influence apparent temperature responses. In addition, some of these apparent discrepancies among studies may be related to the types of measurements used and the length of the monitoring periods (Sierra 2012).

By definition, the temperature sensitivity of SOM decomposition is the change in SOM decomposition rate with temperature under otherwise constant conditions (Fang et al. 2005), but the direct estimation of the temperature response of SOM decomposition is complicated by several compounding factors, including soil moisture (Thongjoo et al. 2005). Soil moisture content regulates several processes involved in the SOM decomposition such as the accessibility of substrates and nutrients for the microorganisms, diffusion rates, and osmotic potentials (Davidson et al. 2006, Pregitzer et al. 2008). These effects are particularly significant for aridlands because most rainfall events are small and spatially heterogeneous (Collins et al. 2008). Because of these pulse-like events, primary production and decomposition may not be closely coupled on short time scales. If decomposition potential exceeds primary production, the nutrient cycling may be more dependent on primary production than the mineralization of stored SOM (Epstein et al. 2002). Several authors have recently called for a greater understanding of microbial processes in belowground ecosystems and therefore the impacts of decomposition on carbon sequestration (e.g. Jones et al. 2002, Mansoni and Porporato 2009).

While soil moisture is of paramount importance to the carbon cycle of arid regions, such New Mexico, temporal and spatial changes in SOM quality and quantity due to inputs of fresh litter material (quality dependent on the C:N ratio, lignin content, etc., Gallo et al. 2005) or the alteration of SOM in the course of decomposition itself. Previous studies have shown that the attenuation and phase shift of both soil temperature and moisture varies with depth (Bauer et al. 2008, Jones et al. 2002, Paul 2001), again complicating the question of how soil moisture and temperature affect belowground processes.

The most common expression for the temperature sensitivity is the Q_{10} equation: $\lambda = \lambda_0 Q_{10}^{(T-T_{ref})/10}$ where λ_0 is the decomposition rate at the reference temperature T_{ref} and Q_{10} is the factor for which the decomposition rate increases for a temperature increment of 10K (Knorr et al. 2005, Vitousek et al. 2004). However, Ise and Moorcraft (2006) devised a decomposition term that is directly proportional to soil temperature and soil moisture: $A = T_d M_d$ where A is the decomposition term, T_d is the function describing the effects of temperature on the decomposition rate and M_d is the function describing the effects of moisture on the decomposition rate. In the CENTURY model, the total SOC in the grid cell is given by:

$$C_{total} = C_{met} + C_{str} + C_{slow} \tag{3.1}$$

where C_{total} is the total SOC in the grid cell and C_{met}, C_{str}, and C_{slow} are SOC densities in metabolic, structural, and slow/passive pools, respectively. The rates of change of SOC in the three pools follow:

$$\frac{dC_{slow}}{dt} = 0.7Ak_{str}C_{str} - Ak_{slow}C_{slow}, \tag{3.2}$$

$$\frac{dC_{met}}{dt} = NPP(F_{met}) - Ak_{met}C_{met}, \tag{3.3}$$

$$\frac{dC_{str}}{dt} = NPP(1 - F_{met}) - Ak_{str}C_{str}, \tag{3.4}$$

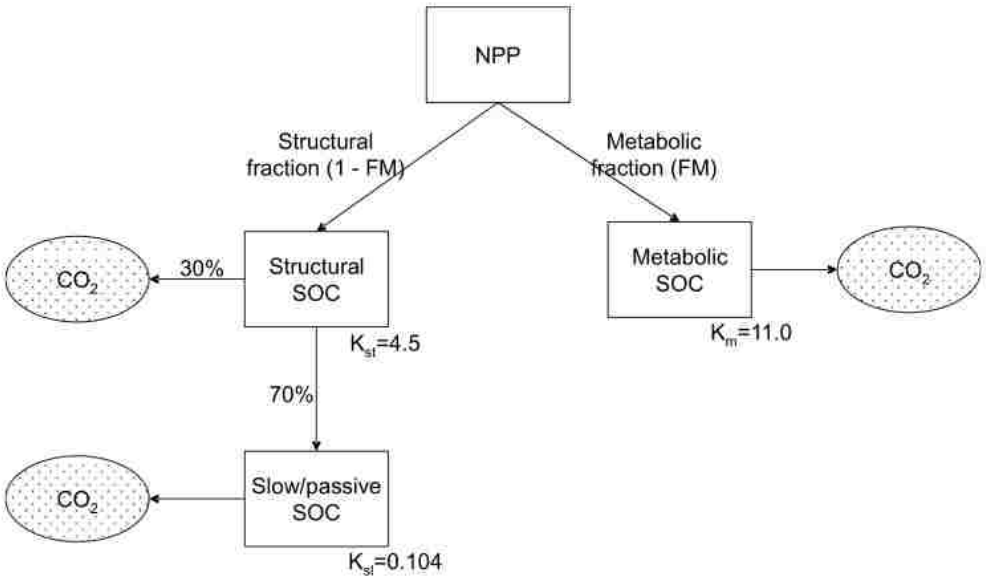

Figure 3.1: Schematic depiction of decomposition model, modified from Parton et al. (1996) and Bolker et al. (1998). NPP is assumed to be equal to the litter input for a steady state, long-term condition. Seventy percent of the Structural SOC pool is gradually transformed into the Slow/passive SOC pool. Each pool has a unique rate of decomposition.

where NPP is the total net primary productivity of the grid cell and F_{met} is a fraction by which NPP goes into the metabolic pool. The function A modifies the intrinsic decomposition rate for each SOC pool based on the temperature and moisture conditions within the grid cell, and it is assumed that there is no transfer of material between the metabolic and slow/passive SOC pools. The amount of SOC in each pool is assumed to reach an equilibrium with constant input and output rates, and we solve the differential equations for an equilibrium (Figure 3.1, Parton et al. 1996).

3.2 Methods and Materials

In this analysis, NRCS (National Resources Conservation Service) SCAN (Soil Climate Analysis Network) and SNOTEL (SNOwpack TELemetry, which also includes soil moisture and temperature) data from the US Department of Agriculture NRCS website (`http://www.wcc.nrcs.usda.gov/`) at 13 sites across the state of New Mexico is used (Figure 3.2 and Table 3.1)). The daily data, including soil moisture and soil temperature, were downloaded from 2010-2012 at depths of 2 inches, 8 inches, and 20 inches. The soil moisture (percent) was collected by a dielectric constant measuring device was derived from the specific soil type equation (e.g. silt, loam). The soil temperature (degrees Celsius) were collected by an encapsulated thermistor. The data were transmitted to the NRCS computer center through meteor burst telemetry and then quality validated against limits. Values that fell outside preset windows were flagged and then examined and edited. Both parameters were graphed and verified to be within an acceptable range.

NRCS SCAN/ SNOTEL Site	Site ID	Location	Soil Type	Elevation (feet)	Biome
Crossroads	2107	Lat: 33 deg; 32 min N Long: 103 deg; 15 min W	loam	4055	Great Plains Grassland
Jornada Exp Range	2168	Lat: 32 deg; 33 min N Long: 106 deg; 42 min W	loam	4360	Chihuahuan Desert
Willow Wells	2108	Lat: 33 deg; 32 min N Long: 103 deg; 38 min W	loam	4537	Great Plains Grassland
Los Lunas Pmc	2169	Lat: 34 deg; 46 min N Long: 106 deg; 46 min W	loam	4846	Chihuahuan Desert
Sevilleta	2171	Lat: 34 deg; 21 min N Long: 106 deg; 41 min W	loam	5233	Chihuahuan Desert
Alacalde	2172	Lat: 36 deg; 5 min N Long: 106 deg; 3 min W	loam	5693	Conifer Woodland
Adam's Ranch #1	2015	Lat: 34 deg; 15 min N Long: 105 deg; 25 min W	loam	6175	Great Plains Grassland
Navajo Whiskey Ck	1138	Lat: 36 deg; 11 min N Long: 108 deg; 57 min W	silt	9050	Colorado Plateau Shrub-Steppe
Palo	1170	Lat: 36 deg; 25 min N Long: 105 deg; 20 min W	silt	9350	Colorado Plateau Shrub-Steppe
Red River Pass #2	715	Lat: 36 deg; 42 min N Long: 105 deg; 20 min W	silt	9850	Colorado Plateau Shrub-Steppe
Shuree	1169	Lat: 36 deg; 47 min N Long: 105 deg; 14 min W	silt	10100	Colorado Plateau Shrub-Steppe
Sierra Blanca	1034	Lat: 33 deg; 24 min N Long: 105 deg; 47 min W	silt	10280	Conifer Woodland
Taos Powderhorn	1168	Lat: 36 deg; 35 min N Long: 105 deg; 27 min W	silt	11057	Colorado Plateau Shrub-Steppe

Table 3.1: Collection sites of data in New Mexico, U.S.A. Measurements of soil moisture and soil temperature were collected at 2 inch, 8 inch, and 20 inch depths.

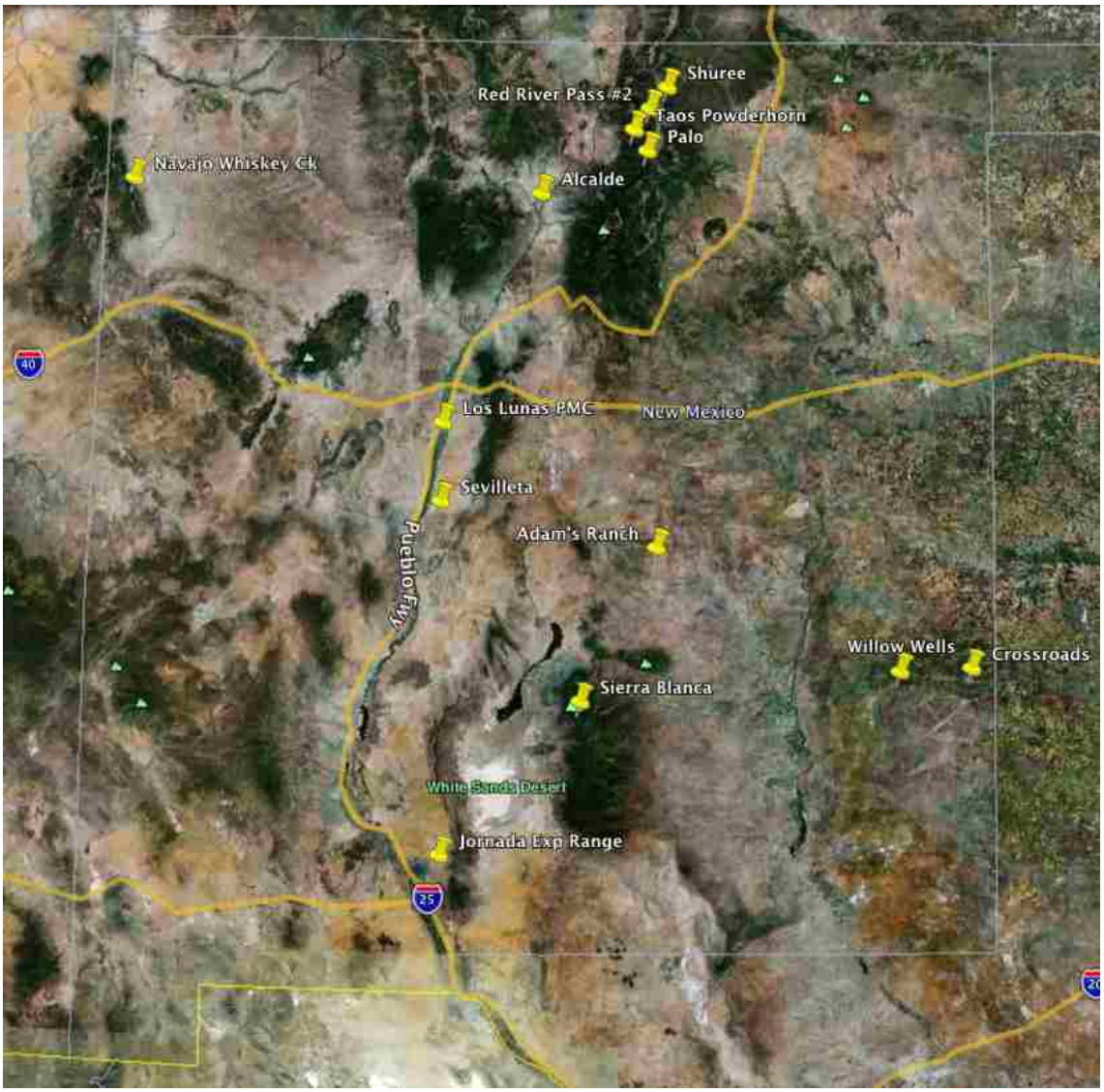

Figure 3.2: SCAN and SNOTEL sites of the NRCS in New Mexico, U.S.A. Daily data from 2010-2012 at soil depths of 2 inches, 8 inches and 20 inches were collected for soil moisture and soil temperature. Figure was created through Google Earth.

The first step of this work was to determine the decomposition variable A from temperature and moisture, which emphasizes the passive carbon pool and answering to the question of using the modified Century model as the more flexible model (Bolker et al. 1998). We defined

$$A = T_d M_d \tag{3.5}$$

The term T_d describes the effects of temperature on the decomposition rate as a function of time and depth

$$T_d(T_m) = t_2 t_1^{(td_a)}, \tag{3.6}$$

where

$$t_1 = \frac{T_{max} - T_m}{T_{max} - T_{opt}} \tag{3.7}$$

with $T_{max} = 45°C$, $T_m = 30$ day moving average, and $T_{opt} = 35°C$ (Ise and Moorcroft 2006). Additionally,

$$t_2 = e^{(\frac{td_a}{td_b}(1 - t_1^{td_a}))} \tag{3.8}$$

where $td_a = 0.2$ and $td_b = 2.63$ (fitted parameters per Ise and Moorcroft 2006). The function M_d describing the effects of moisture on the decomposition rate is also a function of time and depth:

$$M_d(PPT/PET) = \frac{M_d^*}{M_d^* with \frac{PPT}{PET} = 1} \tag{3.9}$$

For New Mexico, the PPT (precipitation) is $\leq$ PET (potential evapotranspiration) and is proportional to soil moisture. Furthermore,

$$M_d^* = \frac{1}{1 + md_a e^{-md_b \frac{PPT}{PET}}} \tag{3.10}$$

with $md_a = 30$ and $md_b = 8.5$ being constants via fitted parameters (per Ise and Moorcroft 2006). When PPT = PET, the moisture conditions are considered optimal and $M_d = 1$, which is the reasoning behind Equation 3.9. If PPT is < PET, the environment is dry and decomposition is moisture limited, but if PPT is > PET, the decomposition rate declines linearly with increasing precipitation, with md_a and md_b set as constants via the original Century model (Parton et al. 1996). We calculated the decomposition term A for New Mexico across a time, depth, and spatial continuum. These data were then used to determine an average value for decomposition across the state of New Mexico.

In order to see how T_d, M_d, and A vary as the soil temperature and moisture vary, a range of values were put into this modified Century model (Figures 3.6 and 3.7, Ise and Moorcroft 2006). The maximum temperature for decomposition was also included (45 C, per Ise and Moorcroft 2006). For the moisture function, PPT/PET values from 0 to 1 were included. Equation 3.5 was then utilized to calculate the decomposition value as a function of both temperature and moisture from values ranging between -30 C and 50 C and PPT/PET from 0 to 1 (Figure 3.8).

3.3 Results

Time series plots of data indicate that seasonal variability as well as pulse-like precipitation events are prominent in New Mexico (example sites shown in Figure 3.3). For instance, the soil temperature values at both the Red River Pass #2 site (silt, 9850 ft) and the Alcalde site (loam, 5693 ft) show strong seasonal variability, but the soil temperatures also vary differently with depth. The lower elevation site, Alcalde, shows temperatures increasing from 2 inches to 20 inches, and then to 8 inches (ranging from -6 C to 35 C). However, the higher elevation site, Red River Pass #2, shows that temperatures are warmest at 20 inches during the summers but also the coldest

at this depth during the winters (ranging from -3 C to 14 C). The moisture plots for these same two sites (Figure 3.3) indicate that the soil moisture at 20 inches at the Alcalde site remains relatively constant through the year but pulse-like precipitation events affect the soil moisture at lesser depths (characteristic of loamy soils with a range from 1 percent to 33 percent moisture). Conversely, the soil moisture at the Red River Pass #2 site is more affected by precipitation events throughout the soil layers, indicating a higher permeability of the silty soil to greater depths (ranging from 0 percent to 28 percent moisture, Figure 3.3).

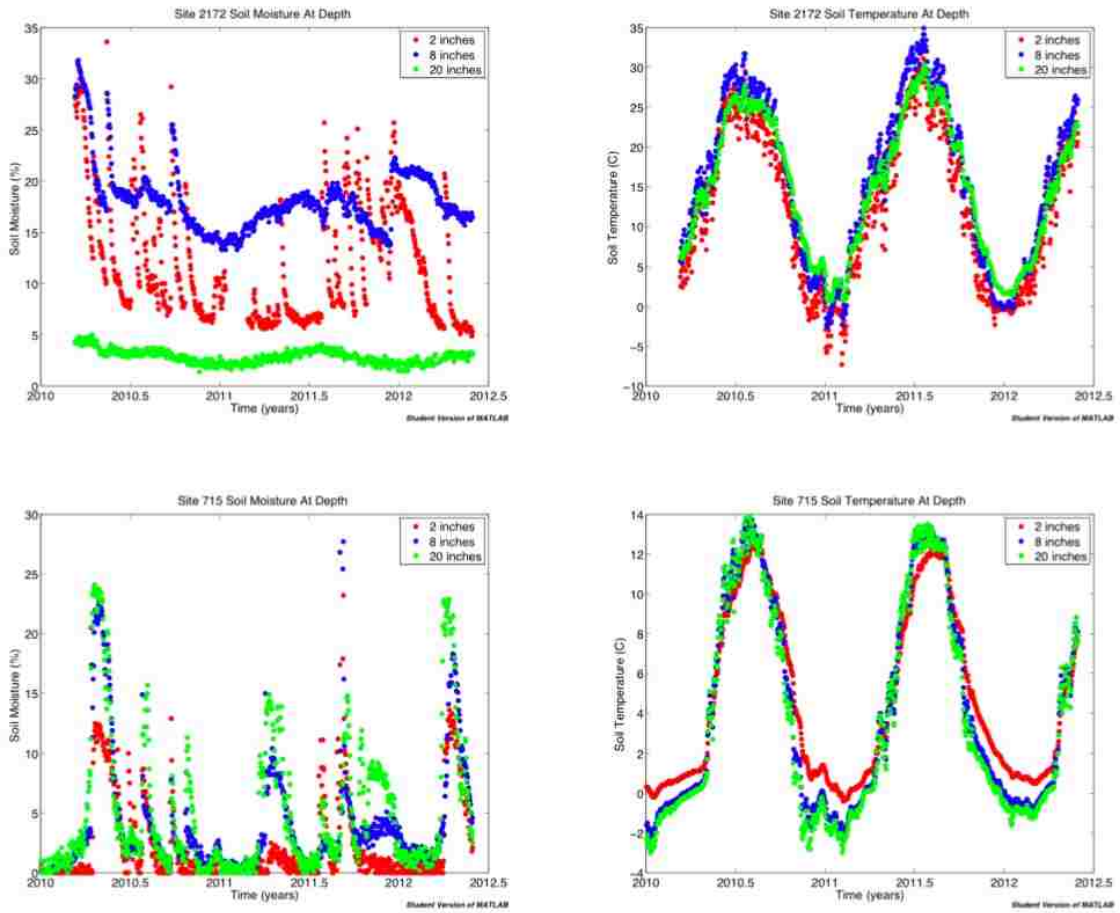

Figure 3.3: Soil moisture (%) and soil temperature (C) at depth for two sites from 2010 May 2012. Site 715 is a high elevation site (Red River Pass #2, 9850 ft) with the predominant soil type being silt. Site 2172 is a lower elevation site (Alcalde, 5693 ft) with the predominant soil type being loam.

Figure 3.4 shows the mean T_d and M_d values as well as the mean A values for the state of New Mexico across 13 sites. The equations described in the methods section were used to calculate the individual site values and then all sites were averaged together over the time series to create a state-wide mean value at every given time at every given depth. It is clear that decomposition varies as a function of temperature, moisture, and depth. The plots suggest that the greatest amount of decomposition, on average, occurs at shallow depths and is highly dependent on pulse-like rain events that occur during warm temperatures. Rainfall events in New Mexico are characteristically small, which indicates that the moisture is generally unable to penetrate to greater depths where further decomposition could occur. Thus, the majority of decomposition takes place in the shallow soil layers. However, it is clear that water penetration through soil is site dependent (Figure 3.3).

Tables 3.2, 3.3, and 3.4 show the mean and maximum T_d, M_d, and A values for each site across the state. These tables average the values across the time series in order to make comparisons across the sites. The minimum value for all three parameters at all sites is zero, meaning that the range of values for all sites goes from 0 to the maximum value. The sites are ordered from the lowest elevation (Crossroads site at 4055 ft) to the highest elevation (Taos Powderhorn site at 11057 ft). The site with the highest mean decomposition value at all three horizons was the Navajo Whiskey Ck site with a mean value of 0.3764 at 2 inches, 0.3435 at 8 inches, and 0.3852 at 20 inches. Again, this value is unitless according to the original model (Ise and Moorcroft 2006).

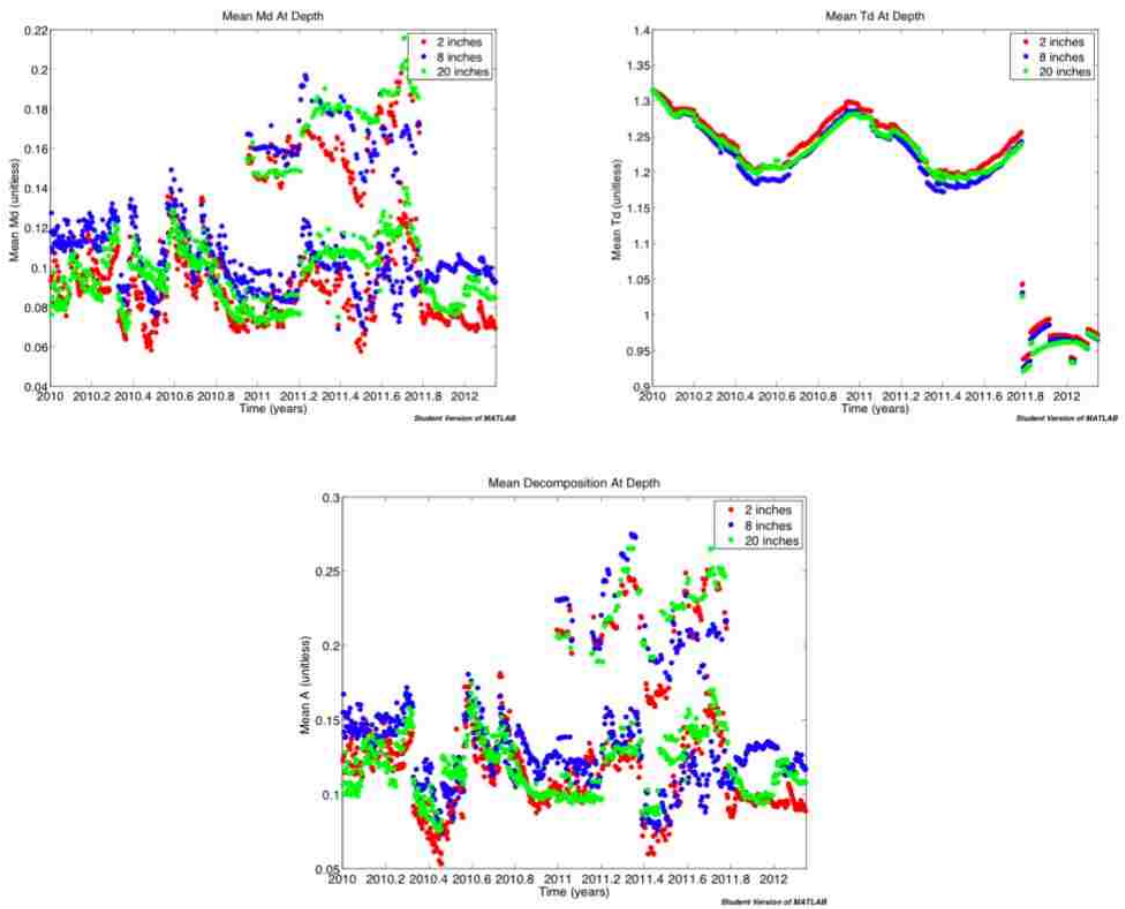

Figure 3.4: Mean Td (temperature function), Md (moisture function), and A (decomposition) values for all 13 SCAN and SNOTEL sites across New Mexico, U.S.A. from 2010 through May 2012. Values at 2 inch, 8 inch, and 20 inch depths are depicted.

Anomalous sites are of interest in this study (Figure 3.5) because they differ from the state average in such ways that indicate site-specific variability. The Taos Powderhorn site at 11057 feet and the Los Lunas Pmc site at 4846 feet both have one anomalous horizon, 2 inches and 20 inches, respectively. It appears that the decrease in decomposition in the 2-inch region at the high-elevation Taos site could be due to cooler temperatures or other compounding factors and that the decrease in decomposition in the 20-inch region at the Los Lunas site could be due to lesser permeability of the soil. The Jornada Exp Range site at 4360 ft is relatively close to the mean throughout the time series and The Navajo Whiskey Ck site at 9050 ft is relatively far from the mean throughout the time series. The Jornada Exp Range is in the northern Chihuahuan desert and is characterized by high amounts of solar radiation, wide diurnal ranges of temperature, low relative humidity, extremely variable precipitation, and high potential rates of evaporation. These characteristics are typical of New Mexico, indicating the reason for the Jornada site being close to the state mean. On the other hand, the Navajo Whiskey site is located on the far western side of the state in the Chuska Mountains, which characteristically receive higher rainfall than the surrounding lowlands and also regular winter snowfall. This higher water content affects the site to the point where there is a relatively large deviation from the statewide mean.

Site	2 inch – mean *Td*	2 inch – max *Td*	8 inch – mean *Td*	8 inch – max *Td*	20 inch – mean *Td*	20 inch – max *Td*
Crossroads (2107)	0.8138	1.3153	0.7967	1.3151	0.8012	1.3148
Jornada Exp Range (2168)	0.9693	1.3154	0.9452	1.3145	0.9552	1.3143
Willow Wells (2108)	0.9747	1.3153	0.9589	1.315	0.9255	1.3148
Los Lunas Pmc (2169)	0.9321	1.3194	0.9106	1.3148	0.9175	1.3145
Sevilleta (2171)	0.8524	1.3249	0.8389	1.3088	0.8358	1.2889
Alacalde (2172)	0.8723	1.3237	0.8547	1.3147	0.8618	1.3143
Adam's Ranch #1 (2015)	0.9341	1.3145	0.9226	1.3144	0.9268	1.3146
Navajo Whiskey Ck (1138)	1.0163	1.3154	1.0116	1.3153	1.0111	1.315
Palo (1170)	0.7126	1.3155	0.7112	1.3127	0.7115	1.3134
Red River Pass #2 (715)	1.0136	1.316	1.0156	1.3238	1.0172	1.3266
Shuree (1169)	0.7128	1.3135	0.7135	1.3157	0.7151	1.318
Sierra Blanca (1034)	1.0337	1.318	1.0405	1.3346	1.0336	1.3152
Taos Powderhorn (1168)	0.7732	1.3205	0.7703	1.3173	0.7705	1.3149

Table 3.2: Mean and maximum T_d values for 13 sites across New Mexico from 2010 to May 2012 (unitless). The minimum value for all sites for T_d is zero.

Site	2 inch – mean *Md*	2 inch – max *Md*	8 inch – mean *Md*	8 inch – max *Md*	20 inch – mean *Md*	20 inch – max *Md*
Crossroads (2107)	0.0449	0.1752	0.0461	0.1465	0.047	0.121
Jornada Exp Range (2168)	0.0324	0.08	0.0364	0.0763	0.0346	0.0597
Willow Wells (2108)	0.0366	0.0871	0.0423	0.1089	0.1036	0.2565
Los Lunas Pmc (2169)	0.0452	0.1632	0.064	0.1323	0.1274	0.5497
Sevilleta (2171)	0.0353	0.1434	0.1011	0.2453	0.055	0.1237
Alacalde (2172)	0.068	0.3692	0.1033	0.3342	0.0303	0.0488
Adam's Ranch #1 (2015)	0.0645	0.2081	0.0682	0.1904	0.0519	0.1667
Navajo Whiskey Ck (1138)	0.2976	0.4963	0.276	0.4985	0.311	0.5049
Palo (1170)	0.0429	0.2438	0.0258	0.0942	0.058	0.2453
Red River Pass #2 (715)	0.0329	0.1944	0.0397	0.2614	0.0444	0.2067
Shurec (1169)	0.161	1.0061	0.1451	1.0061	0.1444	1.0061
Sierra Blanca (1034)	0.0567	0.3192	0.1434	0.4665	0.0262	0.0405
Taos Powderhorn (1168)	0.0782	0.4139	0.0193	0.0344	0.0365	0.0942

Table 3.3: Mean and maximum M_d values for 13 sites across New Mexico from 2010 to May 2012 (unitless). The minimum value for all sites for M_d is zero.

Site	2 inch – mean A	2 inch – max A	8 inch – mean A	8 inch – max A	20 inch – mean A	20 inch – max A
Crossroads (2107)	0.0543	0.2085	0.0551	0.1784	0.0552	0.1559
Jornada Exp Range (2168)	0.0392	0.1045	0.043	0.0981	0.0412	0.0763
Willow Wells (2108)	0.0444	0.0984	0.05	0.1286	0.1218	0.3125
Los Lunas Pmc (2169)	0.0511	0.1949	0.0721	0.1315	0.1547	0.6149
Sevilleta (2171)	0.04	0.1614	0.1095	0.2987	0.0595	0.154
Alacalde (2172)	0.0745	0.3935	0.1169	0.4363	0.035	0.0627
Adam's Ranch #1 (2015)	0.0797	0.2511	0.0831	0.2439	0.0631	0.2144
Navajo Whiskey Ck (1138)	0.3764	0.65	0.3435	0.6524	0.3852	0.656
Palo (1170)	0.0555	0.3196	0.032	0.1233	0.0739	0.3206
Red River Pass #2 (715)	0.0409	0.2421	0.0486	0.3248	0.0551	0.2718
Shuree (1169)	0.1874	1.3055	0.1737	1.3113	0.1746	1.3083
Sierra Blanca (1034)	0.0731	0.3983	0.1815	0.5879	0.0337	0.051
Taos Powderhorn (1168)	0.1021	0.5442	0.025	0.0452	0.0473	0.1236

Table 3.4: Mean and maximum A values for 13 sites across New Mexico from 2010 to May 2012 (unitless). The minimum value for all sites for A is zero.

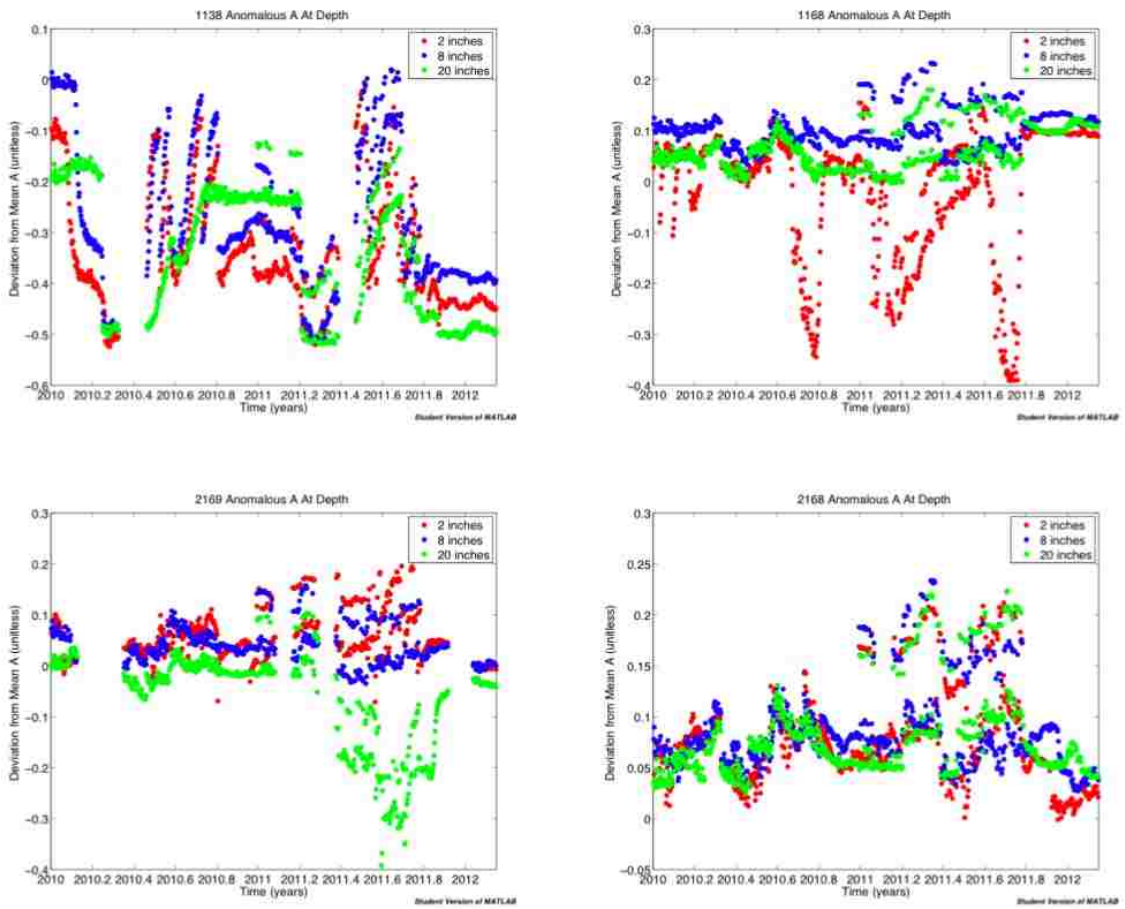

Figure 3.5: Deviation from the decomposition mean at 4 of the 13 sites. Sites 1168 (Taos Powderhorn, 11057 ft) and 2169 (Los Lunas Pmc, 4846 ft) have one anomalous depth, 2 inches and 20 inches, respectively. Site 2168 (Jornada Exp Range, 4360 ft) is relatively close to the mean throughout the time series and site 1138 (Navajo Whiskey Ck, 9050 ft) is relatively far from the mean throughout the time series.

Figures 3.6, 3.7, and 3.8 depict the variability of the temperature function, the moisture function, and the decomposition function, respectively. Per the modified Century model for this analysis, T_d increases as the soil temperature increases, up to 45 C. 45 C is set as the maximum temperature of decomposition activity through the original model (Ise and Moorcroft 2006), which explains the non-realistic behavior of the model at 45 C. Values greater than 45 C are irrevelant. T_d is a function of the maximum temperature, the optimal temperature, and a 30-day moving average of the measured temperature. However, due to the mechanized model, T_d does not increase exponentially as the temperature increases. The small increase in T_d as the temperature increases is due to the mathematical nature of the original model with the set constants for the maximum temperature, the optimal temperature, and the fit parameters of td_a and td_b. Since PPT/PET is directly proportional to soil moisture, it is clear that M_d shows a sigmoid/logarithmic growth curve as the PPT/PET value ranges from 0 to 1. The decomposition function, A, varies as both temperature and moisture vary, as is show in Figure 3.8. According to the results of this model, it is apparent that both high temperatures and soil moisture are required for decomposition to occur.

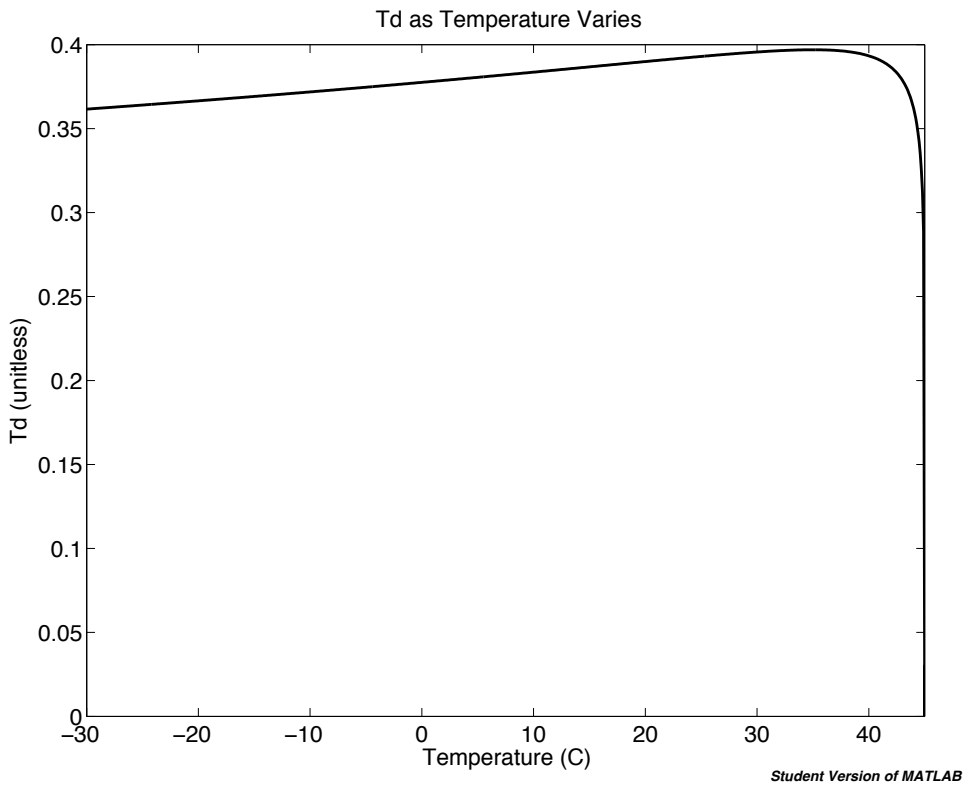

Figure 3.6: Variability of T_d (temp. function) as the soil temperature varies, per the Century model. 45 C is the maximum temperature of decomposition activity per the original model, meaning that values greater than 45 C are erroneous.

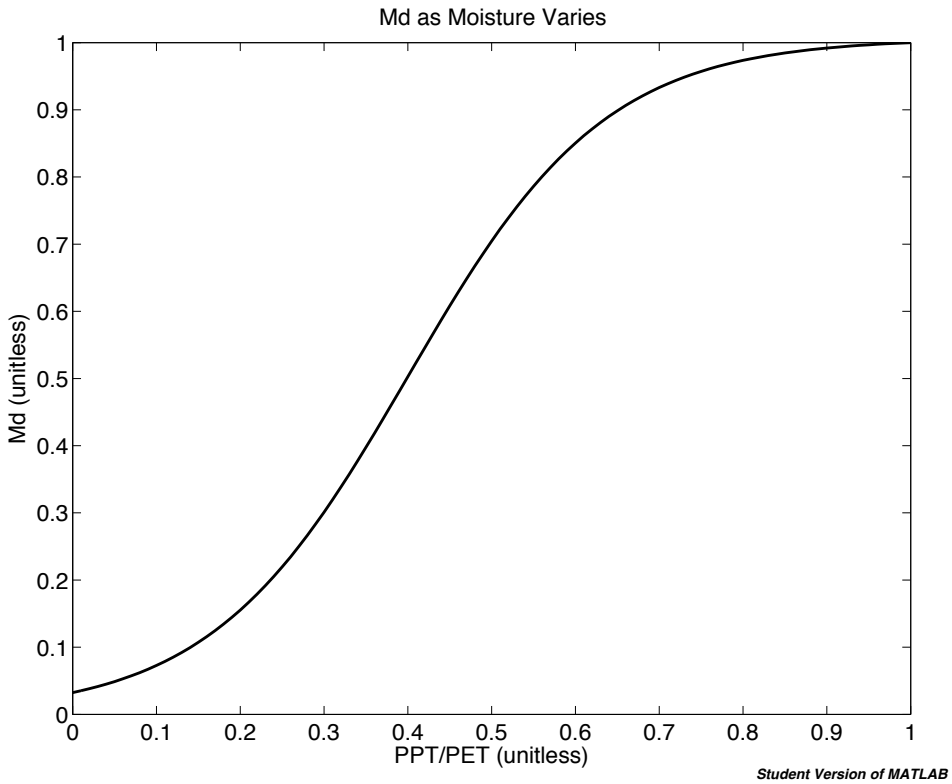

Figure 3.7: Variability of M_d (moisture function) as the ratio of precipitation over potential evaporation varies from 0 to 1. The ratio of PPT/PET is proportional to soil moisture.

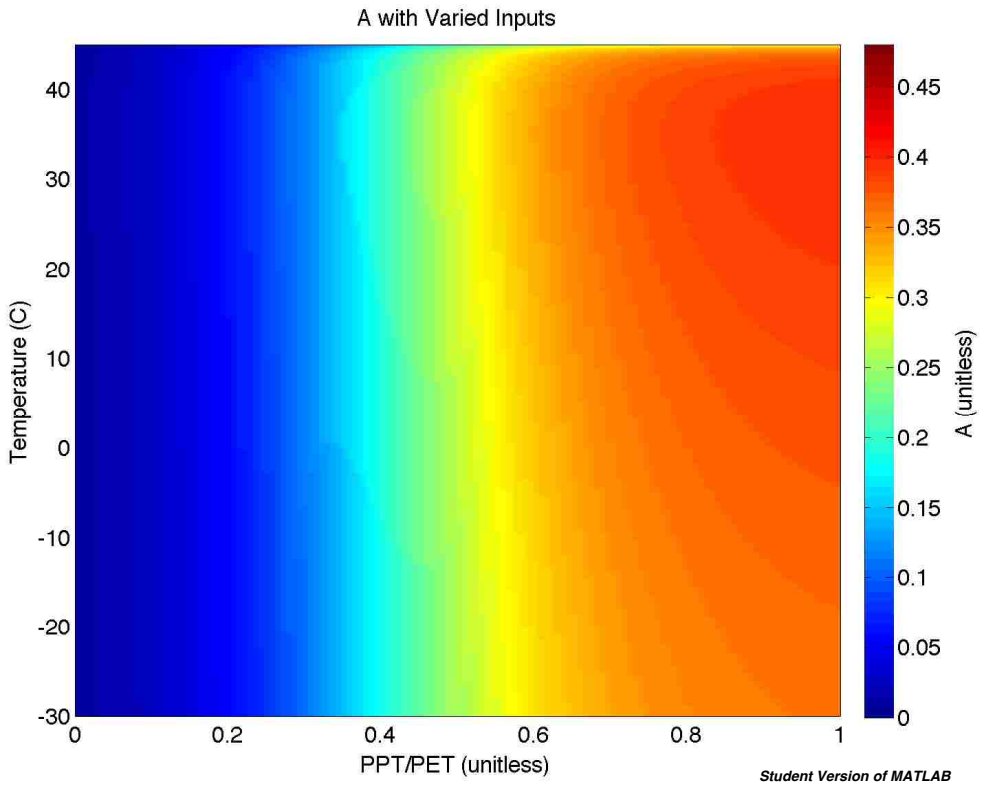

Figure 3.8: Variability of A (decomposition function) with varied soil temperature and moisture inputs. 45 C is the maximum temperature of decomposition activity per the original Century model.

3.4 Discussion

The feedbacks of the carbon cycle have been shown to be very important in predicting climate change over the next century, with a potentially large positive feedback coming from the release of carbon from soils as global temperatures increase (Gholz et al. 2000). The magnitude of this feedback and whether or not it drives the terrestrial carbon cycle to become a net source, rather than a net sink of carbon during the next century depends on the response of soil respiration to temperature. Quantifying decomposition is thus becoming increasingly important in understanding these feedback systems. The uncertainty is large, but is becoming more understood as questions about local systems and thus global systems are answered. The modeling of these ecosystems has demonstrated that climate-nutrient-carbon cycles may have a large impact on atmospheric carbon dioxide concentrations in the coming years (Rastetter et al. 1997).

Decomposition is typically fit to models based on a synthesis of experimental data from microcosm decomposition studies using radio-labeled substrates and consequent fitting of data bases on the experimental results (Del Grosso et al. 2009, Li et al. 1992, Parton et al. 1993, Thornton and Rosenbloom 2005). Several models use this idea to estimate decomposition, including the CENTURY model, the DayCENT model, and the DNDC (DeNitrification-DeComposition) model, but these models assume that the fitted decomposition rates are not limited by the availability of water or mineral nitrogen (Del Grosso et al. 2009, Li et al. 1992, Parton et al. 1993). The work presented here, however, uses soil moisture and temperature to directly calculate the decomposition rate, rather than fitting a decomposition rate to experimental decomposition data.

As seen in Figures 3.3 - 3.5 and Appendices A-C, it is clear that the sites in New Mexico indicate that as the temperature increases, so does the decomposition

rate. This indicates that as global temperatures increase, soil decomposition will also increase (although to an unknown extent) and net carbon stores in terrestrial ecosystems could become a net source for atmospheric carbon, thus further contributing to the positive feedback system of global climate change. Seasonal variability is expected and as more data is collected over time, these feedbacks will be quantifiable and further predictions can be created. In the mean time, it is important to understand that moisture also controls soil decomposition in New Mexico, but that soil type, water permeability, and precipitation events also control this process. The pulse-like events continue to present challenges to the synchronization of soil decomposition and production. The main questions answered through this work are that decomposition does vary with time, depth, and through a spatial context. Previous models have used average decomposition rates for sites, rather than varying decomposition rates through time. However, shortcomings of this work include the use of fitted parameters td_a, td_b, md_a, and md_b (set as constants), missing data and therefore erroneous values, and the use of the soil decomposition submodel without use of the entire water budget submodel.

In comparing the thirteen sites, the results presented here indicate that the biome plays a large role in the decomposition values across the state of New Mexico. The sites found in the Colorado Plateau Shurb-Steppe biome had the highest values of decomposition throughout the sites analyzed (Navajo Whiskey Creek, Palo, Red River Pass #2, Shuree, and Taos Powderhorn at the 20 inch horizon). The sites found in the Conifer Woodland biome had the lowest values of decomposition (Alacalde and Sierra Blanca at the 20 inch horizon). The values calculated here for decomposition are significantly different from current representations within terrestrial ecosystem models (Ise and Moorcroft 2006). In particular, the temperature dependencies of heterotrophic respiration are weaker than the current values, indicating that acceleration in decomposition rates that occur with increasing temperatures will likely be less significant, meaning that temperature and moisture effects tend to converge

over large scale comparisons of decomposition.

In comparison to the DayCENT and the DNDC models, the use of the CENTURY model on a modified daily time-step is able to calculate decomposition rates as a function of time, space, and depth, which indicates that the rate varies continuously. However, this analysis did not take into account the flux of carbon and nitrogen between the atmosphere, vegetation and soil; and definitely has room to improve regarding the growth of plants via nutrient availability, water, and temperature. The nutrient supply is a function of SOM decomposition and external nutrient additions, but only temperature and moisture were analyzed here. Additionally, daily maximum/minimum temperature and precipitation, the timing and descriptions of management events, and soil texture were not included in the determination of the decomposition rate (much like the DayCENT model, Parton et al. 1998). The DayCENT and CENTURY models also include nitrogen dynamic in soil carbon decomposition and consequently show a tendency for reduced heterotrophic respiration (Bonan et al. 2002). Further questions to be answered surround the comparison of ecosystem models, such as the CLM (Bonan et al. 2002) and the DNDC (Li et al. 1992).

3.5 Appendices

3.5.1 Appendix A

The dependence of decomposition on temperature (Td) as a function of time for 13 sites across New Mexico from 2010 through May 2012 at three distinct soil depths (2 inches, 8 inches, and 20 inches).

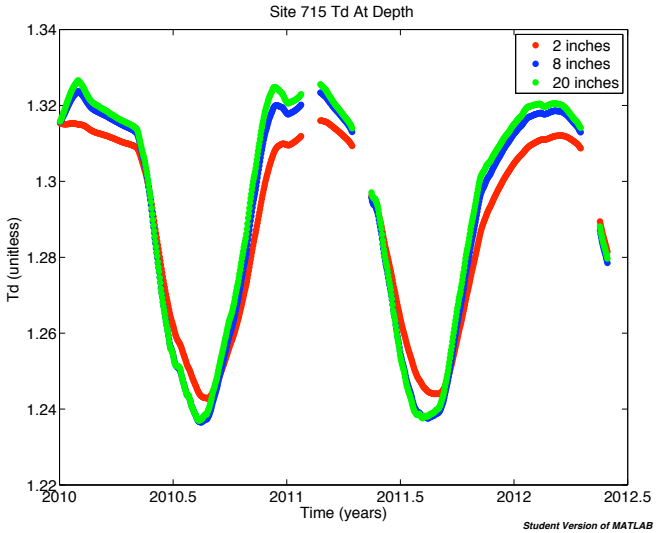
Site 715 Td At Depth
2 inches
8 inches
20 inches
Td (unitless)
1.34
1.32
1.3
1.28
1.26
1.24
1.22
2010
2010.5
2011
2011.5
2012
2012.5
Time (years)
Student Version of MATLAB

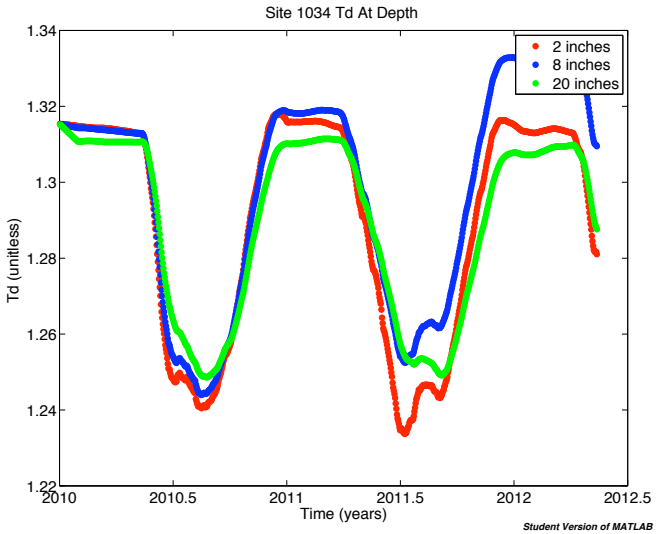
Site 1034 Td At Depth
2 inches
8 inches
20 inches
Td (unitless)
1.34
1.32
1.3
1.28
1.26
1.24
1.22
2010
2010.5
2011
2011.5
2012
2012.5
Time (years)
Student Version of MATLAB

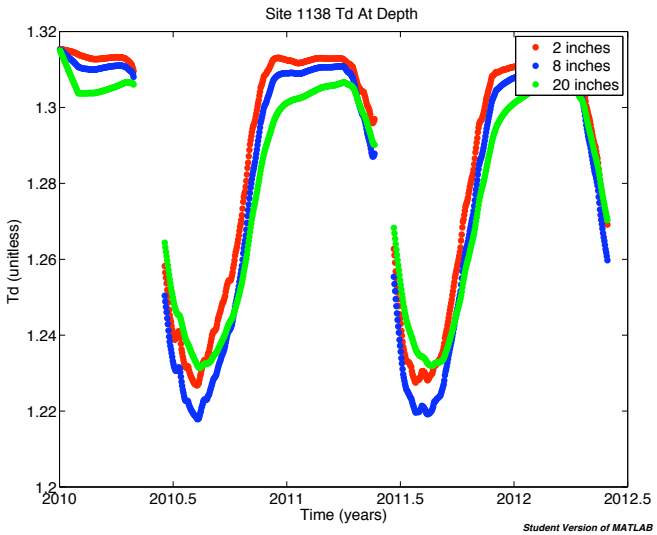
Site 1138 Td At Depth
2 inches
8 inches
20 inches
Td (unitless)
1.32
1.3
1.28
1.26
1.24
1.22
1.2
2010
2010.5
2011
2011.5
2012
2012.5
Time (years)
Student Version of MATLAB

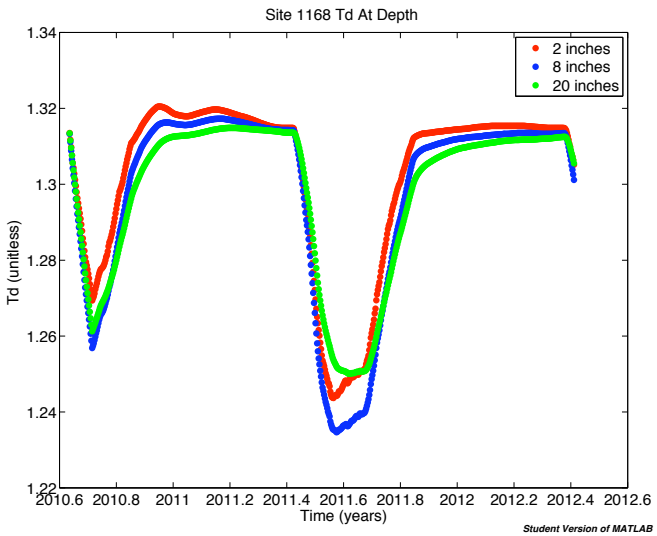
Site 1168 Td At Depth
2 inches
8 inches
20 inches
Td (unitless)
1.34
1.32
1.3
1.28
1.26
1.24
1.22
2010.6
2010.8
2011
2011.2
2011.4
2011.6
2011.8
2012
2012.2
2012.4
2012.6
Time (years)
Student Version of MATLAB

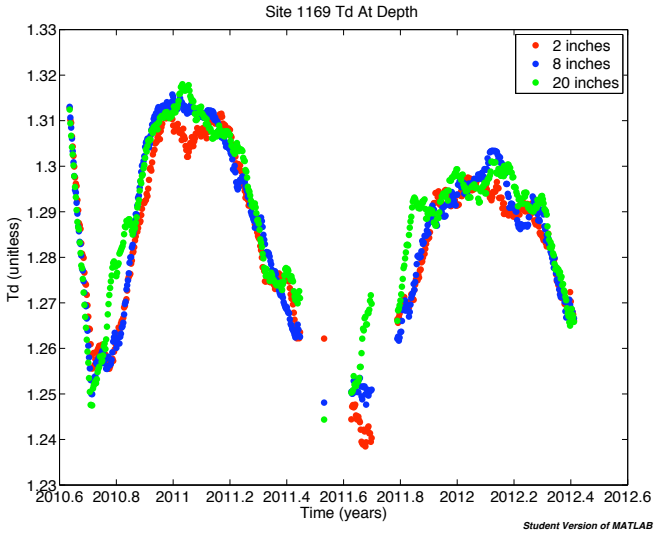
Site 1169 Td At Depth
2 inches
8 inches
20 inches
Td (unitless)
1.33
1.32
1.31
1.3
1.29
1.28
1.27
1.26
1.25
1.24
1.23
2010.6 2010.8 2011 2011.2 2011.4 2011.6 2011.8 2012 2012.2 2012.4 2012.6
Time (years)
Student Version of MATLAB

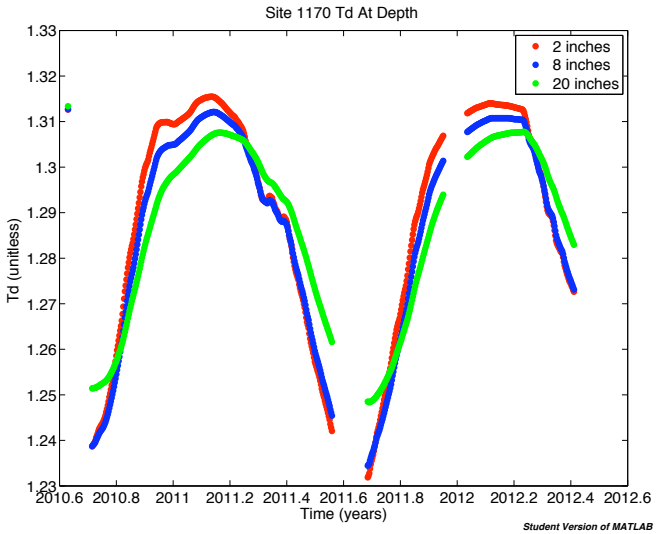
Site 1170 Td At Depth
2 inches
8 inches
20 inches
Td (unitless)
1.33
1.32
1.31
1.3
1.29
1.28
1.27
1.26
1.25
1.24
1.23
2010.6 2010.8 2011 2011.2 2011.4 2011.6 2011.8 2012 2012.2 2012.4 2012.6
Time (years)
Student Version of MATLAB

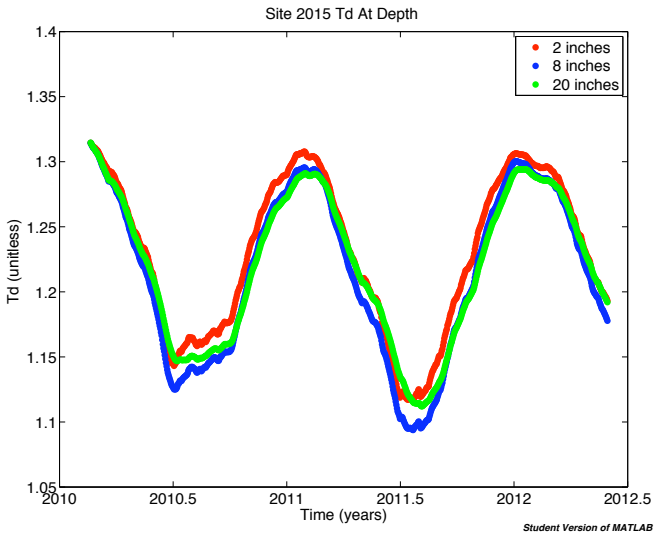
Site 2015 Td At Depth
2 inches
8 inches
20 inches
Td (unitless)
Time (years)
1.4
1.35
1.3
1.25
1.2
1.15
1.1
1.05
2010
2010.5
2011
2011.5
2012
2012.5
Student Version of MATLAB

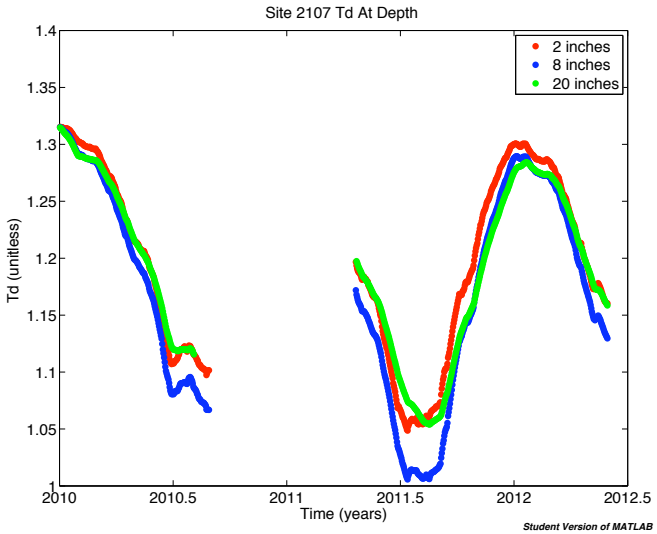
Site 2107 Td At Depth
2 inches
8 inches
20 inches
Td (unitless)
Time (years)
1.4
1.35
1.3
1.25
1.2
1.15
1.1
1.05
1
2010
2010.5
2011
2011.5
2012
2012.5
Student Version of MATLAB

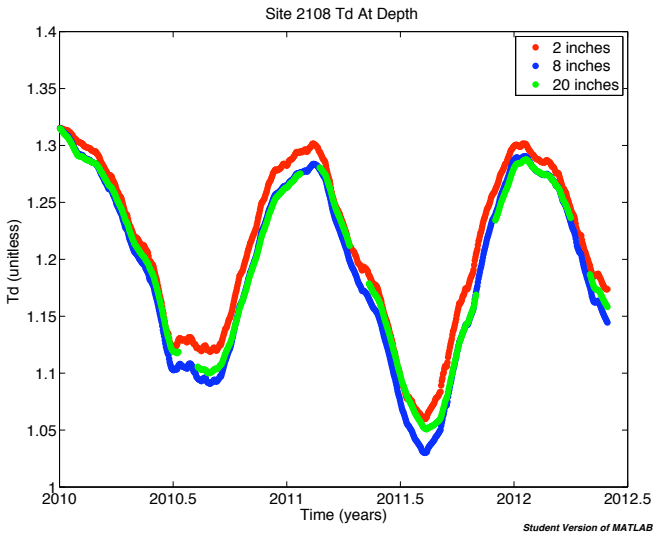
Site 2108 Td At Depth
2 inches
8 inches
20 inches
Td (unitless)
Time (years)
1.4
1.35
1.3
1.25
1.2
1.15
1.1
1.05
1
2010
2010.5
2011
2011.5
2012
2012.5
Student Version of MATLAB

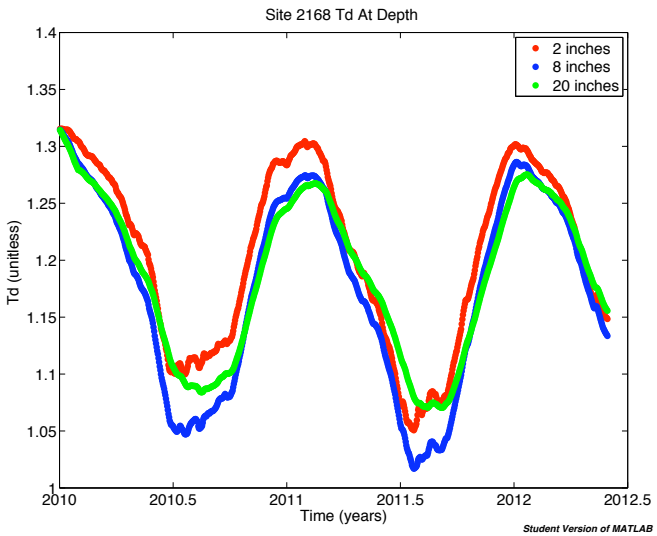
Site 2168 Td At Depth
2 inches
8 inches
20 inches
Td (unitless)
Time (years)
1.4
1.35
1.3
1.25
1.2
1.15
1.1
1.05
1
2010
2010.5
2011
2011.5
2012
2012.5
Student Version of MATLAB

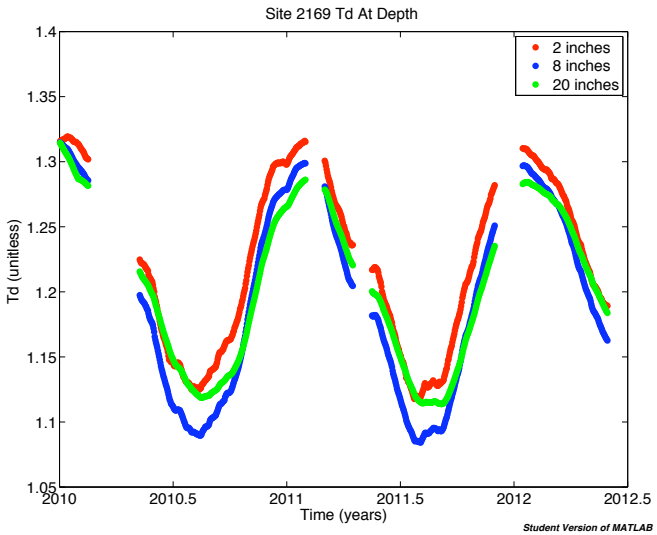
Site 2169 Td At Depth
2 inches
8 inches
20 inches
Td (unitless)
Time (years)
1.4
1.35
1.3
1.25
1.2
1.15
1.1
1.05
2010
2010.5
2011
2011.5
2012
2012.5
Student Version of MATLAB

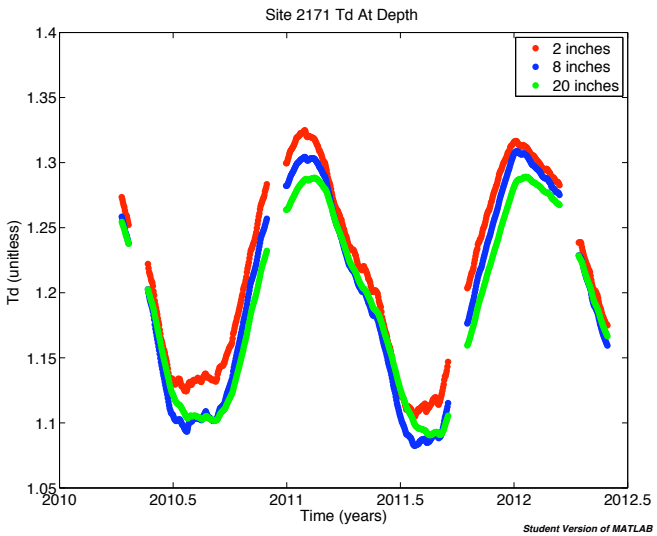
Site 2171 Td At Depth
2 inches
8 inches
20 inches
Td (unitless)
Time (years)
1.4
1.35
1.3
1.25
1.2
1.15
1.1
1.05
2010
2010.5
2011
2011.5
2012
2012.5
Student Version of MATLAB

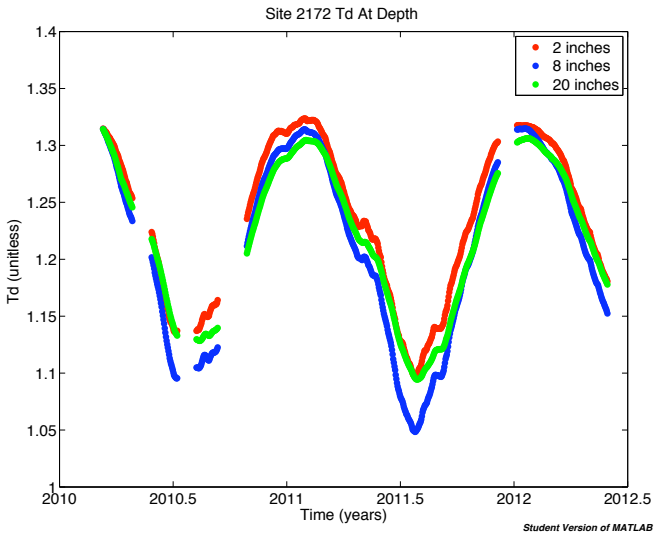
Site 2172 Td At Depth
2 inches
8 inches
20 inches
Td (unitless)
Time (years)
1.4
1.35
1.3
1.25
1.2
1.15
1.1
1.05
1
2010
2010.5
2011
2011.5
2012
2012.5
Student Version of MATLAB

3.5.2 Appendix B

The dependence of decomposition on moisture (Md) as a function of time for 13 sites across New Mexico from 2010 through May 2012 at three distinct soil depths (2 inches, 8 inches, and 20 inches).

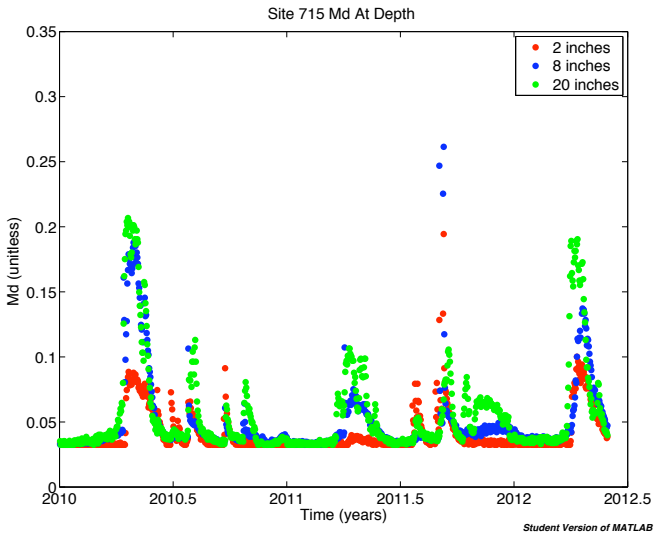
Site 715 Md At Depth
2 inches
8 inches
20 inches
Md (unitless)
0.35
0.3
0.25
0.2
0.15
0.1
0.05
0
2010
2010.5
2011
2011.5
2012
2012.5
Time (years)
Student Version of MATLAB

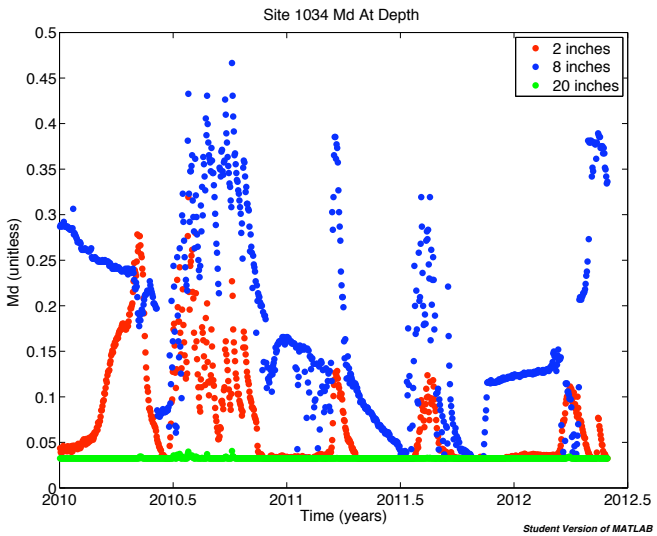
Site 1034 Md At Depth
2 inches
8 inches
20 inches
Md (unitless)
0.5
0.45
0.4
0.35
0.3
0.25
0.2
0.15
0.1
0.05
0
2010
2010.5
2011
2011.5
2012
2012.5
Time (years)
Student Version of MATLAB

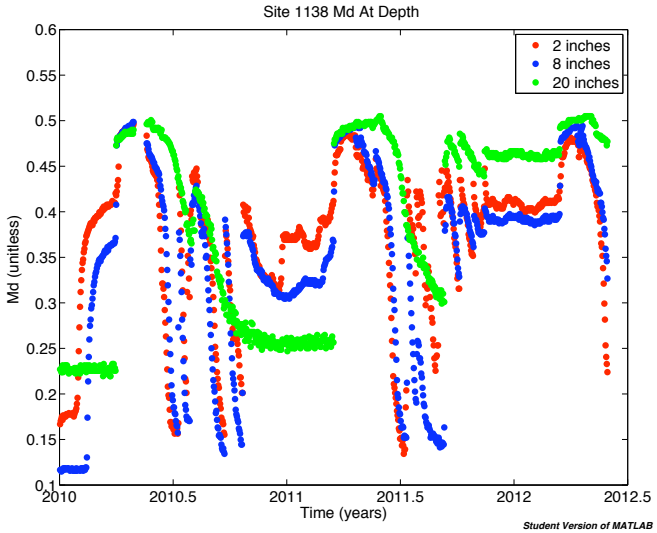
Site 1138 Md At Depth
2 inches
8 inches
20 inches
Md (unitless)
Time (years)
0.6
0.55
0.5
0.45
0.4
0.35
0.3
0.25
0.2
0.15
0.1
2010
2010.5
2011
2011.5
2012
2012.5
Student Version of MATLAB

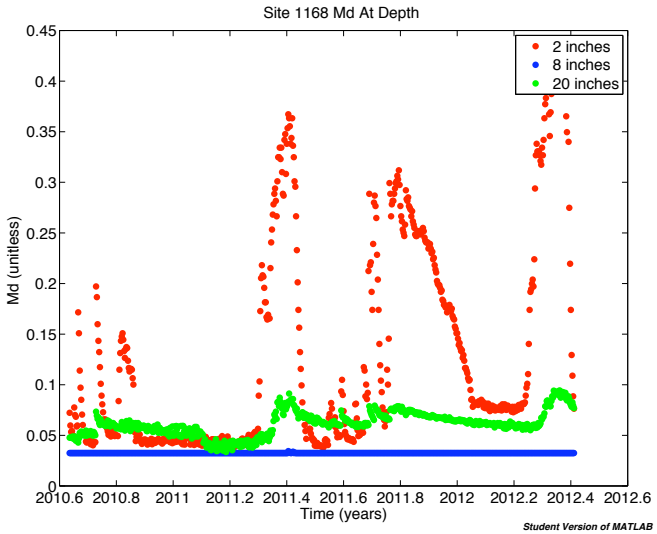
Site 1168 Md At Depth
2 inches
8 inches
20 inches
Md (unitless)
Time (years)
0.45
0.4
0.35
0.3
0.25
0.2
0.15
0.1
0.05
0
2010.6
2010.8
2011
2011.2
2011.4
2011.6
2011.8
2012
2012.2
2012.4
2012.6
Student Version of MATLAB

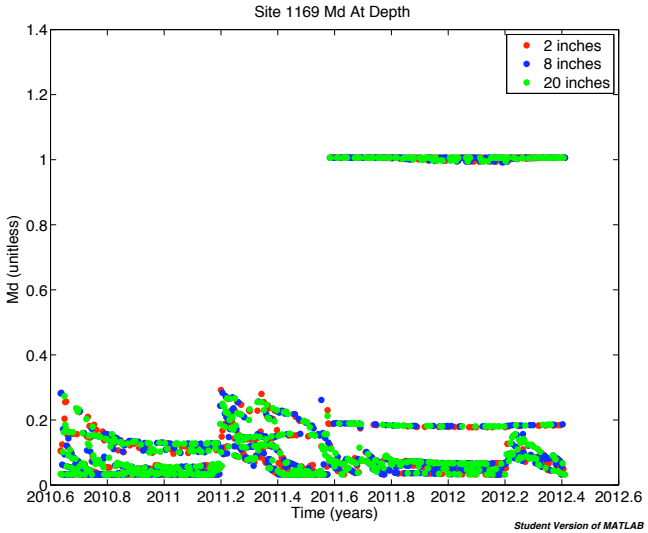
Site 1169 Md At Depth
2 inches
8 inches
20 inches
Md (unitless)
Time (years)
Student Version of MATLAB

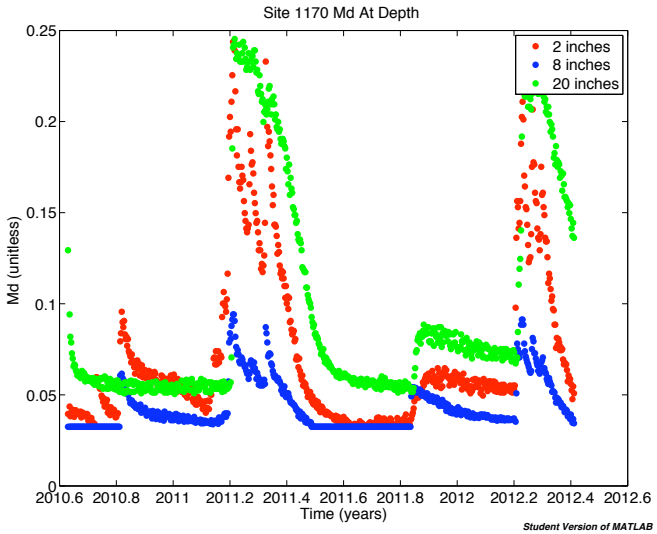
Site 1170 Md At Depth
2 inches
8 inches
20 inches
Md (unitless)
Time (years)
Student Version of MATLAB

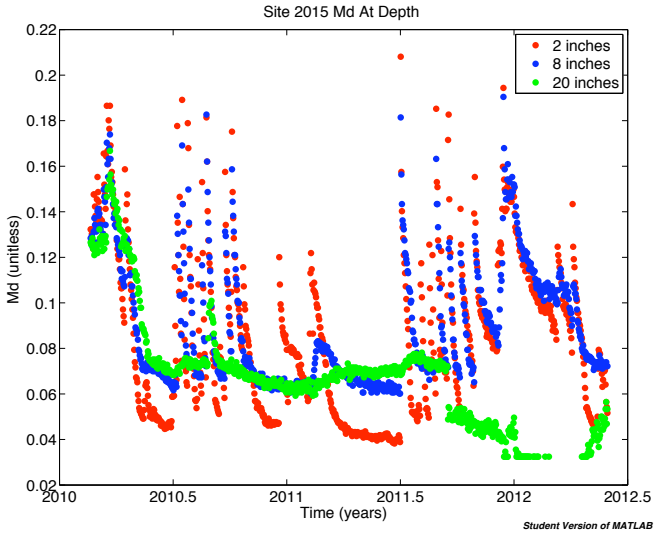
Site 2015 Md At Depth
2 inches
8 inches
20 inches
Md (unitless)
0.22
0.2
0.18
0.16
0.14
0.12
0.1
0.08
0.06
0.04
0.02
2010
2010.5
2011
2011.5
2012
2012.5
Time (years)
Student Version of MATLAB

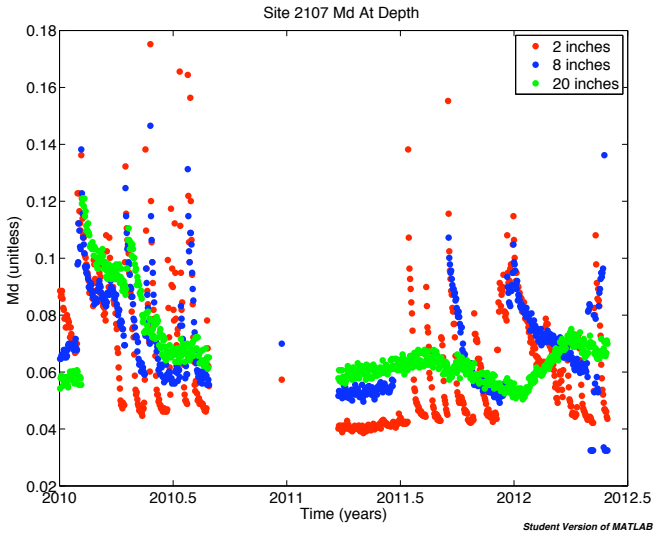
Site 2107 Md At Depth
2 inches
8 inches
20 inches
Md (unitless)
0.18
0.16
0.14
0.12
0.1
0.08
0.06
0.04
0.02
2010
2010.5
2011
2011.5
2012
2012.5
Time (years)
Student Version of MATLAB

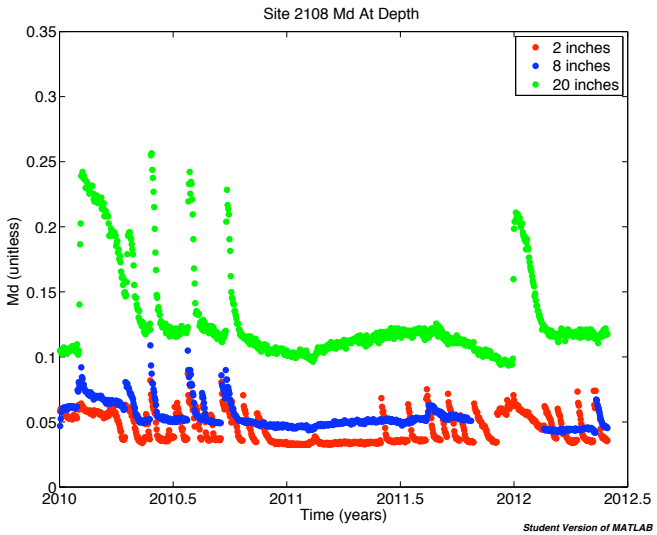
Site 2108 Md At Depth
2 inches
8 inches
20 inches
Md (unitless)
Time (years)
0.35
0.3
0.25
0.2
0.15
0.1
0.05
0
2010
2010.5
2011
2011.5
2012
2012.5
Student Version of MATLAB

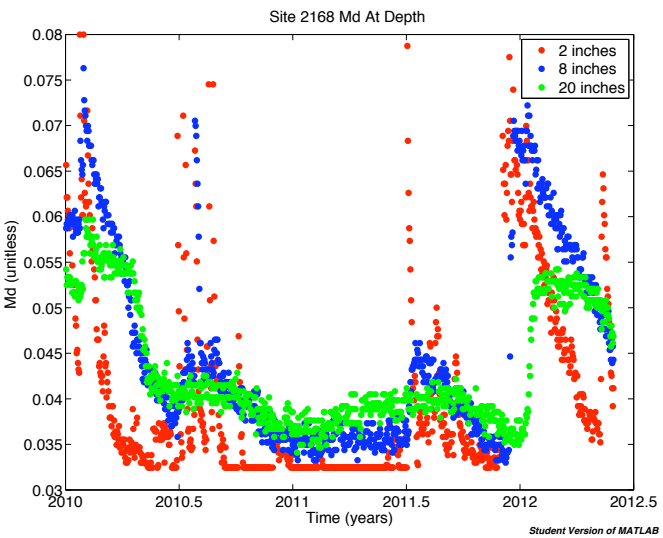
Site 2168 Md At Depth
2 inches
8 inches
20 inches
Md (unitless)
Time (years)
0.08
0.075
0.07
0.065
0.06
0.055
0.05
0.045
0.04
0.035
0.03
2010
2010.5
2011
2011.5
2012
2012.5
Student Version of MATLAB

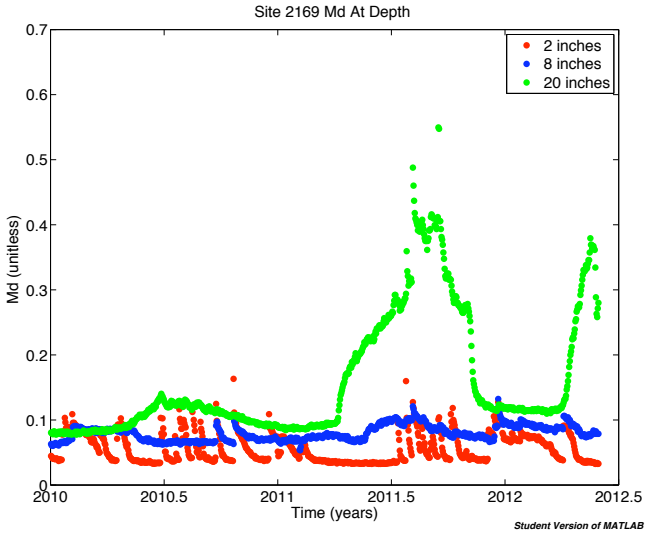
Site 2169 Md At Depth
2 inches
8 inches
20 inches
Md (unitless)
Time (years)
0
0.1
0.2
0.3
0.4
0.5
0.6
0.7
2010
2010.5
2011
2011.5
2012
2012.5
Student Version of MATLAB

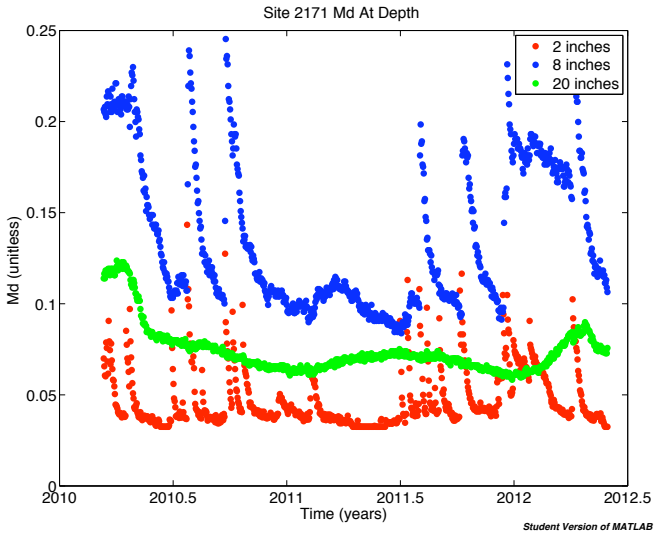
Site 2171 Md At Depth
2 inches
8 inches
20 inches
Md (unitless)
Time (years)
0
0.05
0.1
0.15
0.2
0.25
2010
2010.5
2011
2011.5
2012
2012.5
Student Version of MATLAB

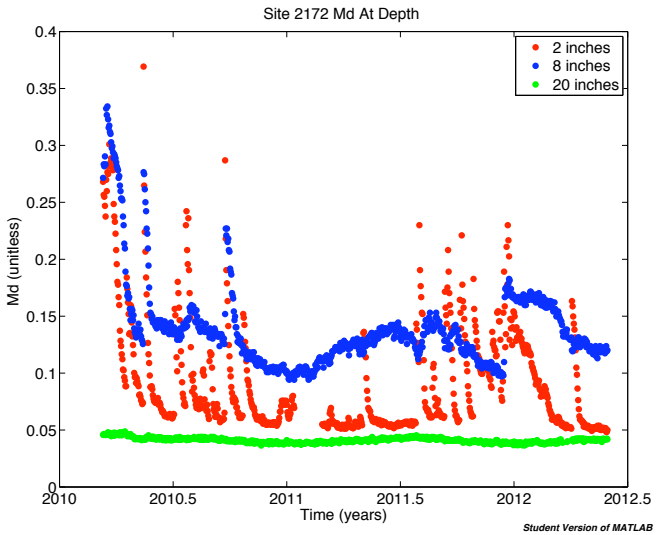
Site 2172 Md At Depth
2 inches
8 inches
20 inches
Md (unitless)
Time (years)
0.4
0.35
0.3
0.25
0.2
0.15
0.1
0.05
0
2010
2010.5
2011
2011.5
2012
2012.5
Student Version of MATLAB

3.5.3 Appendix C

Decomposition (A) as a function of temperature and moisture for 13 sites across New Mexico from 2010 through May 2012 at three distinct soil depths (2 inches, 8 inches, and 20 inches).

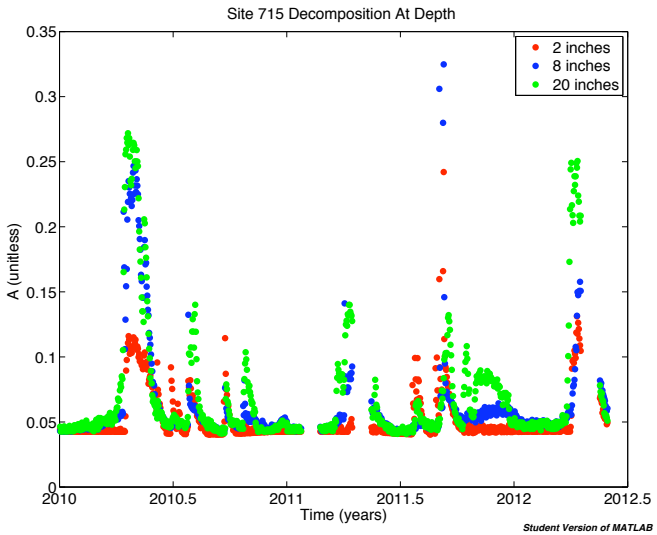
Site 715 Decomposition At Depth
2 inches
8 inches
20 inches
A (unitless)
Time (years)
0.35
0.3
0.25
0.2
0.15
0.1
0.05
0
2010
2010.5
2011
2011.5
2012
2012.5
Student Version of MATLAB

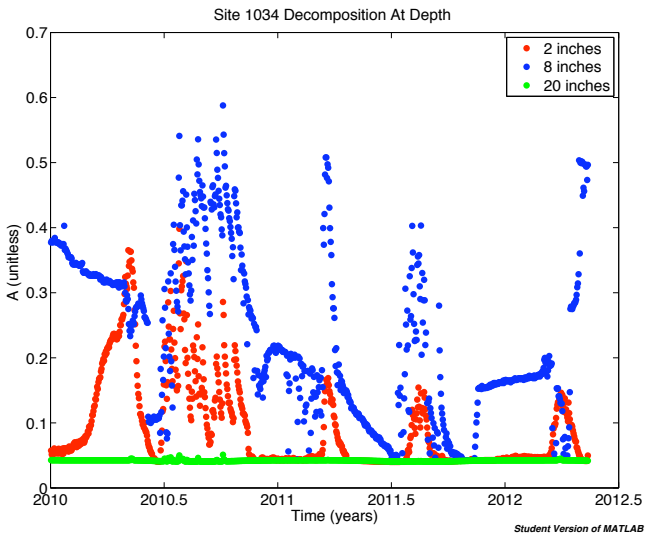
Site 1034 Decomposition At Depth
2 inches
8 inches
20 inches
A (unitless)
Time (years)
0.7
0.6
0.5
0.4
0.3
0.2
0.1
0
2010
2010.5
2011
2011.5
2012
2012.5
Student Version of MATLAB

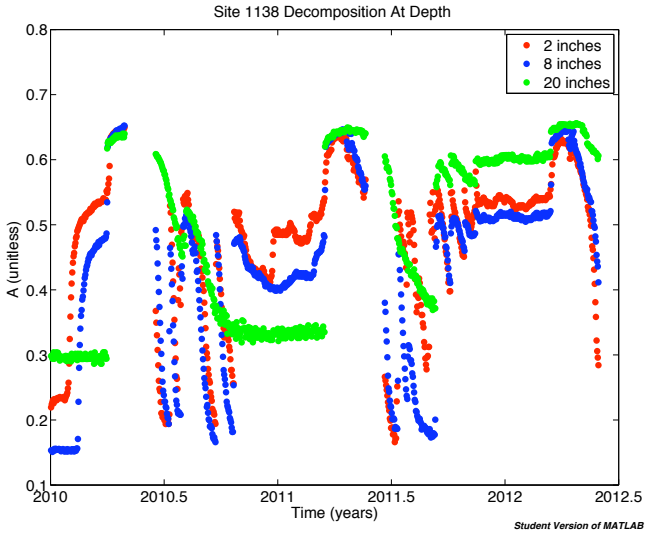
Site 1138 Decomposition At Depth
2 inches
8 inches
20 inches
A (unitless)
Time (years)
0.8
0.7
0.6
0.5
0.4
0.3
0.2
0.1
2010
2010.5
2011
2011.5
2012
2012.5
Student Version of MATLAB

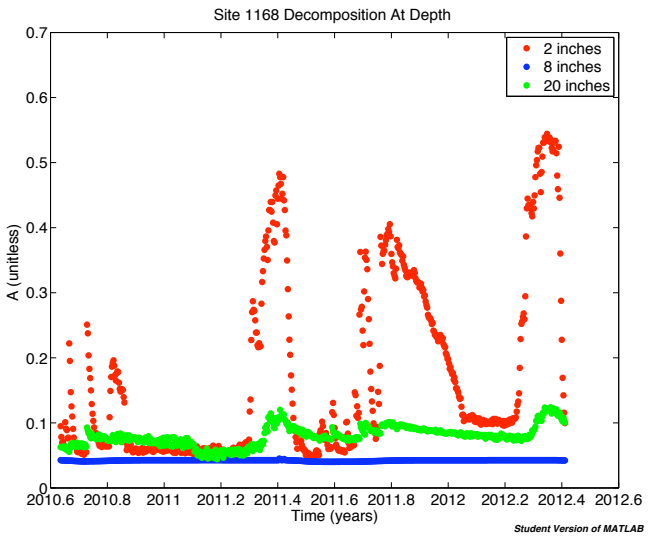
Site 1168 Decomposition At Depth
2 inches
8 inches
20 inches
A (unitless)
Time (years)
0.7
0.6
0.5
0.4
0.3
0.2
0.1
0
2010.6
2010.8
2011
2011.2
2011.4
2011.6
2011.8
2012
2012.2
2012.4
2012.6
Student Version of MATLAB

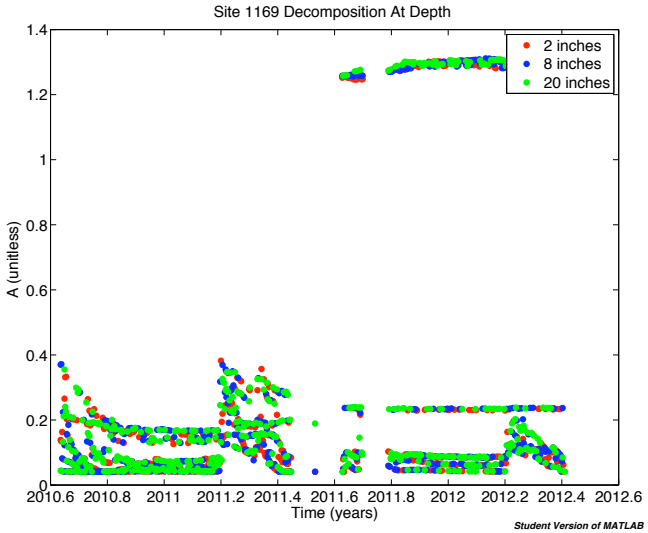
Site 1169 Decomposition At Depth
2 inches
8 inches
20 inches
A (unitless)
Time (years)
Student Version of MATLAB

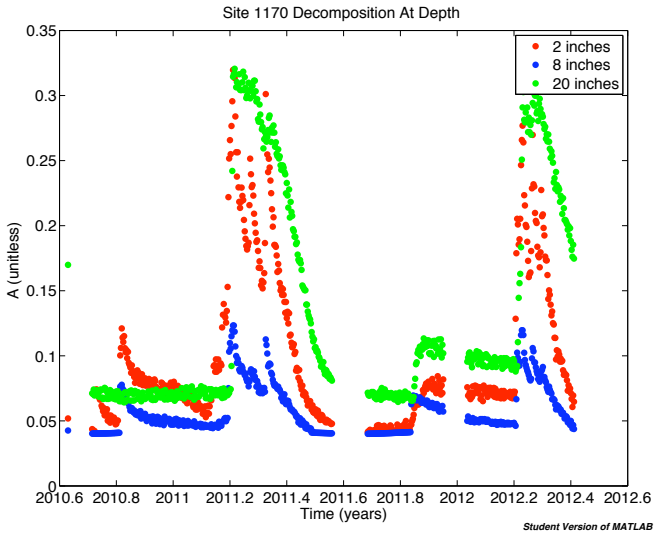
Site 1170 Decomposition At Depth
2 inches
8 inches
20 inches
A (unitless)
Time (years)
Student Version of MATLAB

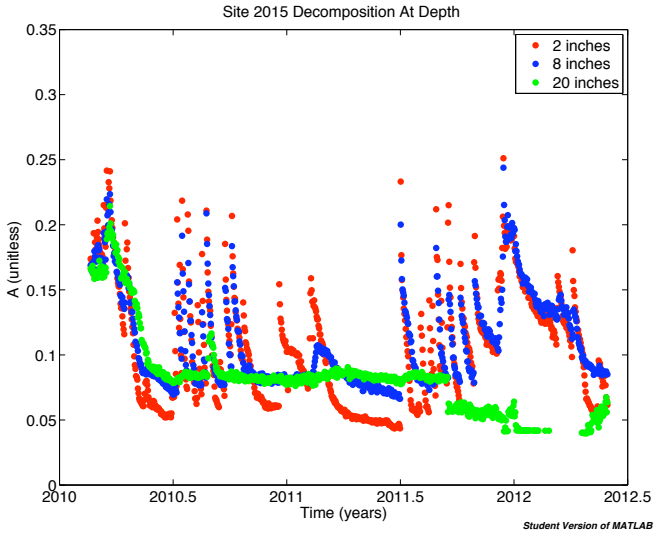
Site 2015 Decomposition At Depth
2 inches
8 inches
20 inches
A (unitless)
Time (years)
0.35
0.3
0.25
0.2
0.15
0.1
0.05
0
2010
2010.5
2011
2011.5
2012
2012.5
Student Version of MATLAB

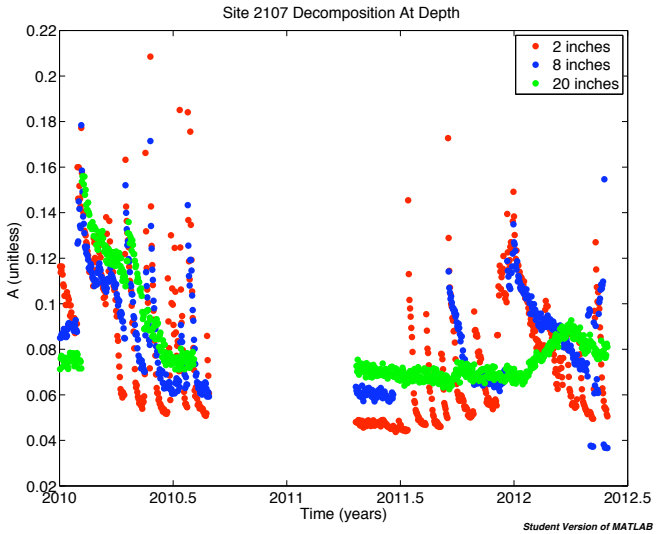
Site 2107 Decomposition At Depth
2 inches
8 inches
20 inches
A (unitless)
Time (years)
0.22
0.2
0.18
0.16
0.14
0.12
0.1
0.08
0.06
0.04
0.02
2010
2010.5
2011
2011.5
2012
2012.5
Student Version of MATLAB

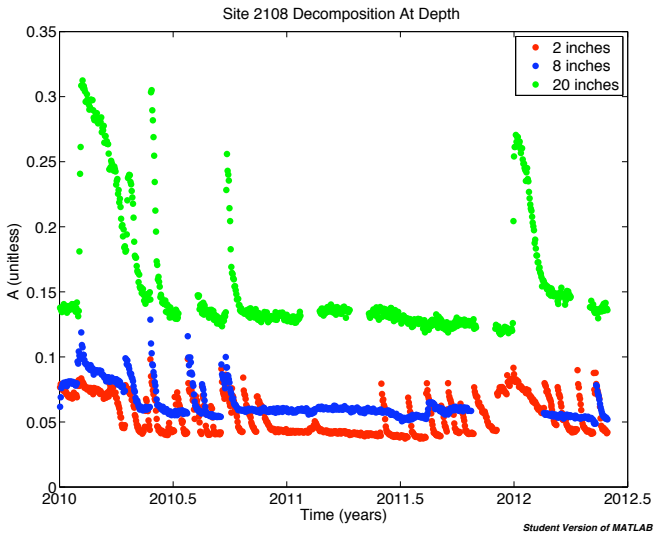
Site 2108 Decomposition At Depth
2 inches
8 inches
20 inches
A (unitless)
Time (years)
0.35
0.3
0.25
0.2
0.15
0.1
0.05
0
2010
2010.5
2011
2011.5
2012
2012.5
Student Version of MATLAB

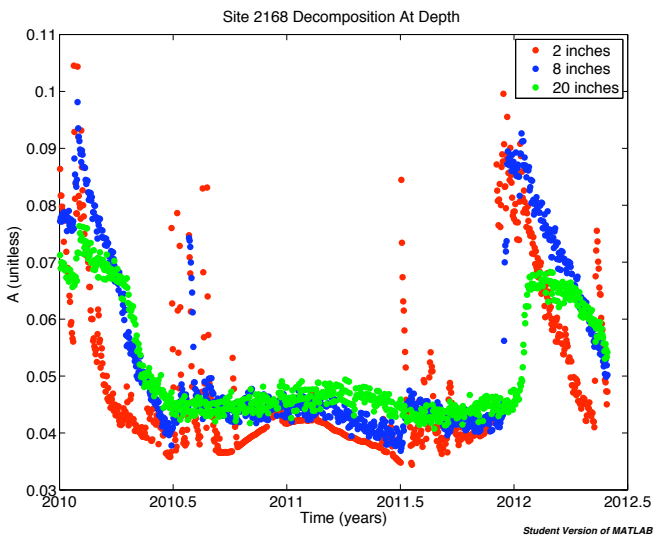
Site 2168 Decomposition At Depth
2 inches
8 inches
20 inches
A (unitless)
Time (years)
0.11
0.1
0.09
0.08
0.07
0.06
0.05
0.04
0.03
2010
2010.5
2011
2011.5
2012
2012.5
Student Version of MATLAB

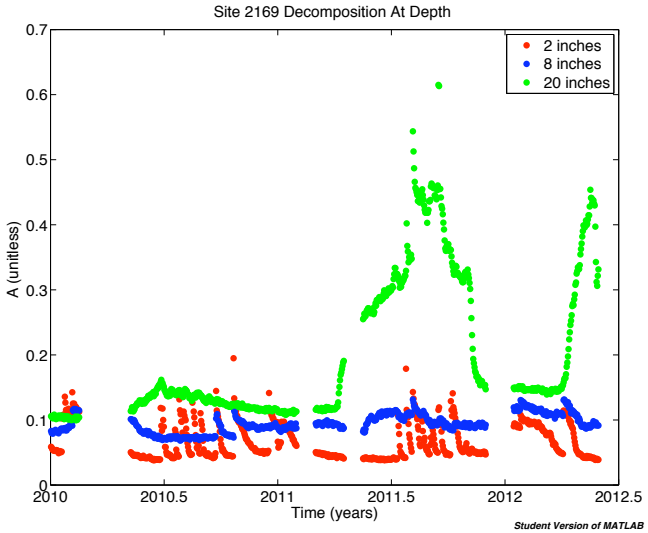
Site 2169 Decomposition At Depth
2 inches
8 inches
20 inches
A (unitless)
Time (years)
0
0.1
0.2
0.3
0.4
0.5
0.6
0.7
2010
2010.5
2011
2011.5
2012
2012.5
Student Version of MATLAB

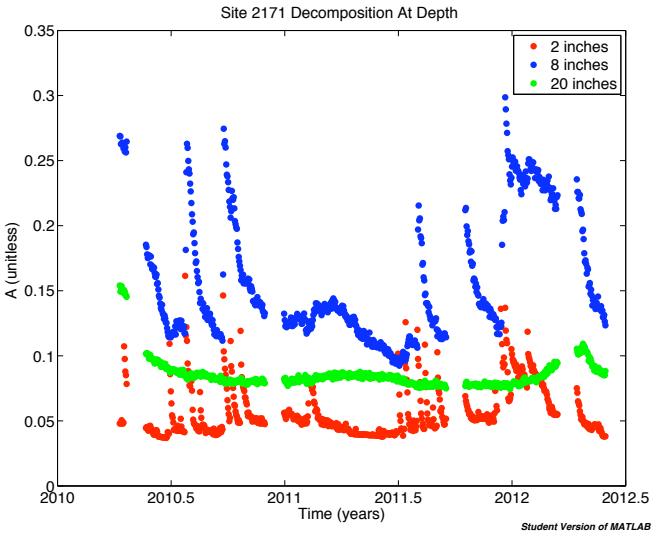
Site 2171 Decomposition At Depth
2 inches
8 inches
20 inches
A (unitless)
Time (years)
0
0.05
0.1
0.15
0.2
0.25
0.3
0.35
2010
2010.5
2011
2011.5
2012
2012.5
Student Version of MATLAB

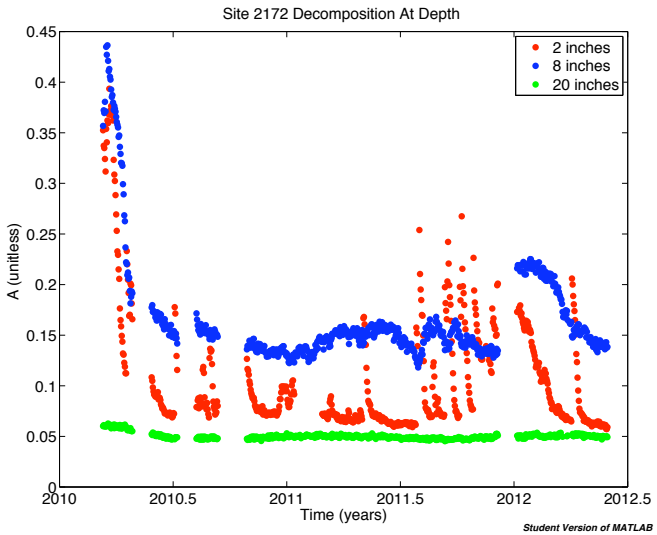
Site 2172 Decomposition At Depth
2 inches
8 inches
20 inches
A (unitless)
Time (years)
0.45
0.4
0.35
0.3
0.25
0.2
0.15
0.1
0.05
0
2010
2010.5
2011
2011.5
2012
2012.5
Student Version of MATLAB

Chapter 4

A Quantitative Look at Science Education

4.1 Introduction

Traditionally, there has been a gap between those who teach science at the K-12 level and those who do science. Few K-12 science teachers ever have science research experiences in their training, yet they attempt to teach students how science works (Druger and Allen 1998). Research scientists are the true experts in science, but they work at universities, colleges, and research institutions and generally have little to do with K-12 education. Several programs in recent years have tried to bridge this disconnect with one example being The Center for Science, Mathematics and Engineering Education at the National Research Council (the operating agency of the National Academy of Sciences, the National Academy of Engineering, and the Institute of Medicine). They have established Resources for Involving Scientists in Education (RISE), with the idea to "effectively engage the scientific community in the systemic reform of K-12 education" (Druger and Allen 1998). Beyond this national

program, many universities have created programs to bring research scientists into K-12 classrooms directly or through professional development. It is not always clear how to make partnerships between teachers and scientists productive, so it is important to carefully design programs to maximize the knowledge transfer (Drayton and Falk 2006).

In order to improve the connection between research scientists and teachers, both ends must reach out to the other. Most often, if asked to present an occasional lecture, or asked to do something on a short-term basis, scientists are willing to help, so it is usually up to the teachers to ask (McKeown 2003). Long-term commitments are harder to come by, but this is where professional development can play a key role. Teaching teachers is ideal, allowing the knowledge to be passed along to the classrooms (Druger and Allen 1998).

In both the research literature and in the everyday approach of teachers, it is commonly assumed that the greatest contribution science teaching can make to society is to spread a broad acquaintance with currently accepted concepts, theories, and methods of problem solving. However, most teachers simply teach scientific facts to students that are then sometimes forgotten soon after the exam. Dewey (1910/1964) stated that "Science has been taught too much as an accumulation of ready-made material with which students are to be made familiar, not enough as a method of thinking, an attitude of mind, after the pattern of which mental habits are to be transformed." So then why is it that still today we are teaching students to memorize facts rather than to understand the process of scientific thinking?

Teachers are told to ensure that their students can do the following: identify questions and concepts that guide scientific investigations, design and conduct scientific investigations, use technology and mathematics to improve investigations and communications, formulate and revise scientific explanations and models using logic and evidence, recognize and analyze alternative explanations and models, and com-

municate and defend a scientific argument (O'Neill and Polman 2004). However, Ma (1999) found four aspects of true knowledge in comparing Chinese students to American students:

1. Connnectedness of material to prior knowledge and new material
2. Multiple Perspectives
3. Basic ideas that the teacher can portray to the students since the teacher knows the most important, fundamental ideas
4. Longitudinal Coherence

To reiterate these four points, several other research studies suggest that struggling (and even failing) to create and carry out empirical investigations in science may teach students more meaningful lessons about how science is pushed forward rather than simply executing cookbook labs or solving carefully formulated problems (Sandoval and Reiser 2003). Because people in many walks of life (including but not limited to careers in pure and applied science) must make decisions on which scientific research and its methods have strong bearing, such practice-based scientific knowledge should have a much more prominent place in schooling. To make this large shift in pedagogy, a long-term investment in teacher professional development plus student-performed research studies would be necessary (O'Neill and Polman 2004).

In addition, various researchers suggest that involving students in processes of inquiry that include the planning of long-term, empirical research has unique and demonstrable benefits compared with the conceptual coverage for which pre-college science education typically strives (O'Neill and Polman 2004). They recommended that educators encourage students to create opinions on scientific matters that may pertain to everyday life, whether they be moral or political. Students should also be

encouraged to have a healthy skepticism of scientific "fact." It is only through further questioning and hypothesizing that scientific discoveries can be made. Despite this, it is all to easy to accept current scientific knowledge as the truth, thus decreasing the furthering of science. Ideally, teachers should emphasize this questioning and further investigation through the scientific process, rather than simply teaching students memorizable facts (Tamir et al. 1998).

Typically, however, the scientific method in science classrooms is taught as discrete, ordered steps meant to guide student inquiry, but research scientists do not use the scientific method in the same manner (Tang et al. 2009). In reality, inquiry is a complex form of human thought that has developed over thousands of years, and it is a cultural legacy that can be employed and changed (Herrenkohl et al. 1999). Because of this, students should not be expected to come to some understanding of the nature of scientific thinking simply by being exposed to interesting materials and problems. Rather, they need to learn the true scientific process from research scientists (White and Frederiksen 1998).

In order to teach the actual scientific process, professional development must play a large role (Jang 2008). One professional development program, for instance, was designed to facilitate change in teachers use of inquiry-based practices in their own classrooms (Jeanpierre et al. 2005). Scientists, teachers, and students formed a learning community, which allowed a tight-knit relationship between research scientists and the classroom environment. A key job of this learning community was to create plans for implementation of inquiry processes, allowing the professional development to assure that the teachers came to understand the nature of science through actual research experience in the field and to help them to build new and personal views of what it meant to practice real science in their own classrooms (Jeanpierre et al. 2005).

Professional development literature emphasizes the need to give teachers ongoing

support as they incorporate changes in their classroom, so it is important that schools and organizations remain in contact with the teachers well after the course has been completed (Jeanpierre et al. 2005).

Buczynski and Hansen (2010) created an Inquiry Learning Partnership for professional development between a university, science center, and two urban school districts to offer teachers specific science content and pedagogical techniques intended to integrate inquiry-based instruction into classrooms. Inquiry-based teaching is strongly recommended by the American Association for the Advancement of Science (AAAS) and the National Research Council (NRC) as a strategy to develop deeper student understanding of science and the ability to apply it to the everyday world (Blanchard et al. 2008).

Studies have indicated that although students can be thoughtful in designing investigations and in planning procedures by thinking about controls, about samples, and about how to organize data collection, students also have trouble focusing on the scientific importance of questions generated and systematically collecting and analyzing data. It is for these reasons that teacher structuring and questioning are crucial in encouraging students to be thoughtful about the various aspects of inquiry (Krajcik et al. 1998).

Because of these recommendations, Buczynski and Hansen (2010), attempted to design a professional development program focusing on inquiry-based teaching and learning. From their pre/post content exams, professional development surveys, focus groups, and assessment data, they found that teachers increased their science content knowledge and began to incorporate inquiry-based techniques into their classrooms. They did, however, determine several issues with their professional development program. They discovered that resources cannot be a limiting factor, time must be maximized, and classroom management must be addressed in the future (Buczynski and Hansen 2010).

Ideally, however, preservice teachers would receive the training necessary to teach science before entering the classroom. Prospective teachers should be taught by science educators with the ability to give them opportunities to enhance their knowledge of the structure, function, and development of science. These science educators can facilitate active participation of prospective teachers in content-specific methods courses, allowing them to understand and appreciate the importance of scientific knowledge (El Khalick and BouJaoude 1997).

El Khalick and BouJaoude (1997) presented an example for preservice teacher training. These preservice teachers would be assigned scientific concepts, asked to present them in alternate forms for different age groups, and then critiqued by the science educators. The scientific accuracy and developmental appropriateness would be evaluated, allowing the preservice teachers to gain as much as possible from the course. To bring this idea to the level of more advanced scientific thinking, preservice teachers could also do an exercise finding the complexities of scientific concepts and common areas of confusion among first-time learners.

Understanding common misconceptions allows teachers to bridge the gaps between complex material. In finding these difficult areas of understanding, preservice teachers can then design activities or instructional sequences that target such conceptions. These types of courses for preservice teachers would allow a constant interplay between learning the conceptual side of science and designing an appropriate teaching method (El Khalick and BouJaoude 1997).

4.2 Background

While the idea of teaching scientific practices is a hot topic, so is the idea of teaching the nature of science and its social practices (Wong and Hodson 2008). Most teachers have good intentions when it comes to teaching science, but all too often students

are left feeling confused and without a solution to what they have learned. In order to reverse this process, it is important to take a step back and to look at science education with a critical eye (Osborne et al. 2003). There must be some level of agreement among the standardized curriculum, allowing students to understand how science works.

Teaching students about the nature of science is as important as developing a knowledge of its content (Osborne et al. 2003) and teaching the nature of science (NOS) needs to become a core rather than a secondary part of the science curriculum according to some authors (Schwartz et al. 2004). However, teaching about the nature of science cannot be a single, simple solution to the problem. No one method and no one group of individuals can provide a universal solution as to what should be the essential elements of a present day science curriculum, and it is for these reasons that teaching about science and certainty of results means also inspecting the reliability and validity of empirical evidence. Osborne et al. (2003) suggested that it might be a mistake to create a curriculum in terms of a requirement to teach the components of the nature of science separately. Rather, they suggested that best practice teaching can be addressed through sets of well chosen case studies with discussions of science and its nature. Since the nature of science is fundamental to the science as a process way of learning, learning about the nature of science should naturally arise from the classroom environment (Osborne et al. 2003).

Wong et al. (2008) presented a two hour self-directed workshop for preservice teachers to construct mind maps on elements of NOS and scientific inquiry and it was found that a few connections were identified (such as links between science, technology, and society, and links between the changing nature of scientific inquiry and newer methods of collecting evidence). They used case studies on topics such as the severe acute respiratory syndrome as an attempt to understand the NOS, but it appears that this topic is greater than simply studying case studies. The nature

of science can also be studied through the scientific process and through thorough understanding of how research scientists do their work. Again, preservice teacher training and professional development may be the key to the understanding of the nature of science (Osborne et al. 2003).

Despite the ideals of science teaching, there have also been several studies regarding science teacher confidence in the classroom. With preservice training and professional development, it is important to determine the long-term effects of the training procedures. Murphy et al. (2007) compared the findings from a survey of teacher confidence in teaching science with the results of a seminal report carried out 10 years prior to the survey distribution. The survey indicated that there were still serious concerns relating to teacher's confidence in properly teaching science. Their study also showed that professional development in science can be effective, but it is important to link the teacher's prior knowledge to the professional development content (Murphy et al. 2007).

Despite this, research has shown that some teachers feel confident teaching concepts to students, but when diagnostically tested, they share many of the same misconceptions of their pupils (Varelas et al. 2005). Because of this, it is clear that more professional development is needed. This could be done through local universities and organizations, or through the establishment of new regional and national Science Learning Centers that could offer more regarding the wider dissemination of good practice in science professional development to schools. It is clear that teachers need the proper training to fully teach students (Murphy et al. 2007).

In order to align scientific research with classroom practices, Ford and Wargo (2006) suggested using routines, roles and responsibilities. These three 'R's include information that implicitly governs school performance and provide a way to study what matters most for student learning about the basics of science as researchers study science. Ideally, this would eliminate common student inquiries such as "Is

this right? and would encourage "This supports my hypothesis." With training such as this and direct apprenticeship with research scientists (Richmond 1998), it is thought that students will learn to be scientists and not simply robots that export textbook facts.

Finally, it should be noted that the classroom is a very complex entity. The constraints that govern the conditions necessary for bringing scientific research into the classroom are extremely varied and cannot be controlled simply (Taylor et al. 2008). Rather, social and cultural environments, along with individual differences between students, are among the factors that need to be understood when furthering our understanding of good teaching and learning inside the science classroom (El Khalick and BouJaoude 1997).

The purpose of this study is to analyze educational research data through a quantitative analysis. By looking at the data and then working backward to find similarities among the studies, we can see how educational research can be analyzed and whether or not scientific practices are performed through research studies that aren't strictly scientific.

4.3 Methods

In order to quantify educational research into objective results, several studies are analyzed for their similarities regarding their respective educational data. Table 4.1 shows the papers used for this analysis, along with metadata on the analysis and a small summary of the research. All of the data collected from the papers in Table 4.1 are then converted to a 0-100 scale, normalizing the values.

To then see how the normalized, quantitative data were related, the mean, median, mode, standard deviation, minimum, and maximum are calculated for each

data set. These values are then compared among the 10 papers described in Table 4.1. If the original works did not present raw data, only the statistical data presented is used in this analysis.

Study	Paper	Data	Summary
1	O'Neill and Polman (2004)	The data are mean assignment scores after interacting with online mentor.	This paper paired students with scientists for a mentoring relationship.
2	Osborne et al. (2003)	The data are the average ratings of the importance of scientific knowledge for secondary education, as surveyed by scientists.	This study interviewed research scientists to determine the best practices for teaching science.
3	El Khalick and BouJaoude (1997)	These values are the results of testing teacher ability compared to scientist ability on a web diagram of a concept.	This study described the knowledge base of a group of science teachers in terms of their knowledge of the structure, function, and development of their disciplines, and their understanding of the nature of science.

Study	Paper	Data	Summary
4	Jeanpierre et al. (2005)	These values are the percentage increase to inquiry based instruction after a professional development course.	This paper studied the outcome of a professional development opportunity that consisted of 2 week long resident institutes for teams consisting of a secondary science teacher and two students.
5	Druger and Allen (1998)	This is the percentage of scientists surveyed that thought K-12 science education is fair.	This paper surveyed research scientists regarding their thoughts on science education.
6	Wong et al. (2008)	These values are the percentage increase after a course on the nature of science (view points).	This paper presented the results of interviews with key scientists involved in research on severe acute respiratory syndrome, together with an analysis of the case studies and aspects of nature of science with authentic scientific inquiry.

Study	Paper	Data	Summary
7	Murphy et al. (2007)	These values are the percentage of teachers feeling confident in teaching science and developing children's science skills.	This paper compared the findings of a large-scale teacher survey on their confidence in teaching science.
8	Wilson et al. (2010)	This is the difference between a commonplace test and an inquiry-based test. The inquiry-based group did 8 percent better than the commonplace group.	This study analyzed the effectiveness of inquiry-based instruction.
9	Buczynski and Hansen (2010)	This is the percent increase from a pre-test to a post-test after professional development for the teacher.	This study analyzed the results of a professional development program with a university and a science learning center.
10	Blanchard et al. (2008)	These are the percent increase from a pre-test to a post-test after teachers participated in an inquiry project.	This study sent teachers through an inquiry project and analyzed the results of their experience and how they related their new-found skills to their classrooms.

Study	Paper	Data	Summary

Table 4.1: Research articles used for a quantitative analysis of educational research.

4.4 Results

In order to see the mean values of all studies, a plot is created with the studies on the vertical axis, as identified by Table 4.1, and the mean (converted to a scale of 0-100) on the horizontal axis. The means are grouped into low, medium, and high categories, allowing further analysis (Figure 4.1).

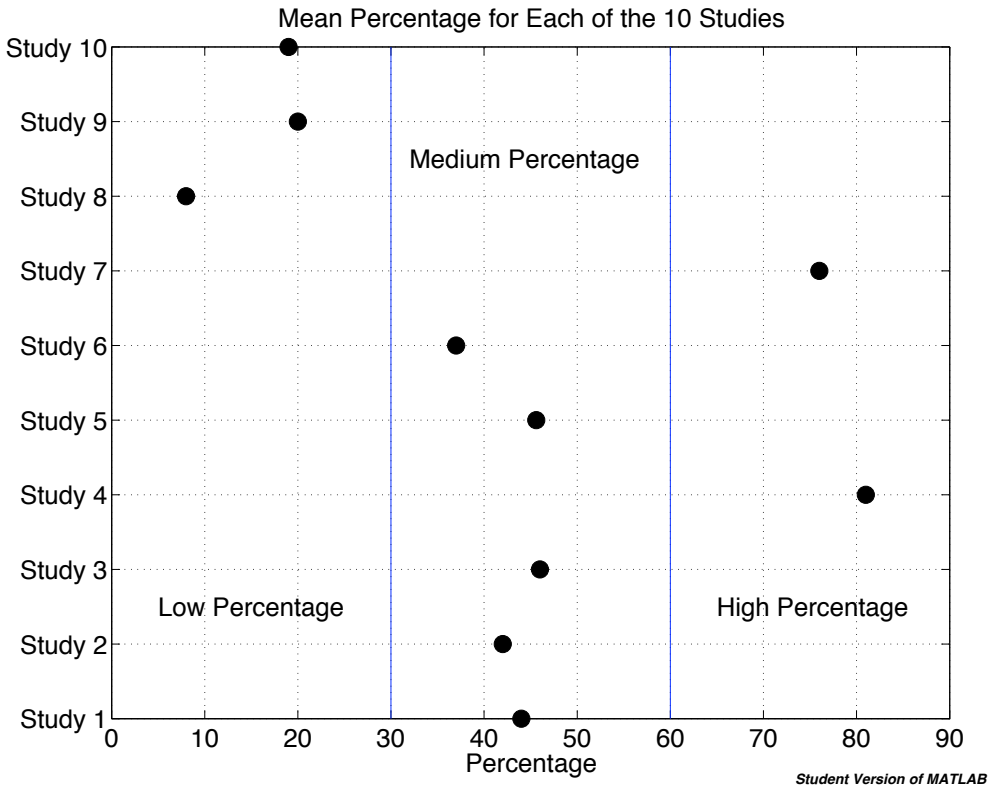

Figure 4.1: Mean value for each of the 10 studies analyzed, normalized on a scale of 0-100.

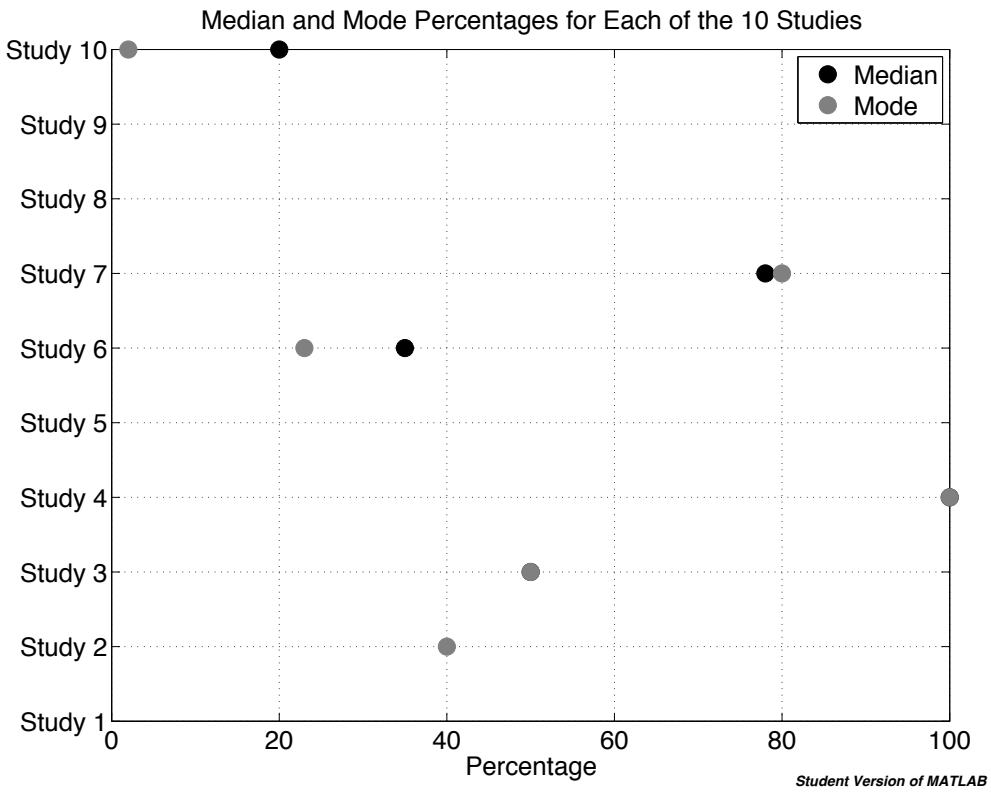

Figure 4.2: Median and mode values for each of the 10 studies analyzed, normalized on a scale of 0-100.

The median and mode for each of the data sets are also calculated and plotted (Figure 4.2). Constraints are due to data availability. If the raw data weren't presented, only the statistical calculations mentioned in the original paper could be utilized.

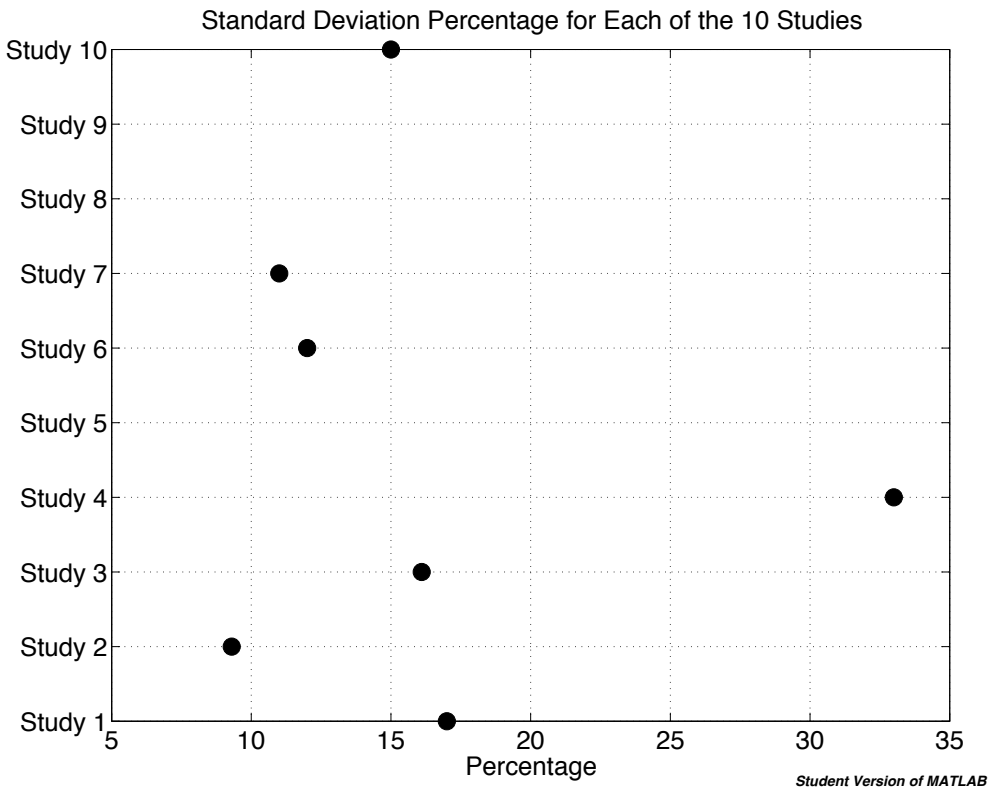

Figure 4.3: Standard deviation for each of the 10 studies analyzed, normalized on a scale of 0-100.

The standard deviation for each of the data sets is also calculated and plotted (Figure 4.3). Constraints are due to data availability. If the raw data weren't presented, only the statistical calculations mentioned in the original paper could be utilized.

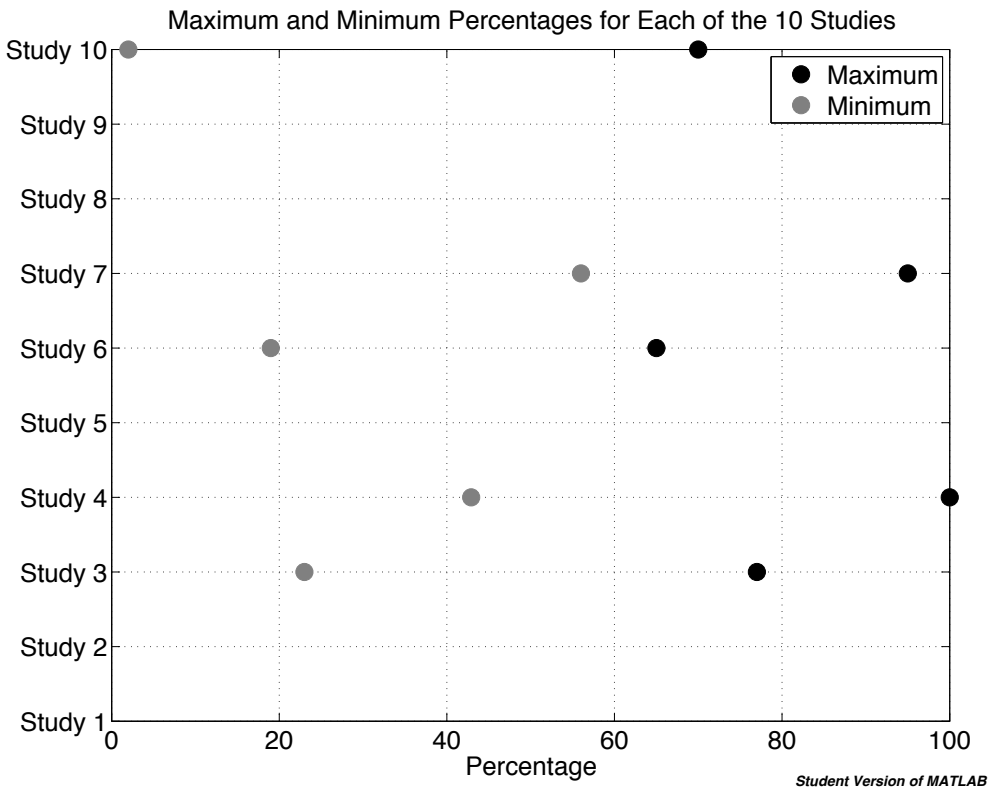

Figure 4.4: Maximum and minimum values for each of the 10 studies analyzed, normalized on a scale of 0-100.

The maximum and minimum for each of the data sets are also calculated and plotted (Figure 4.4). Constraints are due to data availability. If the raw data weren't presented, only the statistical calculations mentioned in the original paper could be utilized.

4.5 Discussion

In looking at Figure 4.1, it is clear that the ten studies analyzed fit into three distinct categories, low, medium, and high. Studies 8, 9, and 10 fall into the low category. Wilson et al. (2010), Buczynski and Hansen (2010), and Blanchard et al. (2008) are the studies in this low category. In comparing them, we can see that all of the data are percent differences between either pre- and post-tests or between two different groups. The notability of this finding is that inquiry-based instruction and professional development with research scientists positively benefits the students.

Studies 1, 2, 3, 5, and 6 fall into the medium category (Figure 4.1). O'Neill and Polman (2004), Osborne et al. (2003), El Khalick and BouJaoude (1997), Druger and Allen (1998), and Wong et al. (2008) are the studies in this medium category. In comparing them, we can see that we have a combination of various types of studies. Two of the studies are specific ratings, with Osborne et al. (2003) rating the importance of scientific knowledge for secondary education and Druger and Allen (1998) rating K-12 science education. Given how these values are collected and averaged, it is reasonable that they fall into the medium category. A second pair of the studies in this category are the results of assessment, with O'Neill and Polman (2004) assessing the importance of students working with online mentors and El Khalick and BouJaoude (1997) assessing teacher ability compared to scientist ability. The final member of this category is the study by Wong et al. (2008) who tested the knowledge of the nature of science following a professional development course. Given this final study, it is more likely that this type of study would fall into the low category with the Wilson et al. (2010), Buczynski and Hansen (2010), and Blanchard et al. (2008) studies, due to the type of data collected. The Wong et al. (2008) study, however, does fall on the low side of the medium category.

Studies 4 and 7 fall into the high category (Figure 4.1). Jeanpierre et al. (2005)

and Murphy et al. (2007) are the studies in this high category. In comparing them, we can see that the two studies are diverse as well. The Jeanpierre et al. (2005) study analyzed the percentage increase to inquiry based instruction after a professional development course while the Murphy et al. (2007) study analyzed the percentage of teachers feeling confident in teaching science and developing children's science skills. Given the nature of these two studies, it would have been thought that the Jeanpierre et al. (2005) study would have fallen into the low category since the data were based on percent increase and that the Murphy et al. study would have fallen into the medium category with the Osborne et al. (2003) and the Druger and Allen (1998) studies since the data were based on ratings.

Given data constraints, the medians and modes could not be calculated for all of the studies (Figure 4.2), but we can see various trends in these calculations for the studies in which the data were available. Study 10 (Blanchard et al. 2008) has a relatively low median and mode while study 7 (Murphy et al. 2007) has a relatively high, and close, median and mode. In comparing these two papers, we can see that the the two papers used different methods for collecting data but both have similar medians and modes, respectively. In other words, both papers have similar "middles" to their data sets with the most re-occurring values being close to the respective middle.

Again, the data are constrained due to the original papers, but the standard deviations for most of the studies are quite reasonable (Figure 4.3). All of the reported standard deviations are less than 20 except study 4 (Jeanpierre et al. 2005). This paper studied the percentage increase to inquiry based instruction after a professional development course, but with this high standard deviation, it is clear that the data are quite spread and are not centered around the average. Jeanpierre et al. (2005) mentioned that their study was subjective but attempted to be as objective as possible. Their data were based on surveys, field notes, and tests, but this is sometimes

seen as an inherent problem with educational research (Jeanpierre et al. 2005).

In comparing educational research to scientific research, there are additional factors at play. How can survey data be quantified? How can field notes be quantified? How can pre- and post-tests be strictly controlled (Jeanpierre et al. 2005)? These are questions that are asked with educational research and it is important to understand that this analysis alone has seen the issues arising from obtaining quantitative data from somewhat qualitative results. Educational data cannot, due to the nature of educational research, be as objective as scientific data (Druger and Allen 1998). It is important to understand these differences and do the best possible analysis with what is presented.

The minimums and maximums of the data sets (Figure 4.4) also provide some insight into data quality. In the studies where the minimums and maximums were available, there is an average range of 52.8 on the 0-100 scale. This information should be taken into account with the other statistical information to come to the conclusion regarding this educational research data. Again, the data presented here are relatively subjective (Jeanpierre et al. 2005) and the complexities of a classroom and educational research must be better understood.

The gap that has existed between science in the classroom and research science has contributed to the subjectivity of educational research data (Jeanpierre et al. 2005). If there is a greater connection between the two, the need for objective research will be presented earlier to students and later-life interests will be pursued with greater scientific meaning. Because few K-12 science teachers have scientific research in their training, they are unable to transfer these skills to their students (Druger and Allen 1998). Several programs created in recent years have tried to bridge this disconnect, and many universities have created programs to bring research scientists into K-12 classrooms directly or through professional development.

Dewey (1910/1964) stated that "Science has been taught too much as an accumulation of ready-made material with which students are to be made familiar, not enough as a method of thinking, an attitude of mind, after the pattern of which mental habits are to be transformed," and to this day, it is thought that the scientific process is not adequately taught in schools, leading to a misunderstanding of scientific data collection and analysis (O'Neill and Polman 2004).

Several research studies suggest that struggling to create and carry out scientific investigations in class may teach students more meaningful lessons about how science is pushed forward rather than simply executing cookbook labs or solving carefully formulated problems (Sandoval and Reiser 2003). In reading the newspaper or magazine articles, it is important for all people to understand science in a way that they can understand a scientific article. For example, O'Neill and Polman (2004) presented the following scenario: "Imagine that you and your spouse are in the midst of trying to conceive your first child. After 2 years of failing to conceive, you have begun to contact fertility clinics. One Sunday the local newspaper reveals concerns about a number of practices at fertility clinics, including the use of specific drugs. Being personally invested in the issue, you read the newspaper article from start to finish. Some of the accounts in the newspaper article are alarming. People have gotten seriously ill, and even died unexpectedly while undergoing fertility treatment. Health care providers have not always warned patients of known risks. But you, personally, are considering some of these drugs, and you desperately want a child. What are you to do?" Given this scenario, it is important to be able to understand the findings of the drugs and understand the tests from a scientific standpoint. Were the researchers objective in their studies? What errors were made in the analysis?

It's because of a situation such as this that the scientific process must be taught in schools. In order to teach the actual scientific process, professional development must play a large role (Jang 2008). Professional development literature emphasizes the

need to give teachers ongoing support as they incorporate changes in their classroom, so it is important that schools and organizations remain in contact with the teachers well after the course has been completed (Jeanpierre et al. 2005).

Buczynski and Hansen (2010), designed a professional development program focusing on inquiry-based teaching and learning. From their assessment data, they found that teachers increased their science content knowledge and began to incorporate inquiry-based techniques into their classrooms. Inquiry-based teaching is strongly recommended by the American Association for the Advancement of Science and the National Research Council as a strategy to develop deeper student understanding of science and the ability to apply it to the everyday world (Blanchard et al. 2008).

However, if preservice teachers receive the training necessary to teach science before entering the classroom, many of the issues described here would be eliminated. Prospective teachers should be taught by science educators with the ability to give them opportunities to enhance their knowledge of the structure, function, and development of science. These science educators can facilitate active participation of prospective teachers in content-specific methods courses, allowing them to understand and appreciate the importance of scientific knowledge (El Khalick and BouJaoude 1997).

In order to align scientific research with classroom practices, it is important to combine preservice training with professional development aided by scientific researchers. There needs to be a greater connection between the scientific community and classrooms, allowing students to learn the proper process from the beginning (O'Neill and Polman 2004). Science is prominent in the everyday lives of most people and it is important for all people to understand the process for decisions that they make in their own lives.

Future work on this analysis will be to contact the authors of the papers used in this study directly in an attempt to increase the data set. Many of the studies used in this analysis simply stated basic statistical values without providing data. It would be interesting to expand upon the quantitative results in an attempt to see if the analyses were in fact objective or if there remained a subjectivity to the studies.

References

Adams, D., and A. Comrie. 1997. The North American Monsoon. Bulletin of the American Meteorological Society **78**:2197–2213.

Anderson-Teixeira, K., J. Delong, A. Fox, D. Brese, and M. Litvak. 2011. Differential responses of production and respiration to temperature and moisture drive the carbon balance across a climatic gradient in New Mexico. Global Change Biology **17**:410–424.

Atkin, O., and M. Tjoelker. 2003. Thermal acclimation and the dynamic response of plant respiration to temperature. Trends in Plant Science **8**:343–351.

Bauer, J., M. Herbst, J. Huisman, L. Weihermuller, and H. Vereecken. 2008. Sensitivity of simulated soil heterotrophic respiration to temperature and moisture reduction functions. Geoderma pages 17–27.

Blanchard, M., S. Southerland, and E. Granger. 2008. No silver bullet for inquiry: Making sense of teacher change following an inquiry-based research experience for teachers. Science Teacher Education **93**:322–360.

Bolker, B., S. Pacala, and W. Parton. 1998. Linear analysis of soil decomposition: Insights from the CENTURY model. Ecological Applications **8**:425–439.

Bonan, G., K. Oleson, M. Vertenstein, and S. Levis. 2002. The land surface cli-

matology of the community land model coupled to the NCAR community climate model. Journal of Climate **15**:31236–3149.

Breshears, D., N. Cobb, and P. Rich. 2005. Regional vegetation die-off in response to global-change-type drought. Proceedings of the National Academy of Sciences **102**:15144–15148.

Buczynski, S., and C. Hansen. 2010. Impact of professional development on teacher practice: Uncovering connections. Teaching and Teacher Education **26**:599–607.

Burkholder, J. L., 1997. Report of the Chief Engineer: Submitting a plan for flood control, drainage, and irrigation of the Middle Rio Grande Conservancy Project. Technical report, State of New Mexico Middle Rio Grande Conservancy District.

Cayan, D., S. Kammerdiener, M. Dettinger, J. Caprio, and D. Peterson. 2001. Changes in the onset of spring in the Western United States. Bulletin of the American Meteorological Society **82**:399–415.

Chilcott, C., R. Dalal, W. Parton, J. Carter, and A. King. 2007. Long-term trends in fertility of soils under continuous cultivation and cereal cropping in southern Queensland IX Simulation of soil carbon and nitrogen pools using CENTURY model. Australian Journal of Soil Research **45**:206–217.

Ciais, P., M. Reichstein, and N. V. et al. 2005. Europe-wide reduction in primary productivity caused by the heat and drought in 2003. Nature **437**:529–533.

Collins, S., R. Sinsabaugh, C. Crenshaw, L. Green, A. Porras-Alfaro, M. Stursova, and L. Zeglin. 2008. Pulse dynamics and microbial processes in aridland ecosystems. Journal of Ecology **96**:413–420.

Daniels, J. 2007. Flood hydrology of the North Platte River headwaters in relation to precipitation variability. Journal of Hydrology **344**:70–81.

Davidson, E., and I. Janssens. 2006. Temperature sensitivity of soil carbon decomposition and feedbacks to climate change. Nature **440**:165–173.

Davidson, E., I. Janssens, and Y. Luo. 2006. On the variability of respiration in terrestrial ecosystems: moving beyond Q_{10}. Global Change Biology **12**:154–164.

Delrieu, G., S. Caoudal, and J. Creutin. 1997. Feasibility of using mountain return for the correction of ground-based X-band weather radar data. Journal of Atmospheric and Oceanic Technology **14**:368–385.

Delucia, E., J. Drake, R. Thomas, and M. Gonzalez-Meler. 2007. Forest carbon use efficiency: is respiration a constant fraction of gross primary production? Global Change Biology **13**:1157–1167.

Dewey, J. 1964. Science as a subject matter and as method. University of Chicago Press.

Dolgonosov, B., K. Korchagin, and N. Kirpichnikova. 2008. Modeling of annual oscillations and 1/f-noise of daily river discharges. Journal of Hydrology **357**:174–187.

Drayton, B., and J. Falk. 2006. Dimensions that shape teacher-scientist collaborations for teacher enhancement. Science Teacher Education **90**:734–761.

Druger, M., and G. Allen. 1998. A study of the role of research scientists in K-12 science education. The American Biology Teacher **60**:344–349.

Dungait, J., D. Hopkins, A. Gregory, and A. Whitmore. 2012. Soil organic matter turnover is governed by accessibility not recalcitrance. Global Change Biology **18**:1781–1796.

El Khalick, F. A., and S. BouJaoude. 1997. An exploratory study of the knowledge base for science teaching. Journal of Research in Science Teaching **34**:673–699.

Eliasson, P., R. McMurtrie, D. Pepper, M. Stromgren, S. Linder, and G. Agren. 2005. The response of heterotrophic CO_2 flux to soil warming. Global Change Biology **11**:167–181.

Epstein, H., I. Burke, and W. Lauenroth. 2002. Regional patterns of decomposition and primary production rates in the U.S Great Plains. Ecology **83**:320–327.

Falge, E., D. Baldocchi, and R. Solson. 2005. Gap filling strategies for defensible annual sums of net ecosystem exchange. Agricultural and Forest Meterology **107**:43–69.

Fang, C., P. Smith, J. Moncrieff, and J. Smith. 2005. Similar response of labile and resistant soil organic matter pools to changes in temperature. Nature **433**:57–59.

Field, C., D. Lobell, H. Peters, and N. Chiariello. 2007. Feedbacks of terrestrial ecosystems to climate change. Annual Review of Environment and Resources **32**:1–29.

Finzi, A., R. Norby, C. Calfapietra, A. Gallet-Budyoonek, B. Gielen, W. Holmes, M. Hoosbeek, C. Iversen, R. Jackson, M. Kubiske, J. Ledford, M. Liberloo, R. Oren, A. Polle, S. Pritchard, D. Zak, W. Schlesinger, and R. Ceulemans. 2007. Increases in nitrogen uptake rather than nitrogen-use efficiency support higher rates of temperate forest productivity under elevated CO_2. Proceedings of the National Academy of Sciences **104**:14014–14019.

Ford, M., and B. Wargo. 2006. Routines, roles, and responsibilities for aligning scientific and classroom practices. Science Teacher Education **91**:133–157.

Gallo, M., R. Sinsabaugh, and S. Cabaniss. 2005. The role of ultraviolet radiation in litter decomposition in arid ecosystems. Applied Soil Ecology **34**:82–91.

Gholz, H., D. Wedin, S. Smitherman, M. Harmon, and W. Parton. 2000. Long-term

dynamics of pine and hardwood litter in contrasting environments: toward a global model of decomposition. Global Change Biology **6**:751–765.

Gifford, R. 1994. The global carbon cycle: a viewpoint on the missing sink. Functional Plant Biology **21**:1–15.

Gosz, J., D. Moore, G. Shore, H. Grover, W. Rison, and C. Rison. 1995. Lightning estimates of precipitation location and quantity on the Sevilleta LTER, New Mexico. Ecological Applications **5**:1141–1150.

Graf, W. 2006. Downstream hydrologic and geomorphic effects of large dams on American rivers. Geomorphology **79**:336–360.

Grosso, S. D., D. Ojima, W. Parton, E. Stehfest, M. Heistermann, B. DeAngelo, and S. Rose. 2009. Global scale DAYCENT model analysis of greenhouse gas emissions and mitigation strategies for cropped soils. Global and Planetary Change **67**:44–50.

Guo, J., L. Tsang, E. Josberger, A. Wood, J. Hwang, and D. Lettenmaier. 2003. Mapping the spatial distribution and time evolution of snow water equivalent with passive microwave measurements. IEEE Transactions on Geoscience and Remote Sensing **41**:612–621.

Guralnik, V., and J. Srivastava. 1999. Event detection from time series data. Journal of the Association for Computing Machinery pages 33–42.

Hamed, K. 2008. Trend detection in hydrologic data: The Mann-Kendall trend test under the scaling hypothesis. Journal of Hydrology **349**:350–363.

Hameed, S. 1984. Fourier analysis of Nile flood levels. Geophysical Resarch Letters **1**:843–845.

Hanson, R., M. Newhouse, and M. Dettinger. 2004. A methodology to asess relations between climatic variability and variations in hydrologic time series in the southwestern United States. Journal of Hydrology **287**:252–269.

Herrenkohl, L., A. Palincsar, L. DeWater, and K. Kawaski. 1999. Developing scientific communities in classrooms: A sociocognitive approach. The Journal of The Learning Sciences **8**.

Hidalgo, H., T. Das, M. Dettinger, D. Cayan, D. Pierce, T. Barnett, G. Bala, A. Mirin, A. Wood, C. Bonfils, B. Santer, and T. Nozawa. 2009. Detection and attribution of streamflow timing changes to climate change in the Western United States. Journal of Climate **22**:3838–3855.

Hogberg, P., A. Nordgren, N. Buchmann, A. Taylor, A. Ekblad, M. Hogberg, G. Nyberg, M. Ottosson-Lofvenius, and D. Read. 2001. Large scale forest girdling shows that current photosynthesis drives soil respiration. Nature **411**:789–792.

Hong, J., and J. Kim. 2011. Impact of the Asian monsoon climate on ecosystem carbon and water exchanges: a wavelet analysis and its ecosystem modeling implications. Global Change Biology **17**:1900–1916.

Hughes, M., and H. Diaz. 2008. Climate variability and change in the drylands of western North America. Global and Planetary Change **64**:111–118.

IPCC, 2007. Climate Change 2007: The Physical Science Basis Summary for Policy Makers.

Ise, T., and P. Moorcroft. 2006. The global-scale temperature and moisture dependencies of a soil organic carbon decomposition: an analysis using a mechanistic decomposition model. Biogeochemistry **80**:217–231.

Jain, A., and S. P. Indurthy. 2003. Comparative analysis of event-based rainfall-runoff modeling techniques - deterministic, statistical, and artificial neural networks. Journal of Hydrologic Engineering pages 93–98.

Jang, S. 2008. The effects of integrating technology, observation and writing into a teacher education method course. Computers and Education **50**:853–865.

Jeanpierre, B., K. Oberhauser, and C. Freeman. 2005. Characteristics of professional development that effect change in secondary science teachers' classroom practices. Journal of Research in Science Teaching **42**:668–690.

Jones, C., P. Cox, and C. Huntingford. 2003. Uncertainty in climate-carbon-cycle projections associated with the sensitivity of soil respiration to temperature. Tellus **55B**:642–648.

Knorr, W., I. Prentice, J. House, and E. Holland. 2005. Long-term sensitivity of soil carbon turnover to warming. Nature **443**:298–301.

Knowles, N., M. Dettinger, and D. Cayan. 2006. Trends in snowfall versus rainfall for the Western United States. Journal of Climate **19**:4545–4559.

Krajcik, J., P. Blumenfeld, R. Marx, K. Bass, and J. Fredricks. 1998. Inquiry in project-based science classrooms: Initial attempts by middle school students. The Journal of The Learning Sciences **7**:313–350.

Krishna, A. 2005. Snow and glacier cover assessment in the high mountains of Sikkim Himalaya. Hydrological Processes **19**:2375–2383.

Kurc, S., and E. Small. 2007. Soil moisture variations and ecosystem-scale fluxes of water and carbon in semiarid grassland and shrubland. Water Resources Research **43**.

Labat, D. 2005. Recent advances in wavelet analyses: Part 1. A review of concepts. Journal of Hydrology **314**:275–288.

Leon, C., P. Julien, and D. Baird. 2009. Case study: Equivalent widths of the Middle Rio Grande, New Mexico. Journal of Hydraulic Engineering **134**:306–315.

Leung, L., Y. Qian, X. Bian, W. Washington, J. Han, and J. Roads. 2004. Mid-century ensemble regional climate change scenarios for the western United States. Climatic Change **62**:75–113.

Li, C., S. Frolking, and T. Frolking. 1992. A model of nitrous oxide evolution from soil driven by rainfall events: 1. Model structure and sensitivity. Journal of Geophysical Research **97**:9759–9776.

Luyssaert, S., I. Inglima, and M. J. et al. 2007. CO_2 balance of boreal, temperate, and tropical rainforests derived from a global database. Global Change Biology **13**:2509–2537.

Ma, L. 1999. Knowing and Teaching Elementary Mathematics: Teachers' Understanding of Fundamental Mathematics in China and the United States (Studies in Mathematical Thinking and Learning Series). Routledge.

Mansoni, S., and A. Porporato. 2009. Soil carbon and nitrogen mineralization: Theory and models across scales. Soil Biology and Biochemistry **41**:1355–1379.

Mantilla, R., V. Gupta, and O. Mesa. 2006. Role of coupled flow dynamics and real network structures on Hortonian scaling of peak flows. Journal of Hydrology **322**:155–167.

Maurer, E., I. Stewart, C. Bonfils, P. Duffy, and D. Cayan. 2007. Detection, attribution, and sensitivity of trends toward earlier streamflow in the Sierra Nevada. Journal of Geophysical Research **112**:D11118.

McKeown, R. 2003. Working with K-12 schools: Insights for scientists. BioScience **53**:870–875.

McMurtrie, R., B. Medlyn, and R. Dewar. 2001. Increased understanding of nutrient immobilization in soil organic matter is critical for predicting the carbon sink strength of forest ecosystems over the next 100 years. Tree Physiology **21**:831–839.

Molotch, N., and S. Margulis. 2008. Estimating the distribution of snow water equivalent using remotely sensed snow cover data and a spatially distributed snowmelt model: A multi-resolution, multi-sensor comparison. Advances in Water Resources **31**:1503–1514.

Moorhead, D., and R. Sinsabaugh. 2006. A theoretical model of litter decay and microbial interaction. Ecological Monographs **76**:151–174.

Mote, P. 2003. Trends in snow water equivalent in the Pacific Northwest and their climatic causes. Geophysical Resarch Letters **30**:1601–1605.

Murphy, C., P. Neil, and J. Beggs. 2007. Primary science teacher confidence revisited: ten years on. Educational Research **49**:415–430.

Neff, J., A. Townsend, G. Gleixner, S. Lehman, J. Turnbull, and W. Bowman. 2002. Variable effects of nitrogen additions on the stability and turnover of soil carbon. Nature **419**:915–917.

Norbiato, D., M. Borga, M. Sangati, and F. Zanon. 2007. Regional frequency analysis of extreme precipitation in the eastern Italian Alps and the August 29, 2003 flash flood. Journal of Hydrology **345**:149–166.

O'Neill, D., and J. Polman. 2004. Why educate "little scientists?" Examining the potential of practice-based scientific literacy. Journal of Research in Science Teaching **41**:234–266.

Osborne, J., S. Collins, M. Ratcliffe, R. Millar, and R. Duschl. 2003. What "ideas-about-science" should be taught in school science? A Delphi study of the expert community. Journal of Research in Science Teaching **40**:692–720.

Parton, W., 1996. Evaluation of soil organic matter models using long term datasets, Chapter the CENTURY model, pages 283–293 . Springer-Verlag, Berlin, Germany.

Parton, W., M. Hartman, D. Ojima, and D. Schimel. 1998. DAYCENT and its land surface submodel: description and testing. Global and Planetary Change **19**:35–48.

Parton, W., J. Scurlock, D. Ojima, T. Gilmanov, D. Schimel, T. Kirchner, J. Menaut, T. Seastedt, E. G. Moya, A. Kamnarut, and J. Kinyamario. 1993. Observations and modeling of biomass and soil organic matter dynamics for the grassland biome worldwide. Global Biogeochemical Cycles **7**:785–809.

Paul, K., 2001. Temperature and moisture effects on decomposition.

Pelletier, J., and D. Turcotte. 1997. Long-range persistence in climatological and hydrological time series: analysis, modeling and application to drought hazard assessment. Journal of Hydrology **203**:198–208.

Peterson, D., R. Smith, M. Dettinger, D. Cayan, and L. Riddle. 2000. An organized signal in snowmelt runoff over the western United States. Journal of the American Water Resources Association **36**:421–432.

Piao, S., P. Ciais, and P. F. et al. 2008. Net carbon dioxide losses of northern ecosystems in response to autumn warming. Nature **451**:49–52.

Platt, W., and J. Connell. 2003. Natural Disturbances and directional replacement of species. Ecological Monographs **73**:507–522.

Portmann, R., S. Solomon, and G. Hegerl. 2009. Spatial and seasonal patterns in climate change, temperatures, and precipitation across the United States. Proceedings of the National Academy of Sciences **106**:7324–7329.

Pregitzer, K., A. Burton, D. Zak, and A. Talhelm. 2008. Simulated chronic nitrogen deposition increases carbon storage in Northern Temperate forests. Global Change Biology **14**:142–153.

Randerson, J., C. Field, I. Fung, and P. Tans. 1999. Increases in early season ecosystem uptake explain recent changes in the seasonal cycle of atmospheric CO_2 at high northern latitudes. Geophysical Resarch Letters **26**:2765–2769.

Rastetter, E., G. Agren, and G. Shaver. 1997. Responses of N-limited ecosystems to increased CO_2: A blanced-nutrition, coupled-element-cycles model. Ecological Applications **7**:444–460.

Redmond, K., and R. Koch. 1991. Surface climate and streamflow variability in the Western United States and their relationship to large-scale circulation indices. Water Resources Research **27**:2381–2399.

Reichstein, M., D. Papale, and R. Valentini. 2007. Determinants of terrestrial ecosystem carbon balance inferred from European eddy covariance flux sites. Geophysical Resarch Letters **34**.

Renard, B., and M. Lang. 2007. Use of a Gaussian copula for multivariate extreme value analysis: Some case studies in hydrology. Advances in Water Resources **30**:897–912.

Reuters, 1996. Southwest drought threatens broad economic damage. News.

Richmond, G. 1998. Scientific apprenticeship and the role of public schools: General education of a better kind. Journal of Research in Science Teaching **35**:583–587.

Riebsame, W., S. Changnon, and T. Karl. 1991. Drought and natural resources management in the United States. Westview Press pages 11–92.

Rustad, L., J. Campbell, G. Marion, R. Norby, M. Mitchell, A. Hartley, J. Cornelissen, J. Gurevitch, and GCTE-NEWS. 2001. A meta-analysis of the response of soil respiration, net nitrogen mineralization, and aboveground plant growth to experimental ecosystem warming. Oecologia **126**:543–562.

Sabo, J., and D. Post. 2008. Quantifying periodic, stochastic, and catostrophic environmental variation. Ecological Monographs **78**:19–40.

Sandoval, W., and B. Reiser. 2003. Explanation-driven inquiry: Integrating conceptual and epistemic scaffolds for scientific inquiry. Science Education **88**:345–372.

Sang, Y., D. Wang, J. Wu, Q. Zhu, and L. Wang. 2009. The relation between periods' identification and noises in hydrologic series data. Journal of Hydrology pages 165–177.

Schaefli, B., D. Maraun, and M. Holschneider. 2007. What drives high flow events in the Swiss Alps? Recent developments in wavelet spectral analysis and their application to hydrology. Advances in Water Resources **30**:2511–2525.

Scheffer, M., S. Carpenter, J. Foley, C. Folke, and B. Walker. 2001. Catostrophic shifts in ecosystems. Nature **413**:591–596.

Schepers, H., J. van Beek, and J. Bassingthwaighte. 1992. Four methods to estimate the fractal dimension from self affine signals. IEEE Eng. Med. Biol. pages 57–64.

Schwartz, R., N. Lederman, and B. Crawford. 2004. Developing views of nature of science in an authentic context: An explicit approach to bridging the gap between nature of science and science inquiry. Science Teacher Education **88**:610–645.

Scott, R. 2006. Partitioning of evapotranspiration and its relation to carbon dioxide exchange in the Chihuahuan Desert. Hydrological Processes **20**:3227–3243.

Serreze, M., M. Clark, and R. Armstrong. 1999. Characteristics of the Western United States snowpack from snow telemetry SNOTEL data. Water Resources Research **35**:2145–2160.

Shi, S., X. Ye, Z. Dong, and Y. Zhang. 2007. Real-time simulation of large-scale dynamic river water. Simulation Modelling Practice and Theory **15**:635–646.

Sierra, C. 2012. Temperature sensitivity of organic matter decomposition in the Arrhenius equation: some theoretical considerations. Biogeochemistry **108**:1–15.

Smith, L., D. Turcotte, and B. Isacks. 1998. Stream flow characterization and feature detection using a discrete wavelet transform. Hydrological Processes **12**:233–249.

Stewart, I. 2009. Changes in snowpack and snowmelt runoff for key mountain regions. Hydrological Processes **23**:78–94.

Stoy, P., G. Katul, and M. Siqueira. 2008. Role of vegetation in determining carbon sequestration along ecological succession in the southeastern United States. Global Change Biology **14**:1409–1427.

Swayze, G., R. Clark, A. Goetz, T. Chrien, and N. Gorelick. 2003. Effects of the spectrometer band pass, sampling, and signal-to-noise ratio on spectral identification using the Tetracorder algorithm. Journal of Geophysical Research - Planets **108**:5105–5135.

Tamir, P., R. Stavy, and N. Ratner. 1998. Teaching science by inquiry: assessment and learning. Journal of Biological Education **33**:27–32.

Tang, X., J. Coffey, A. Elby, and D. Levin. 2009. The scientific method and scientific inquiry: Tensions in teaching and learning. Science Education **94**:29–47.

Tate, R. 2000. Impact of individual soil properties on microbial activity. John Wiley.

Taylor, A., M. Jones, B. Broadwell, and T. Oppewal. 2008. Creativity, inquiry, or accountability? Scientists' and teachers' perceptions of science education. Science Education **92**:1058–1075.

Thongjoo, C., S. Miyagawa, and N. Kawakubo. 2005. Effects of soil moisture and temperature on decomposition rates of some waste materials from agriculture and agro-industry. Plant Production Science **8**:475–481.

Thornton, P., and N. Rosenbloom. 2005. Ecosystem model spin-up: Estimating steady state conditions in a coupled terrestrial carbon and nitrogen cycle model. Ecological Modelling **189**:25–48.

Varelas, M., R. House, and S. Wenzel. 2005. Beginning teachers immersed into science: Scientist and science teacher identities. Science Education **89**:492–516.

Velasco-Forero, C., D. Sempere-Torres, E. Cassiraga, and J. Gomez-Hernandez. 2009. A non-parametric automatic blending methodology to estimate rainfall fields from rain gauge and radar data. Advances in Water Resources pages 986–1002.

Vitousek, P., D. Turner, W. Parton, and R. Sanford. 1994. Litter decomposition on the Mauna Loa Environmental Matrix, Hawai'i: Patterns, mechanisms, and models. Ecology **75**:418–429.

Vivoni, E., C. Aragòn, L. Malczynski, and V. Tidwell. 2009. Semiarid watershed response in central New Mexico and its sensitivity to climate variability and change. Hydrology and Earth System Sciences **13**:715–733.

Walton, R., and H. Hunter. 2009. Isolating the water quality responses of multiple land uses from stream monitoring data through model calibration. Journal of Hydrology **378**:29–45.

Wang, G., T. Jiang, R. Blender, and K. Fraedrich. 2008. Yangtze 1/f discharge

variability and the interacting river-lake system. Journal of Hydrology **351**:230–237.

Webb, E., G. Pearman, and R. Leuning. 1980. Correction of flux measurements for density effects due to heat and water vapour transfer. Quarterly Journal of the Royal Meterological Society **22**:5918–5932.

White, B., and J. Frederiksen. 1998. Inquiry, modeling, and metacognition: Making science accessible to all students. Cognition and Instruction **16**:3–118.

Wilson, C., J. Taylor, S. Kowalski, and J. Carlson. 2010. The relative effects of equity of inquiry-based and commonplace science teaching on students' knowledge, reasoning, and argumentation. Journal of Research in Science Teaching **47**:276–301.

Wong, J., L. Han, J. Bancroft, and R. Stewart, 2010. Automatic time-picking of first arrivals on noisy microseismic data. CREWES.

Wong, S., and D. Hodson. 2008. From the horse's mouth: What scientists say about scientific investigation and scientific knowledge. Science Education **93**:109–130.

Wong, S., D. Hodson, J. Kwan, and B. Yung. 2008. Turning crisis into opportunity: Enhancing student-teachers' understanding of nature of science and scientific inquiry through a case study of the scientific research in severe acute respiratory syndrome. International Journal of Science Education **30**:1417–1439.

Zhang, X., F. Zwiers, G. Hegerl, F. Lambert, N. Gillett, S. Solomon, P. Stott, and T. Nozawa. 2007. Detection of human influence on twentieth-century precipitation trends. Nature **448**:461–466.